AD_____

Award Number: DAMD17-99-1-9504

TITLE: Characterization of Genetic Alterations in Ovarian Cancer

PRINCIPAL INVESTIGATOR: David I. Smith, Ph.D.

CONTRACTING ORGANIZATION: Mayo Foundation
Rochester, Minnesota 55905

REPORT DATE: October 2002

TYPE OF REPORT: Annual

PREPARED FOR: U.S. Army Medical Research and Materiel Command
Fort Detrick, Maryland 21702-5012

DISTRIBUTION STATEMENT: Approved for Public Release;
Distribution Unlimited

REPORT DOCUMENTATION PAGE

Form Approved
OMB No. 074-0188

1. AGENCY USE ONLY (Leave blank)	2. REPORT DATE	3. REPORT TYPE AND DATES COVERED
	October 2002	Annual (1 October 2001 - 30 September 2002)

4. TITLE AND SUBTITLE
Characterization of Genetic Alterations in Ovarian Cancer

5. FUNDING NUMBER
DAMD17-99-1-9504

6. AUTHOR(S)
David I. Smith, Ph.D.

7. PERFORMING ORGANIZATION NAME(S) AND ADDRESS(ES)

Mayo Foundation
Rochester, Minnesota 55905

E-Mail: smith.david@mayo.edu

8. PERFORMING ORGANIZATION REPORT NUMBER

9. SPONSORING / MONITORING AGENCY NAME(S) AND ADDRESS(ES)

U.S. Army Medical Research and Materiel Command
Fort Detrick, Maryland 21702-5012

10. SPONSORING / MONITORING AGENCY REPORT NUMBER

11. SUPPLEMENTARY NOTES

Report contains color.

12a. DISTRIBUTION / AVAILABILITY STATEMENT

Approved for Public Release; Distribution Unlimited

12b. DISTRIBUTION CODE

13. ABSTRACT ***(Maximum 200 Words)***

Ovarian cancer is a highly lethal malignancy specific to women. We have set up the infrastructure at Mayo for an Ovarian Cancer Research Program utilizing the rich resources of clinical material and linking work from molecular geneticists with that of dedicated clinicians. What we are proposing to do is to combine several powerful strategies to clone many of the genes involved in ovarian cancer development. The first project focuses on identifying genes that are over-expressed or under-expressed during the development of ovarian cancer using subtraction suppression hybridization cDNA libraries and Gene Expression Array Analysis in collaboration with Millennium Predictive Medicine. The second project focuses on the role of gene amplification in familial versus sporadic ovarian cancer. Genes that show loss of expression in ovarian cancer and that are derived from chromosomal regions that are lost during ovarian cancer progression will be investigated in Project #1 as potential tumor suppressors. The third project is to characterize two common fragile sites, FRA6F (6q21) and FRA6E (6q26) which are derived from chromosomal regions frequently deleted in ovarian cancer and that also contain genes involved in replication senescence. Thus we have three interactive projects whose overall focus is to identify key genetic targets in the development of ovarian cancer.

14. SUBJECT TERMS	15. NUMBER OF PAGES
ovarian cancer	122
	16. PRICE CODE

17. SECURITY CLASSIFICATION OF REPORT	18. SECURITY CLASSIFICATION OF THIS PAGE	19. SECURITY CLASSIFICATION OF ABSTRACT	20. LIMITATION OF ABSTRACT
Unclassified	Unclassified	Unclassified	Unlimited

Table of Contents

Introduction

Of the cancers unique to women, ovarian cancer has the highest mortality rate. Very little is known about the genetic alterations that result in the development of this lethal disease. However, it is clear that there may be many genetic changes that occur which lead to this disease. The purpose of this Program Project is to use the strategy of transcriptional profiling to identify large numbers of aberrantly regulated genes in primary ovarian tumors. In our collaboration with Millennium Predictive Medicine, we have been using microarrays containing 25,000 human genes to monitor the level of expression of these genes in ovarian tumors as compared to normal ovarian epithelial cells. This work will also be complemented with the construction of subtraction suppression hybridization cDNA libraries to identify additional aberrantly regulated genes, not on the microarrays. There are then three interconnected projects that will analyze some of the aberrantly regulated genes identified using transcriptional profiling. The first project's goal is to characterize the down-regulated genes and to test these as candidate tumor suppressor genes. The second project's goal is to analyze over-expressed genes in both sporadic and hereditary ovarian cancer to characterize regions of amplification in sporadic versus hereditary ovarian tumors. The third project's goal is to study the expression of genes that are localized to regions containing common fragile sites. The overall goal of this work is to better characterize the key genetic alterations that lead to the development of ovarian cancer. We have made significant progress on all of these projects in the last year of support. In addition, the support from the Department of Defense has enabled us to establish a newly recognized Translational Program in Ovarian Cancer as part of the Mayo Clinic Cancer Center. In addition, thanks to the support of the Department of Defense, our Ovarian Group feels that it is now ready to compete for SPORE funding in Ovarian Cancer. We are therefore putting together our proposal for the February 1, 2003 deadline.

This Program Project was approved for three years of funding. However, due to time delays in getting approval for all of our Human and Animal Subject Research, the work described in this grant did not actually start until almost 9 months after the planned start date. If this grant had started on the proposed start date, we would now be writing our final Progress Report. Due to the delay however, we have received permission from the Department of Defense to extend this grant until the end of October 2003. What we will be describing below is the progress made upon completing two years of funding. We will, therefore, be submitting our final Progress Report next year.

PROJECT #1: Down-Regulated Genes in Ovarian Cancer. Viji Shridhar, P.I.

INTRODUCTION

The specific goal of this project is to identify genes that are down regulated during the development of ovarian cancer with an expression-based strategy. The two main strategies are:

1) In collaboration with Millennium Predictive Medicine (MPMx, Cambridge, MA), we will use their 25K cDNA gene expression arrays to screen for changes in expression of primary ovarian tumors and cell lines; and
2) Generate suppression subtraction cDNA libraries between ovarian tumors from patients with different stages of the disease and normal ovarian epithelial cells

Genes identified from this preliminary screening will be characterized in the following ways:

(A) The expression profiles of down regulated genes will be confirmed by Northern and semi-quantitative RT-PCR analysis in primary tumors and cell lines.
(B) The down-regulated genes from (1) will be analyzed on a corresponding Southern blot of DNA from primary ovarian tumors and cell lines to identify any altered bands at the genomic level.
(C) Identify corresponding BAC clones and map it to specific chromosomal regions either by FISH or by radiation hybrid mapping panel.
(D) Test candidate genes for mutations using high throughput capabilities of denaturing high performance liquid chromatography.
(E) The final specific aim of this project is to correlate the expression of down regulated genes in a significant proportion of a large panel of primary ovarian tumors from patients for whom we have extensive outcome data. This will allow us to determine the clinical significance of alterations in these genes.

Key Research Accomplishments

(1) In an attempt to understand early events in ovarian carcinogenesis and to explore steps in its progression, we have applied multiple molecular genetic techniques to the analysis of 21 early stage (stage I/II) and 17 advanced stage (stage III/IV) ovarian tumors. These techniques included expression profiling seven each of early and late stage tumors with cDNA micro-arrays containing approximately 18,000 expressed sequences, and comparative genomic hybridization to address the chromosomal locations of copy number gains as well as losses. **Results from the analysis indicate that "early stage" ovarian cancers exhibit profound alterations in gene expression, many of which are similar to those identified in late stage tumors. However, differences observed at the genomic level suggest differences between the early and late stage tumors and provide support for a progression model for ovarian cancer development.** The manuscript describing these results is published in *Cancer Research* (2001; 61:5895-5904), a copy of which is included in the Appendix.
(2) In order to identify novel tumor suppressor genes involved in ovarian carcinogenesis, we generated four down regulated suppression subtraction cDNA libraries from two early stage (stage I/II) and two late stage (stage III) primary ovarian tumors each subtracted against cDNAs derived from normal ovarian epithelial cell brushings. Approximately 600-700 distinct clones were sequenced from each library. Comparison of down regulated clones obtained from early and late stage tumors revealed genes that were unique to each library suggesting tumor specific differences. We found 45 down regulated genes that were common in all four libraries. We also identified several genes whose role in tumor development has yet to be elucidated, in addition to several under-expressed genes whose potential role in carcinogenesis has previously been described. The differential expression of a subset of these genes was confirmed by semi-quantitative RT-PCR using GAPDH as control in a panel of 15

stage I and 15 stage III tumors of mixed histological subtypes. Chromosomal sorting of library sequences revealed that several of the genes mapped to known regions of deletion in ovarian cancer. Loss of heterozygosity analysis revealed multiple genomic regions with a high frequency of loss in both early and late stage tumors. In order to determine if loss of expression of some of the genes corresponds to loss of an allele by LOH, we utilized a microsatellite marker for one of the novel genes on 8q and have shown that loss of expression of this novel gene correlates with loss of an allele by LOH. In conclusion, our analysis has identified down regulated genes, which map to known as well as novel regions of deletions and may represent potential candidate tumor suppressor genes involved in ovarian cancer. **While some of the genes identified from these libraries were also identified as down regulated genes by transcriptional profiling of the same tumor, we identified several known and unknown genes of very low abundance only in the SSH libraries. The data from the SSH library analysis also revealed that there were many genes which were differentially expressed in both early and late stage tumors.** The manuscript describing the results from this analysis was published in *Cancer Research*; the manuscript is in the Appendix.

The expression of the down regulated genes were characterized in the following ways:

(A) By Northern and semi-quantitative RT-PCR analysis. Please see the attached manuscripts for details.

(B) Southern blot analysis is still ongoing. We have not detected any altered bands at the genomic level with some of the down-regulated genes tested.

(C) Chromosomal mapping of corresponding BACS will not be performed due to the extensive chromosomal sequences available as a result of the Human Genome Project. For most of the genes identified from these screens, chromosomal positions are known.

(D) Mutation screening using DHPLC for some of the genes is ongoing.

(E) The clinical significance of alterations in these genes is also ongoing.

PROGRESS REPORT - Year 3

Based on the high throughput screening…

(1) We validated the expression levels of 100 different genes by semiquantitative RT-PCR in a panel of ovarian cancer cell lines and a subset of these genes (10) by light cycler analysis in primary ovarian tumors.

(2) We selected the following genes for a more detailed analysis

GENES	Chromosomal Location
hSulf 1	8q13
hSulf 2	20q12-13
Nesprin	6q25
HtrA1	10q26.3
A novel gene	5q15
A novel gene on X	Xq22
PEG3	19q13.3

For each of these genes, we have done the following analyses:

1. Loss of heterozygosity within and the flanking region of the gene locus;
2. Southern blot analysis to look for altered bands;
3. Northern analysis in cell lines and primary ovarian tumors;
4. Mutation screening of exons by DHPLC analysis; and
5. Methylation analysis by MS-PCR.

Results from these analyses identified…

1. LOH analysis identified a novel region of deletion on 8q and 20q.
2. We have identified two genes with altered bands in 1 of 20 primary tumors in two different genes (Nesprin and HtrA1) at the southern level.
3. Northern blot analysis of all of the above genes truly reflected the results obtained with semi-quantitative RT-PCR.
4. Mutational analysis was performed on the following genes:
   a) hSulf 1 (exons 5-13 of 21 exons);
   b) All three exons of the novel gene on chromosome X;
   c) All 21 exons of the novel gene on 5q; and
   d) All 9 exons of HtrA1. No tumor specific mutations were seen in any of these genes.
5. Methylation analysis of the novel gene on chromosome X (which we named PAPX) revealed that the gene was expressed monoallelically. Loss of expression of this gene in all the cell lines tested and in 20 primary tumors was due to methylation of a specific SmaI site in intron 1 on the active X.
6. Clinical correlation associated with alterations in these genes is ongoing.

****

PROJECT #2: Characterization of the Role of Amplified Oncogenes in the Development of Familial and Sporadic Ovarian Cancer. Fergus Couch, Ph.D.

BACKGROUND:

The specific goal of this project is to identify genes that are amplified and overexpressed during the development of ovarian cancer. The goal is to also use these genes to test the hypotheses 1) that gene amplification contributes significantly to the development and progression of ovarian cancer, and 2) that familial and sporadic ovarian tumors have different progression pathways.

To achieve this goal, we proposed the following four major aims:

Specific Aim #1: Assembly of collections of frozen familial and sporadic ovarian tumors.

Specific Aim #2: Assessment of the extent of gene amplification in familial and sporadic tumors.

Specific Aim #3: Identification of novel amplicons and amplified genes in familial and sporadic ovarian tumors.

Specific Aim #4: Characterization of the oncogenic activity of candidate oncogenes.

RESULTS:

Specific Aim #1/Task 1: The description of the completion of Specific Aim 1 was provided in the previous annual report.

Specific Aim #2/Task 2: In our previous report, we described the results of CGH studies of a series of early and late stage ovarian tumors. These studies resulted in the identification of a number of known regions of amplification containing previously described oncogenes such as Cyclin D1, c-Myc, AIB-1, ZNF217, Cyclin E, and PI3KCA. A number of other amplified regions including 1p, 1q, 8p, 11p, 12p, 16p, and 19p were also identified. Oncogenes associated with ovarian cancer have not previously been identified in these regions.

Specific Aim #3/Task 3: Our goal in this section was to identify novel amplified and over-expressed genes in ovarian tumors. We previously reported that we had profiled a total of 78 ovarian tumors and 5 normal ovarian epithelial cell samples on a 30,000 gene expression array in

collaboration with MPMx. By analyzing 50 gene moving median profiles of each tumor we identified 15 putative regions of amplification and the candidate genes within these regions.

In the last year we attempted to verify that these candidate regions are actually amplified in the tumors using Fluorescent *In Situ* Hybridization (FISH) studies. Tissue microarrays containing three 0.6 μm cores from 48 of the 78 tumors were generated. These arrays were then hybridized with Bacterial Artificial Chromosome (BAC) probes from the candidate regions along with relevant centromeric probes (Vysis Inc.) and a ratio of BAC probe signals to centromeric signals in 60 nuclei from each sample was calculated to determine if amplification was present. No amplification was detected using probes for N-myc on chromosome 2p24.1, E2F1 on chromosome 20q11.2, and RAB7 and MCM2 minichromosome maintenance deficient 2 (mitotin) on chromosome 3q. These negative results led us to question the ability of the moving median window analysis of gene expression data to identify regions of amplification with high specificity. While this approach may successfully identify some regions of amplification, the high background of non-amplified regions suggests that it may take considerable effort to find those few amplicons.

With this in mind, we took a different approach to identifying amplified regions and genes in ovarian tumors. In collaboration with Dr. Barbara Weber from the University of Pennsylvania, we have profiled 26 of the same group of ovarian tumors on gCGH arrays. These arrays contain 4,000 BAC clones spotted in duplicate on glass slides. DNA from tumors is fluorescently labeled with cy3 dye by nick translation and mixed in equal proportion with cy5 labeled normal genomic DNA. The complex probe is then hybridized to the array and the intensity of fluorescent signal at both the cy3 and cy5 fluorescent ratios for each spot is measured with a scanner. The fluorescence intensity is normalized to the median intensity value for each array and the cy3/cy5 ratio is calculated. The intensity ratio for each BAC can then be plotted against the position of the BAC in the genome. Careful analysis of control samples with known levels of amplification of certain genes has determined that the lower boundary for amplification (≥5 gene copies) using this technique is 1.75, while the boundary for loss of heterozygosity (LOH) or deletion is 0.75. Alternatively, by plotting $\log_2$ (intensity ratio) against chromosomal position, a more uniform spread of the intensity data can be achieved. With this approach the lower boundary for amplification is 0.75 and the upper limit for LOH is -0.5. The Weber group has developed CGH browser software to facilitate this process. An example of a plot is shown in Figure 1. Selected BACs on these plots can be directly linked to the BAC ID and to FISH mapping data from the Human Genome Project.

Using this approach we have visually identified a number of regions of amplification and loss throughout the genome of each tumor. Specifically, we have identified 44 independent regions of amplification in this set of tumors. However, the majority of these amplification events are found in less than 10% of the tumors. A total of 9 regions were identified in greater than 10% of the tumors. These include 8q11, 8q21, 8q24, 18p11, 18q12, 19p12, 19q13.2, 19q13.4, and 20q13. Of particular interest is the 8q24 region that is amplified in 40% of the tumors. We confirmed that the most highly amplified gene in this region of amplification in the tumors is the c-myc gene. We have now focused our efforts on the 19q13.2 and 19q13.4 amplicons that were identified in 18% of the tumors. We have determined that the 19q13.2 amplicon contains the AKT2, c-AXL, CLG, and XRCC1 candidate oncogenes, while the 19q13.4 amplicon contains the PRPF31 and TCF3 candidate oncogenes. We have begun to evaluate amplification of these specific genes by Southern blot of the tumor DNA with gene specific probes.

Further efforts on this study involve:

1) completing gCGH array analysis of 30 sporadic ovarian tumors and 10 BRCA1 and BRCA2 mutant ovarian tumors;
2) selecting the most common regions of amplification in these tumors;
3) correlating expression and amplification data from the tumors in order to identify amplified and over-expressed candidate oncogenes; and
4) validating amplification of specific regions by FISH and Southern blotting, with particular emphasis on 19q13.2 and 19q13.4.

Specific Aim #4/Task 4: Work on this area has not yet begun because we have been contributing all of our effort to the gCGH studies. However, we are particularly interested in evaluating the oncogenic activity associated with the CLG gene from 19q13.2 and the TCF3 gene from 19q13.4.

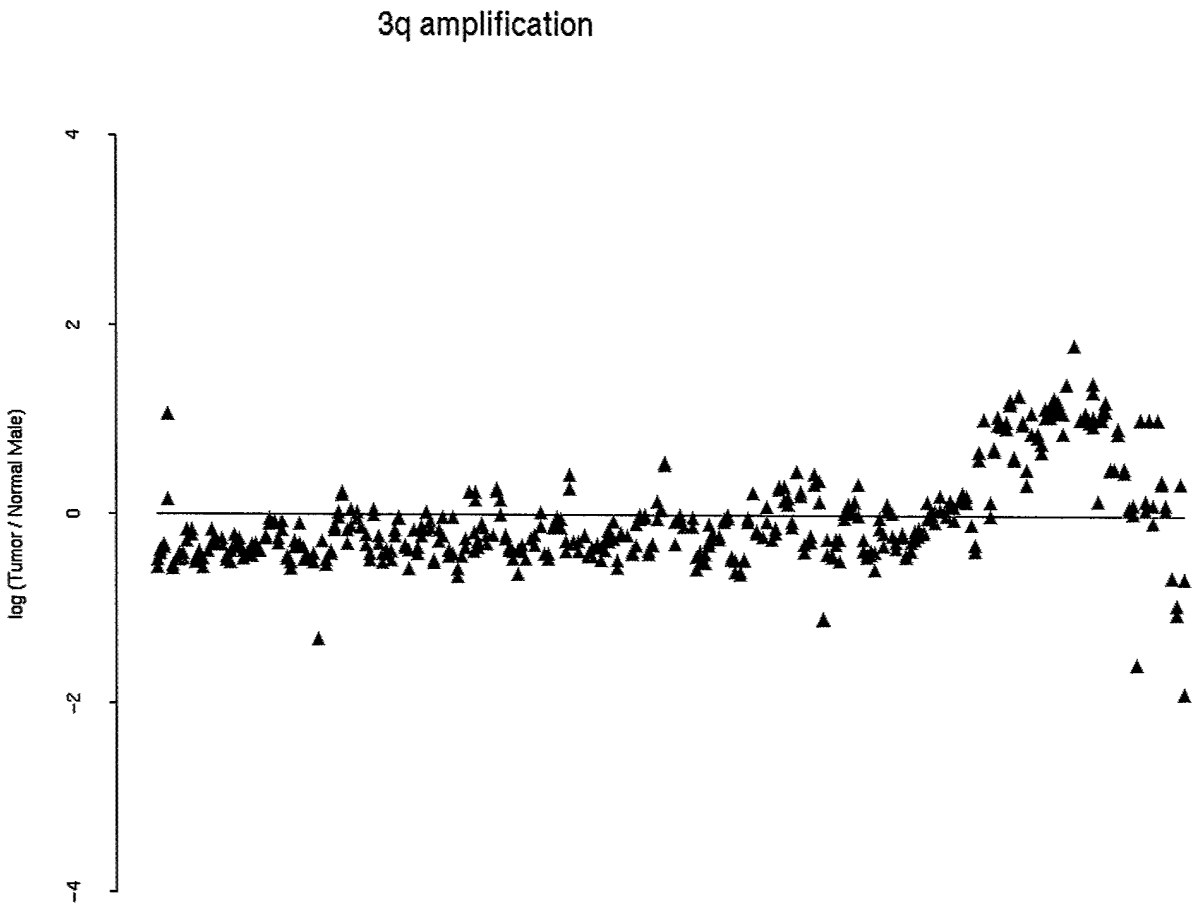

Figure 1. Amplification on chromosome 3q in an ovarian tumor as detected by gCGH. The $\log_2$(intensity ratio) for each BAC on chromosome 3 was plotted against the relative chromosomal position of the BAC. Duplicate intensity values for each BAC are plotted. Points of greater than 0.75 on the y-axis are considered amplified.

****

PROJECT #3: Common Fragile Sites and Ovarian Cancer. David I Smith, P.I.

There were four specific aims to our original proposal. **Specific Aim #1:** The cloning and characterization of FRA6E (6q21) and FRA6F (6q26) as these two common fragile sites are derived from chromosomal regions that are frequently deleted during the development of ovarian cancer. **Specific Aim #2:** The isolation of genes from the FRA6E and FRA6F regions, followed by examining each of them as potential tumor suppressor genes or as sensors of genomic damage. **Specific Aim #3:** The third specific aim was to perform clinical correlative studies in ovarian cancer with our impressive resource of fresh frozen ovarian tumors with full clinical follow-up. **Specific Aim #4:** The final specific aim, and the one that linked this project to the other projects within this Program Project Grant, was to characterize aberrantly expressed genes derived from chromosomal bands containing common fragile sites, to determine if these genes actually do reside within common fragile site regions. We feel that we have continued to make excellent progress towards the completion of these goals.

Specific Aim #1: Our first goal was to characterize two common fragile site (CFS) regions derived from regions on the long arm of chromosome 6 that were frequently deleted during the development of ovarian cancer. Although our plan called for us to characterize both CFS regions, we have focused most of our efforts on the characterization of the FRA6E (6q26) region, and have collaborated with the group of Dr. Barbanti-Brodano (University of Ferrara, Italy) who have been analyzing the 6q21 region. In collaboration with Dr. Barbanti-Brodano, we have recently published a paper on the cloning of the FRA6F CFS in *Oncogene* (see the *Key Research Accomplishments* section for details on this and other papers published in the past year).

As mentioned, we have focused most of our attention on the characterization of the FRA6E CFS. The common fragile sites are characterized by hybridizing fluorescently labeled large-insert clones (usually cosmids or BACs) to metaphase spreads produced from aphidicolin-treated lymphocytes and then observing where the labeled clones hybridize relative to aphidicolin-induced decondensation/breakage within specific common fragile site regions. Since the regions of instability where decondensation/breakage occurs is considerably larger than the labeled clones, an individual clone can hybridize proximal, distal or actually crossing the region with a decondensation/break. Clones which hybridize with approximately equal frequency proximal and distal to breaks in different metaphases are considered to reside within the "center" of the common fragile site region. Clones which hybridize more frequently proximal than distal to breaks are considered to reside on the proximal side of the common fragile site region. Finally, if a clone hybridizes always on one side of a fragile site (in at least 20 metaphases with good discernible breakage within the common fragile site) that clone is outside of the common fragile site region. Utilizing this assay we were able to determine that the "center" of this common fragile site actually resides on the telomeric end of the entire region of instability. In the past year the development of the human genome sequence has been quite dramatic. Re-examination of the region of aphidicolin-induced instability has revealed that FRA6E actually spans 4 megabases and the PARK2 gene covers the distal half of the CFS region. Thus, PARK2 is the second largest known human gene.

Specific Aim #2: Our second specific aim was to identify genes that resided within the FRA6E common fragile site and to determine the level of expression of these genes in ovarian cancer cell lines and in primary ovarian tumors. We have identified a total of eight genes that reside within this 2.2 megabase region of instability. The Figure below shows all our results on the physical characterization of the FRA6E region. Included on this figure is the BAC contig which we have constructed across this region. This contig is now completely sequenced without any gaps. Also included on the figure below are the FISH results with several of the BACs from the contig. The centromeric end of FRA6E contains a number of small genes including IGF2R, a gene which has

been demonstrated to be mutated in some forms of cancer and has been called a putative tumor suppressor.

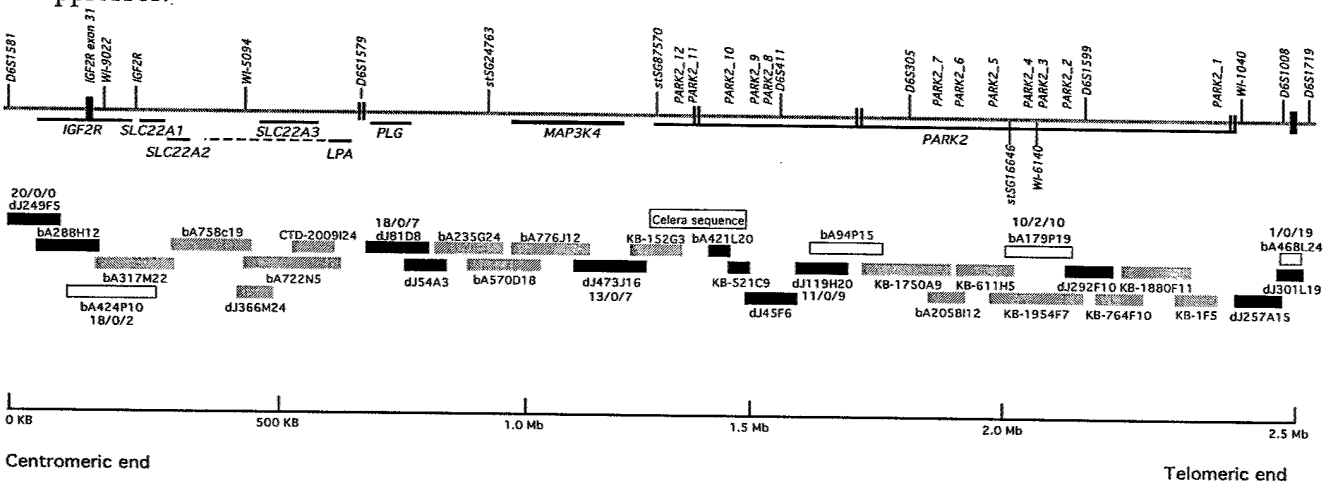

As described last year in our Progress Report, the PARK2 gene spans the center of the FRA6E CFS. There are many similarities between the structure of PARK2 and its relationship to the FRA6E CFS and two other very interesting CFS genes, FHIT and WWOX. Our group has been studying the WWOX gene and the FRA16D (16q23.2) CFS that surrounds it, using similar techniques that we utilized to characterize FHIT and FRA3B (3p14.2). What is clear from all these studies is that each of these highly unstable regions (and indeed FRA3B, FRA16D and FRA6E are all among the most active of the CFSs) spans a very large genomic region. Contained within the center of these unstable regions (defined not as the geographic center, but where clones hybridize with approximately equal frequency proximal and distal to the region of aphidicolin induced breakage) are very large, very interesting genes. FHIT has been demonstrated to be a tumor suppressor and there is some preliminary evidence suggesting that WWOX may also be a tumor suppressor gene. In addition, mutations in WWOX have been observed in ovarian tumors (Paige et al; WWOX: a candidate tumor suppressor involved in multiple tumor types. *Proc Natl Acad Sci USA* 2001; 98:11417-11422) and that this gene behaves as a suppressor of tumor growth (Bednarek et al. WWOX, the FRA16D gene, behaves as a suppressor of tumor growth. *Cancer Res* 2001: 61:8068-8073).

We then went on to examine the expression of each of the genes from FRA6E and found that half of them showed a loss of expression in ovarian cancer cell lines and primary tumors, and that Parkin was down-regulated in 80% of the primary ovarian tumors analyzed (using semi-quantitative RT-PCR). Additionally, loss of heterozygosity (LOH) analysis of primary ovarian tumors using polymorphic markers in the 6q26 region revealed markers that mapped within the large Parkin gene had the highest LOH of any of the markers within the FRA6E region. Our data summarizing our work on the characterization of the entire FRA6E region and the expression analysis of genes within that region in ovarian cancer cell lines and primary tumors was submitted for publication in *Oncogene*. The reviewers were enthusiastic about our results but requested several additional experiments that we have just completed. This paper was thus returned to *Oncogene* for review.

One of the stated goals under Specific Aim #2 was to analyze genes that map within the common fragile sites to determine if they are mutational targets in ovarian cancer cell lines and primary tumors. We have used a combination of different techniques to look for mutations within these genes, including analyzing cell lines and primary tumors for homozygous deletions, as well as CSGE analysis for smaller alterations. We did not detect any homozygous deletions in any of the FRA6E genes in our resource of ovarian cancer cell lines or primary tumors. However, as part of a collaboration with Dr. Lewis Roberts who works on hepatocellular carcinoma, we have

detected a homozygous deletion in the PARK2 in one HCC cell line. We are currently characterizing this homozygous deletion which appears to be complex (thus far we have found two distinct homozygous deletions in the middle of PARK2 in this one cell line).

We have not identified any mutations in PARK2 in ovarian tumors. However, this result is very similar to what has been observed for FHIT. Although there are a number of alterations in the FRA3B region in many different cancers, there has only been a single published report demonstrating a point mutation in FHIT. We have spent a great deal of time analyzing what appear to be tumor-specific alternative PARK2 transcripts. This is also very similar to what has been observed for FHIT and WWOX. Utilizing RT-PCR analysis we have found that many ovarian cancers have numerous alternative PARK2 transcripts. We have purified many of these and sequenced them, and in most instances, we detect deletions of entire exons, suggesting that what we are seeing is alternative splicing that is tumor specific. Similar to frequent observations of FHIT in various cancers, we still detect the full-length, apparently wild-type transcript of PARK2 in all the ovarian cancer cell lines and primary tumors.

We have analyzed PARK2 heterozygous deletions using real-time PCR. This analysis reveals that there are clearly multiple heterozygous deletions in this region in ovarian cancer. What we do not know is if the net result is that both copies of PARK2 are inactivated, similar to what is observed in the FRA3B region. In order to determine if there is any PARK2 protein made, we have begun to analyze PARK2 expression utilizing commercially available antibodies. This analysis, which we recently completed for the ovarian cancer cell lines, has shown that PARK2 levels are dramatically decreased in the cell lines. We are now analyzing PARK2 expression in primary ovarian tumors. In addition, we are about to begin RNAi experiments to inactivate PARK2 expression in short-term cultures of normal ovarian epithelium. These would then be analyzed to determine: (1) the changes in gene expression as a result of PARK2 inactivation; and (2) the resulting phenotypic changes to the normal ovarian epithelial cells.

Specific Aim #3: The third specific aim was to perform clinical correlative studies in ovarian cancer with our impressive resource of fresh frozen ovarian tumors with full clinical follow-up. We have isolated RNA from over 100 primary ovarian tumors representing different histologies (serous, clear-cell, and mucinous ovarian tumors), and different stages and grades. Unfortunately, low stage, low grade serous tumors represent less than 1% of all serous tumors in our repository, although low stage, low grade mucinous or endometrioid tumors are more common. We have also analyzed ovarian tumor samples from patients that appeared to have chemosensitive tumors (resulting in disease-free survival of greater than 3 years), as well as patients that appear to be chemoresistant (tumor progresses in less than 6 months).

Unfortunately, our analysis of PARK2 mRNA expression has yielded conflicting results. While we detected down-regulation of PARK2 in many ovarian cancer cell lines and primary tumors using semi-quantitative RT-PCR, we did not find the same thing using real-time PCR. We struggled with this for a while until we realized that very different results are obtained depending upon which real-time primers are utilized . Presumably some regions of PARK2 are considerably down-regulated (or deleted) while others are not. Now that we have the Western's working with PARK2 antibodies, we will do this analysis at the protein level to determine if there is any clinical importance to the loss of PARK2 expression.

Specific Aim #4: The final specific aim was to characterize aberrantly expressed genes derived from chromosomal bands containing common fragile sites to determine if these genes actually do reside within common fragile site regions. One of the stated goals of this Program Project Grant was to encourage interactions and collaborations between the three separate Projects. When we analyzed the transcriptional profiling results obtained by Dr. Shridhar, we found that many of the

consistently down-regulated genes were derived from chromosomal bands that contain common fragile sites. We chose a sub-set of these genes to determine which were derived from a common fragile site region. The genes that were chosen were picked based upon a number of criteria including whether they were genes that were previously described as being important in the development of ovarian cancer (such as NOEY2), or whether the gene was derived from a chromosomal region that has been shown to be consistently deleted in ovarian cancer. The Table below lists the genes that were chosen for further study.

Gene	Image Clone	Accession	Band	CFS
NOEY 2	345680	W72033	1p31	FRA1C
RGP4	429349	AA007419	1q21	FRA1F
FHIT	-	XM043137	3p14.2	FRA3B
PDGFRA	52096	H23235	4q12	FRA4B
FST	434768	AA701860	5p14; 5q11	FRA5E; Hecht et al 1988
M6P/IGF2R[a]	67055	T70421	6q26	FRA6E
PLG[a]	875979	T73187	6q26	FRA6E
SLC22A3[a]	127120	R08121	6q26	FRA6E
CAV-1	-	XM057981	7q31.2	FRA7G
CAV-2	-	NM001233	7q31.2	FRA7G
TESTIN	-	?	7q31.2	FRA7G
PSAP	291255	N72215	10q21-22	FRA10C; FRA10D
TSG101	123087	R02529	11p15	FRA11C; FRA11D; FRA11E
TPM1	341328	W58092	15q22.1	FRA15A
WWOX	-	NM016373	16q23.2	FRA16D

In order to determine if any of these genes resided within a common fragile site region, we first needed to identify BAC clones that spanned each of these genes. In some instances, BAC clones could be identified electronically. For the majority of the genes chosen however, we needed to screen the Research Genetics BAC pools to identify BAC clones that spanned these genes. Once the BACs were isolated, they were used as FISH-based probes to determine if they localized within a common fragile site region. If a BAC clone always hybridized proximal or distal to the region of aphidicolin-induced decondensation/breakage in 20/20 metaphases examined, that clone localizes outside of the CFS region of instability. Clones which hybridized with approximately equal frequencies proximal and distal to the region of decondensation/breakage were derived from the "center" of that CFS region. Clones which hybridized more frequently distal to the region of breakage were derived from the distal portion of the CFS. We could thus localize BACs as either outside the respective CFS region, within the center of those regions, or at the "ends" of that CFS region. We analyzed the BAC clones that were identified to span each of the 10 genes chosen and found that 9 of the genes localized within a CFS region. Three of the genes (FST, IGF2R, and PDGFRA) localized to the ends of their respective CFS. The remaining six genes (NOEY2, PSAP, TPM1, SLC22A3, PLG, and TSG101) localized within the "centers" of their respective fragile sites. This work has enabled us to localize a number of CFS regions that were not previously characterized. This work has been recently published in *Genes, Chromosomes and Cancer* (the reference is listed under Key Research Accomplishments).

Our goal in the final year of this Program Project is to continue to analyze PARK2 to determine how frequently PARK2 is inactivated in ovarian cancers and whether there is any clinical correlation between loss of PARK2 expression and the development of ovarian cancer. In addition, we are initiating functional studies to determine if loss of PARK2 is associated with any important phenotypic changes in normal ovarian epithelial cells.

****

ADMINISTRATION CORE

Background: The premise of our entire program project grant is that ovarian cancer develops upon a background of significant genetic alterations and that we can combine several powerful strategies, based in a rich tissue repository, to clone many of the genes involved in ovarian cancer development.

Objective: The overall purpose of the Administration Core is to support and oversee the work done by all three projects and the three other cores.

Relevance to Ovarian Cancer: There is ample data that frequent genetic alterations underlie the development of epithelial ovarian cancer. This is the premise underlying our entire program project grant. The Administration Core integrates all our efforts to (1) determine which of these myriad genetic abnormalities are relevant and (2) identify the biologic function of the relevant alterations.

Support Provided to Research Projects by Administration Core: The Administration Core performs these functions:

- Continues to build our tissue repository
- Obtains clinical and follow-up data to match tissue specimens
- Develops a system to provide ready access to tissue repository
- Links tissue and clinical data via a relational database
- Coordinates pathology review for all specimens
- Provides statistical support to all projects and cores
- Oversese all projects and cores including budgets
- Manages all human subject issues including approvals through the Mayo Institutional Review Board and the Department of Defense Human Subjects Reviews Groups; address all patient/family questions about research participation
- Organizes meetings of investigators and external advisors
- Maintains a liaison with education and outreach specialists within the Mayo Women's Cancer Program and Mayo Clinic Cancer Center (MCCC)
- Formalizes a partnership with representatives of the advocacy community

Methodology and Design: Our methods for the repository/database and statistical support are described here and in the following *Results* section.

Tissue repository: The Ovarian Program has stored specimens of a variety of ovarian tumors since 1991. At the present time we have 1,390 ovarian specimens in a fresh, frozen state, approximately 70% of which are epithelial or borderline in origin, with the remaining samples being benign or non-epithelial tumors. Over 90% of the epithelial samples have undergone tumor grade and morphology review by Dr. Gary Keeney, a pathologist specializing in gynecologic malignancies. The details regarding tissue acquisition and pathology review are provided in the following section on the Tissue Acquisition Core facility. The clinical information from patients providing tissue specimens is currently being abstracted from the medical records – this will

include key risk factors such as family history and follow-up data. In the Results section below, we provide the current status of the tissue repository, clinical information, and relational database. Dr. Steve Iturria in the Section of Biostatistics has provided statistical support for the genetic analyses. His duties have included maintaining all data files in a secure environment, performing diagnostics to ensure data quality, extracting data sets for analyses, and assisting investigators in the identification and use of appropriate statistical methods.

Results:

Tissue repository: At the present time, we have nearly 1400 ovarian tumors in a fresh frozen state. This maintains the anticipated accrual of 100-125 new ovarian tumor specimens annually. Sectioned tumors for RNA preparation or purified DNA have been provided to all three projects of this program project grant. In addition, tissue arrays from the Mayo Clinic Tissue Registry collection of paraffin blocks have been constructed for efficient use of tissue for FISH and immunohistochemical analyses.

Chart abstraction for clinical follow-up: To date, we have abstracted 675 charts and this work is proceeding on schedule. Significant effort is taken to provide the most current follow-up data available for patients who have completed their initial course of treatment. Clinical data for newly abstracted charts are currently entered into the new relational database rather than the older SAS-based database.

Relational database: At the present time, inventory and tracking information for the ovarian tissue repository are housed in an Access database, created to store information by tumor code numbers (patient identification is not distributed to individual investigators or cores). The clinical data and follow-up information are housed in a clinical database. The new web-based clinical database is undergoing the final audit of a test series of downloaded charts before all previously abstracted charts are downloaded from SAS into the new system. We anticipate that the extensive pre-implementation testing and modifications made in 2002 will allow a smooth transition. The change to a web-based system will increase the efficiency of data retrieval as well as promote data integrity.

Statistical support: The statistical support that Dr. Iturria has provided thus far to the specific projects includes:

(Project #3) Examined the down-regulation of genes near known fragile sites in ovarian cancer. Tumor vs. normal expression ratios for genes lying in known fragile sites were contrasted with those of genes not lying in known fragile sites. Potentially unknown fragile sites were identified by constructing moving average plots for the tumor vs. normal expression ratios on each chromosome.

(Project #2) Identified over-expressed genes in ovarian cancer. Cluster analyses were performed to identify sets of genes that had common expression profiles across multiple experiments. Clusters which exhibited a pattern consistent with over-expression in tumors were identified. Various other gene-ranking methods were used to identify genes demonstrating significant increased expression in ovarian tumors. Moving average analyses were carried out to identify entire regions of gene amplification.

(Project #1) Identified under-expressed genes using methods similar to those used above.

Oversight: Drs. Smith and Hartmann communicate multiple times per week to ensure the fluid progress of all the projects and cores. They each interact independently with project and core leaders to address issues as they arise.

Human subjects issues; patient/family contact: We have developed a protocol for direct patient contact as we continue to build our tissue/clinical data repository. The steps for this protocol are as follows:

A. Tumor sent from Surgical Pathology to Tumor Acquisition Core Facility.
B. Tumor Acquisition Core sends e-mail notification of tumor received to Study Coordinator.
C. Surgical pathology results reviewed to determine appropriate participation level.
D. Patient contacted by Study Coordinator regarding participation in Ovarian Tumor Study.
E. Consent form signed, blood request ordered, and questionnaire completed.
F. Materials filed in master file along with Patient Enrollment Master Sheet.

All patient/family contact materials have recently been approved by the Mayo IRB and the Department of Defense Human Subjects Review Group so that we may continue this work until October 2003.

Coordination of meetings: Our Ovarian Cancer Research group meets the third Monday of every month from 10:30 a.m.–12:00 noon. Fifteen to 20 individuals attend including the project leaders, core leaders, technicians, and trainees involved in this ovarian cancer effort. At these meetings investigators present their scientific data for discussion, and new questions and collaborations are generated. Moreover, our Executive Committee meets monthly to assure smooth operations among the projects and within the MCCC. Dr. Hartmann meets weekly with the study abstracter and the laboratory personnel involved in sample acquisition.

Maintain liaison with education and outreach specialists within the Mayo Women's Cancer Program and MCCC. Ms. Julie (Quam) Ponto is the nurse coordinator for the Women's Cancer Program and routinely attends our scientific sessions, as does Ms. Lisa Copeland of MCCC Communications. The issues of gynecologic cancer patients are routinely addressed at our MCCC public education events which occur in the fall and spring each year.

Formalize a partnership with representatives of the advocacy community. In the past year, we have developed an even closer working relationship with the Minnesota Ovarian Cancer Alliance (MOCA). At the present time, 11 Mayo staff members serve on the MOCA Medical Advisory Board. Dr. Hartmann has been asked to serve on their grant review group. We are committed to incorporating direction and guidance from the patient advocacy community as we conduct our research and map out strategies for future studies. Recently, two of the members of our Program (David I Smith and Chaplain Mary E. Johnson) received grants from MOCA. Dr. Smith received support to further characterize the role of PARK2 in the development of ovarian cancer. Chaplain Johnson received support to study whether a patient's sense of well-being and religious convictions have any effect on her ultimate clinical outcome. Members of our Program continue to play an active role with MOCA. In addition, we have also named Deborah Collyar, a well known patient advocate, to our External Advisors Committee. Dr. Collyar will also assist us in our work preparing the Ovarian SPORE application.

Conclusions:

We have built upon our prior infrastructure in women's cancers within the MCCC to upgrade our database, mobilize needed resources to investigators in a timely manner, and provide a smooth organizational structure for the conduct of our ovarian cancer genetics research. We feel that our Program has matured greatly since receiving Department of Defense funding and that we are now in an excellent position to be competitive for Ovarian SPORE funding.

****

TISSUE ACQUISITION CORE FACILITY

The Tissue Acquisition Core provides a coordinated, centralized, and dedicated program for procurement and processing of biospecimens obtained from ovarian cancer patients and from populations of women at risk of developing ovarian cancer. Clinically annotated human biospecimens have historically been one of the most valuable and unique resources available for translational research at Mayo Clinic Rochester and the GOAL of the Core is to procure a tissue and/or a blood specimen from every ovarian cancer patient seen at Mayo Clinic. The Core will coordinate acquisition of both normal and neoplastic ovarian tissues, process blood samples, provide investigators with DNA and RNA, and will continue to bank biospecimens for future translational research. The Core will also serve as a resource of expertise, collaborative support, and service for pathology, immunohistochemistry, *in situ* hybridization, laser capture microdissection construction of tissue arrays, RT-PCR, and digital image analysis. The Core will interface and be electronically integrated with the Ovarian Cancer Patient Registry and the Biostatistics Core to provide investigators clinically annotated biospecimens. The collection, banking, and use of biospecimens will be performed with appropriate patient consent and institutional approval. The Core will interact and collaborate with other federally-funded Ovarian Cancer Programs to promote resource sharing and integrate scientific projects.

Dr. Gary Keeney has verified the initial tumor grade and morphology determinations of over 90% of all the epithelial cancers in our repository. His review has significantly decreased ambiguity about tumor morphologies and grades. This has allowed identification and exclusion of "ovarian tumors" deriving from a non-ovarian primary cancer.

Tumors that are to be used in assays are first sectioned and stained with hematoxylin and eosin. Dr. Wilma Lingle, Laboratory Medicine and Pathology and Head of the Tissue Acquisition and Processing Core Facility, looks at each slide and determines the percentage of the frozen section that is comprised of malignant cells. Only samples containing >70% tumor are used for analysis. This quality control measure is repeated each time a tumor is used, resulting in sequential analysis of tumor quality every 200-300 microns. Because of a consolidation of tumor acquisition and processing protocols within the last year, new tumors are screened prospectively for the percentage of the block comprised of malignant tissue. This has already made the determination of appropriate specimens for specific projects more efficient.

****

BIOLOGICAL FUNCTION CORE

The purpose of the Biological Function Core is to provide normal ovarian epithelial specimens for the studies outlined in Projects 1-3 and assess the functional consequences of the genetic alterations detected during completion of Projects 1-3. To perform this analysis, we proposed to: (1) generate new cell lines from primary ovarian cancers and normal ovarian epithelium; (2) transect these cell lines with appropriate plasmids to recapitulate the genetic alterations identified in Projects 1-3; (3) assess the effects of this transfection on proliferation rate, clonogenicity, and ability to form tumors in nude mice; (4) determine the effects of the transfected constructs on sensitivity of cell lines *in vitro* to agents commonly used to treat ovarian cancer; and (5) examine the effects of the genetic alterations on the therapeutic modalities when control or transfected cells are grown as xenografts in nude mice.

Hypothesis: The functional studies are being undertaken to determine whether the genetic alterations detected in ovarian cancer cells alter the proliferative rate, apoptotic threshold, and/or drug sensitivity of the tumor cells *in vitro* and *in vivo*.

Relevance to ovarian cancer: These activities are designed to: i) provide additional samples and models that can be used to study the biology of ovarian cancer vs. normal ovarian surface epithelium; ii) demonstrate how individual genetic alterations contribute to the cancer phenotype; and iii) potentially identify new gene products that can be investigated as possible therapeutic targets.

Core Facility Support Provided to Research Projects: As indicated below, the Biological Function Core has provided normal ovarian surface epithelial cells as normal controls in support of Projects 1-3. In addition, the Core has taken genes identified in Project 3 and demonstrated their effects on drug sensitivity. Finally, the Core has begun to develop cell lines and animal models required for assessment of additional genes that are in the process of being identified in Projects 1-3.

Results:

Task 1: Provision of normal ovarian surface epithelial cells for study controls. Uncultured brushings of normal ovaries (documented to contain sheets of normal ovarian surface epithelial cells) and cultures of ovarian surface epithelium have been provided to the Smith, Shridhar, and Couch laboratories to provide normal controls for Projects 1-3. In addition, normal ovarian surface epithelial cells bearing a temperature-sensitive SV40 large T antigen (described in the 2000 progress report) have been provided to the three labs to provide additional controls for experiments emanating from Projects 1-3.

Task 2: Optimization of current cell lines and development of new cell lines. As indicated below, many functional studies will involve expression of cDNA encoding a particular transcript into cells that have low levels or lack that transcript. To facilitate these studies, we optimized the transfection efficiency and geneticin-induced killing in each of six currently available low-passage ovarian cancer cell lines. We have also inserted a deoxycycline-sensitive transcriptional regulator into these six lines so that potentially toxic genes can be expressed in these cell lines in a conditional fashion. Because these genes might have different effects in a p53 wildtype background than a p53 mutant or p53 null background, over the past year we have also characterized the p53 status of all six of the cell lines. In an attempt to generate additional cell lines, ~30 fresh ovarian cancers were put into tissue culture under standard conditions (in addition to the 66 reported last year). Of these 30, two (one that turned out to be from a patient with a mixed Mullerian tumor and one from a patient with recurrent ovarian cancer) spontaneously gave rise to cell lines.

We have also explored an additional strategy for developing ovarian cancer cell lines. William Cliby, who is a member of the Biological Function Core, has injected approximately 10 fresh ovarian cancer samples directly into nu/nu mice. None of the subsequent growths were successfully passaged to additional mice. Two tumors retrieved and placed into tissue culture did not grow into cytokeratin-positive (i.e. epithelial) cultures. Discussions with laboratories successfully using other tumor model systems to generate xenografts have been helpful for identifying strategies that should improve these results.

Task 3: Assess the effect of genetic alterations on proliferation rate and cloning efficiency in vitro. In the 2000 progress report we described work on a gene call MC-J, which is silenced by methylation in ~70% of epithelial ovarian cancers. The work is now completed (Shridhar V. *et al.* Loss of expression of a new member of the DNAJ protein family confers resistance to chemotherapeutic agents used in the treatment of ovarian cancer. *Cancer Res.* 2001; 61:4258-65). The Biological Function Core has been assisting in the analysis of two additional genes, HTRA and PAPX, over the past year.

HTRA is a serine protease that contains an insulin-like growth factor binding domain at its amino terminus (Zumbrunn J, Trueb B. Primary structure of a putative serine protease specific for IGF-binding proteins. *FEBS Lett.* 1996; 398:187-192). Early studies demonstrated that HTRA expression in fibroblasts is suppressed by SV-40-transformation. Dr. Shridhar's work has resulted in the demonstration that HTRA mRNA is diminished in >50% of ovarian cancer specimens relative to normal ovarian surface epithelium. To assess the functional consequences of HTRA down-regulation, the OV167 ovarian cancer cell line (which lacks HTRA expression) was transfected with HTRA under the control of the constitutive cytomegalovirus promoter or with empty vector. The growth rates of parental cells, empty vector controls, and HTRA transfectants were comparable as were colony-forming efficiencies.

PAPX is an X-linked gene with no strong homology to any other gene in the database. Dr. Shridhar's data demonstrated that PAPX mRNA is diminished in all of the ovarian cancer cell lines tested and in >70% of ovarian cancer specimens relative to normal ovarian surface epithelium. The Biological Function Core has worked with Dr. Shridhar to try to create stable transfectants expressing PAPX cDNA behind the constitutive cytomegalovirus promoter. When stable transfectants were not obtained, transient transfection experiments were performed, which showed that all transfected successfully cells appeared to be undergoing apoptosis. Efforts are currently under way to develop cell lines expressing PAPX under the inducible control of the tetracycline-regulated tet-on system. This cell line will then be utilized to examine the role of PAPX in cell survival and proliferation. In the meantime, the Biological Function Core has also developed a polyclonal serum that recognizes the PAPX protein and has utilized this serum to confirm at the protein level that PAPX is downregulated in six different ovarian cancer cell lines relative to normal ovarian surface epithelium. This antiserum is being utilized to characterize the colonies resulting from PAPX transfection.

Task 4: Assess the effect of genetic alterations on sensitivity to various treatments in vitro. OV167 cells transfected with **HTRA** or empty vector were examined for sensitivity to cisplatin, paclitaxel, and topotecan *in vitro*. HTRA transfection slightly increased the sensitivity to topotecan and paclitaxel. Larger effects (a 3- to 5-fold change in IC_{90}) were observed with cisplatin. This enhanced sensitivity was also reflected in a more rapid induction of apoptosis after addition of cisplatin to the HTRA-transfected cells. Ongoing studies suggest that the alteration in cisplatin sensitivity does not reflect any change in cisplatin accumulation.

This same approach will be applied to the **PAPX** transfectants once they become available.

Task 5: Assess the effect of genetic alterations on tumorigenicity and drug sensitivity in vivo. All six of the low passage ovarian cancer cell lines were injected into the flanks of nu/nu mice. Interestingly, despite success with commercially available cell lines, none of the Mayo cell lines formed tumors when injected either subcutaneously or intraperitoneally. At present we are injecting minced fresh tumor specimens into nu/nu mice in an attempt to establish xenografts that can be utilized to a) serve as another potential source of cell lines (see Task 1) and b) further assess the effect of genes identified in Projects 1-3 on tumorigenicity and *in vivo* drug sensitivity.

Xenograft experiments using commercially available cell lines that have been engineered to overexpress a gene discovered to be downregulated in projects #1 and #3 are in progress.

****

MOLECULAR CYTOGENETICS CORE FACILITY

We are extremely fortunate to have an outstanding molecular cytogeneticist working with our ovarian Program. Dr. Robert Jenkins is responsible with starting our Ovarian Program (with Dr. Hartmann), and he has done much work over the years on the characterization of many of the ovarian tumor specimens already collected. We do not request any funding from the Department of Defense to support this Core as it is supported entirely by the Mayo Clinic Cancer Center. Nevertheless, the Core continues to provide support for routine cytogenetic and molecular cytogenetic services to members of the Ovarian Cancer Program. Investigators on the grant are welcome to use the course facilities and have ready access to Dr. Jenkins' expertise. The Core's help in providing comparative genomic hybridization to characterize 25 of our specimens was highlighted in Dr. Shridhar's August 2001 *Cancer Research* paper comparing the genomic differences between early and late stage ovarian cancer (see manuscripts published). This Core has provided excellent service to the Program Project as we have been able to use comparative genomic hybridization to characterize 25 of the ovarian tumor specimens. We will also be transcriptionally profiling the same ovarian tumors, and thus will have both expression and cytogenetic information on the same set of tumors.

Conclusions:
We feel that we have made excellent progress toward our stated goals in the last year of support for this Program Project. In the past we depended upon the expression profiles for ovarian tumors determined by our colleagues at Millennium Predictive Medicine. However, there are a number of problems with that collaboration and the resulting data. The major problem is that we are not free to share this data with other investigators, and we have severe limitations on publishing genes that Millennium is interested in pursuing. As a result in the past year, we initiated work in collaboration with the M.D. Anderson Ovarian SPORE headed by Dr. Robert Bast. Indeed, David I Smith actually has a subcontract on the M.D. Anderson SPORE Project #1 to work with the M.D. Anderson group. We utilized the Affymetrix U95 A-E set of gene expression chips to analyze the expression of 45 primary ovarian tumors (including 10 early stage tumors from the Mayo Clinic) as compared to pools of brushings of normal ovarian epithelium. Our plan is to also perform comparative genomic hybridization (in collaboration with Dr. Joe Gray at the University of California, San Francisco) on the same tumor samples so that we can directly compare mRNA expression and DNA copy number. This will facilitate a number of our studies including the work of Dr. Fergus Couch searching for new amplicons in ovarian cancer.

The support provided by the Department of Defense has really enabled the Ovarian Program of the Mayo Clinic Cancer Center to grow and develop. The competing renewal for the Mayo Clinic Cancer Center will be submitted in June 2003 and the Ovarian Program is going to be included as one of the translational programs in that renewal. In addition, the support has enabled us to build our Ovarian Cancer infrastructure so that we feel that we are well prepared for the February 1st Ovarian Cancer SPORE competition.

We are not proposing any major changes at the present time from our original proposal.

****

REPORTABLE OUTCOMES:

Manuscripts Published

- Shridhar V, Sen A, Chien J, Staub J, Avula R, Kovats S, Lee J, Lillie J, Smith DI. Identification of under-expressed genes in early and late stage primary ovarian tumors by suppression subtraction hybridization. *Cancer Res*, 2002; 62:262-270.
- Smith DI. Transcriptional profiling develops molecular signatures for ovarian tumors. Cytometry 2002: 47:60-62.
- Denison SR, Becker NA, Ferber MJ, Phillips LA, Kalli KR, Lee J, Lillie J, Smith DI, and Shridhar V. Transcriptional profiling reveals several common fragile site genes are down-regulated in ovarian cancer. *Genes Chromosom Cancer* 2002; 34:406-415.
- Morelli C, Karayiann E, Magnanini C, Mungall AJ, Thorland E, Negrini M, Smith DI, Barbanti-Brodano G. Cloning and characterization of the common fragile site FRA6F haboring a replicative senescence gene and frequently deleted in human tumors. *Oncogene* 2002; 21: 7266-7276.
- Becker NA, Thorland EC, Denison SR, Phillips LA, and Smith DI. Evidence that instability within the FRA3B regions extends for four megabases. *Oncogene* In Press, 2002.
- Callahan G, Denison SR, Phillips LA, Shridhar V, and Smith DI. Characterization of the common fragile site, FRA9E, and its potential role in ovarian cancer. *Oncogene*, 2003, In Press.

Manuscripts Submitted

- Chien J, Bible KC, Staub J, Lee YK, Hu S-I, Smith DI, Crowl RM, Kaufmann SH, Shridhar V. Down-regulation of the serine protease HtrA1 modulates oxidant- and cisplatin-induced cell death in ovarian cancer.
- Lai J, Chien J, Staub J, Avula R, Mathews T, Greene E, Smith DI, Kaufamnn SH, Roberts L, Shridhar V. Loss of hSulf, a novel sulfatase that modulates heparin binding growth factor signaling, in ovarian carcinoma.

Manuscript in Preparation

- Chien J, Staub J, Avula R, Smith DI, Kaufmann SH, Shridhar V. A down regulated pro-apoptotic transcriptional regulatory gene, PAPX, in ovarian cancer.
- Denison SR, Callahan G, Phillips LA, and Smith DI. Evidence for a role of a common fragile site (FRA6E) in autosomal recessive juvenile Parkinsonism and ovarian cancer. Submitted to *Oncogene* 10/28/02.

Abstracts:

- Shridhar V, Pandita A, Lee J, Iturria S, Staub J, Avula R, Sen A, Calhoun R, Couch F, James CD, Hartmann L, Lillie J, Smith DI. Comprehensive analysis of genetic alterations in ovarian cancer. Oncogenomics meeting in Tucson, Arizona, January 25-27, 2001.
- Becker N, Phillips LA, Smith DI. FRA3B is larger than published data and completely contains two genes. Amer. Assoc. for Cancer Research 42:A333, 2001.
- Callahan G, Denison S, Shridhar V, Smith DI. Cloning and characterization of FRA9E. Amer. Assoc. for Cancer Research 42:A338, 2001.
- Denison SR, Phillips LA, Shridhar V, Smith DI. FRA6E (6q26), a 1 MB gene-rich common fragile site. Amer. Assoc. for Cancer Research 42:A346, 2001.
- Avula R, Stuab U, Sen A, Lee J, Hartmann L, Lillie J, Smith DI, Shridhar V. Identification of differnetially expressed genes in early and late stage primary ovarian tumors by suppression subtraction hybridization. Amer. Assoc. for Cancer Research 42:A1729, 2001.
- Shridhar V, Pandita A, Lee J, Iturria S, Staub J, Avula R, Sen A, Calhoun E, Couch F, James CD, Hartmann L, Lillie J, Smith DI. Comprehensive analysis of genetic alterations in ovarian cancer. Amer. Assoc. for Cancer Research 42:A2307, 2001.

- Phillips LA, Becker N, Hartmann L, Smith DI. A relationship between common fragile site expression and nucleotide excision repair? Amer. Assoc. for Cancer Research 42:A4866, 2001.
- Aderca I, Montoya DP, Krummel KA, Nagorney DM, Smith DI, Roberts LR. The FRA16D common chromosomal fragile site co-localizes with a region of LOH on chromosome 16 in hepatocellular carcinoma. Digestive Diseases Week 2001.
- Becker N, Denison S, Callahan G, Thorland E, Ferber M, Phillips L, Smith DI. Expression of common fragile site genes in cancer-derived cell lines. Amer. Association for Cancer Research, 2002.
- Smith DI, Denison S, Callahan G, Ferber M, Becker N, Phillips L. Common fragile site regions may contain many important tumor suppressor genes. Cancer Genetics and Tumor Suppressor Cold Spring Harbor Meeting, 2002.
- Lai J-P, Staub J, Avula A, ChienJ, Smith DI, Roberts LR, Shridhar V. A novel sulfatase domain-containing gene hSULF promotes apoptosis in ovarian carcinoma. AACR Special Conference –Apoptosis and Cancer, Waikoloa, HI, Feb 13-17, 2002, A-81
- Lai J-P, Staub J, Avula A, Montoya D, Greene E, Smith DI, Shridhar V_2 Roberts LR. Proapaoptotic effects of a novel sulfatase domain contating protein, hSulf in hepatocellular carcinoma. AACR Special Conference –Apoptosis and Cancer, Waikoloa, HI, Feb 13-17, 2002, B-42
- Chien J, Staub J, Avula R, Kaufmann SH, Bible KC, Lee Y-K, Smith DI, Hu. S-I, Crowl RM, Shridhar V. Human HtrA identified as a differentially expressed gene product in ovarian cancer, is involved in stress response. AACR Special Conference –Apoptosis and Cancer, Waikoloa, HI, Feb 13-17, 2002, A-20
- Chien J, Staub J, Avula R, Hartmann LC, Smith DI, Kaufmann SH, Shridhar, V. A novel proapoptotic protein is down regulated by hypermethylation in ovarian cancer. AACR Special Conference –Apoptosis and Cancer, Waikoloa, HI, Feb 13-17, 2002, B-54.
- Lai J-P, Staub J, Avula A, ChienJ, Smith DI, Roberts LR, Shridhar, V. Characterization of a novel sulfatase domain-containing gene hsulf in ovarian carcinoma. AACR 92nd Annual Meeting, April5-9, 2002 (San Fransisco, CA)
- Lai J-P, Staub J, Avula A, Montoya D, Smith DI, Shridhar V, Roberts LR. A novel sulfatase domain-containing gene hSULF promotes apoptosis in hepatocellular carcinoma cells. AACR 92nd Annual Meeting, April5-9, 2002 (San Fransisco, CA).
- Smith DI, Denison SR, Becker NA, Ferber MJ, Callahan G, Phillips LA, Shridhar V. Genes in common fragile sites are frequently down-regulated and potential mutational targets in ovarian cancer. Oncogenomics 2002: Dissecting cancer through genome research. Dublin, Ireland May 1-5, 2002.
- D.I. Smith, V. Shridhar, L.Hartmann, J.Chien, J.Lillie. Development of a molecular signature for ovarian epithelial cancer. 10th International congress of Human Genetics, May15-19, 2001 (Vienna, Austria), C009
- Chien J., Staub J., Avula R., smith D.I., and Shridhar V. Aberrant expression of perlecan in ovarian cancer. AACR-91st Annual Meeting, March 24-28, 2001 (New Orleans, LA), 12:A1723.
- Avula, R., staub J., Sen A., Lee J., Hartmann L., Lillie J., Smith D.I., and Shridhar V. Identification of differentially expressed genes in early and late stage primary ovarian tumors by suppression subtraction hybridization. AACR-91st Annual Meeting, March 24-28, 2001 (New Orleans, LA), 12:A1729.
- Shridhar V., Pandita A., Lee J., Iturria S., staub J., Avula R., Sen A., Calhoun E., Couch F., James D., Hartmann L., Lillie J., and Smith D.I. Comprehensive analysis of genetic alterations in ovarian cancer. AACR-91st Annual Meeting, March 24-28, 2001 (New Orleans, LA), 16:A2307.

- Shridhar V, Pandita A, Lee J, Iturria S, Staub J, Avula R, Sen A, Calhoun E, Couch F, James D, Hartmann L, Lillie J, Smith DI. Comprehensive analysis of genetic alterations in ovarian cancer. Oncogenomics conference, January 25-27, 2001 (Tuscon, AR), A33.
- Shridhar V, Callahan G, Staub J, Avula R, Hartmann LC, and Smith DI. Identification of novel genes not expressed in primary ovarian tumors and cell lines. AACR-91st Annual Meeting, April 1-5, 2000 (San Farnsisco, CA), 41:A1983.
- Smith DI, Sen A, Avula R, Staub J, Lee J, Hartmann L, Lillie J, and Shridhar V. Identification of differentially expressed genes in early and late stage primary ovarian tumors by the construction of subtraction suppression hybridization cDNA libraries. Amer. J. Hum. Genet. 67:A505, 2000.

Dr. D.I. Smith Presentations

- Common fragile sites and Cancer- Presented to the Department of Microbiology and Molecular Genetics, SUNY Stonybrook, Nov. 19, 2001.
- Star Trek is here today: Implications of the Human Genome Project. Presented to the Mayo Foundation Nurses - April 15 and 22nd, 2002.
- Large common fragile site genes are mutational targets in ovarian cancer. Fox Chase Cancer Center, Philadelphia, PA, April 16, 2002.
- Large common fragile site genes are mutational targets in ovarian cancer. University of Michigan Cancer Center, Ann Arbor, MI, April 19, 2002.
- Implications of the Human Genome Project. Presented to the NCI-CPEN Workshop, June 14, 2002.
- Using expression profiling to study the biology of ovarian cancer. Presented at Shaw College of the Chinese University of Hong Kong. September 27, 2002.

[CANCER RESEARCH 62, 262–270, January 1, 2002]

Identification of Underexpressed Genes in Early- and Late-Stage Primary Ovarian Tumors by Suppression Subtraction Hybridization[1]

Viji Shridhar,[2] Ami Sen, Jeremy Chien, Julie Staub, Rajeswari Avula, Steve Kovats, John Lee, Jim Lillie, and David I. Smith

Department of Experimental Pathology, Division of Laboratory Medicine, Mayo Clinic, Rochester, Minnesota 55905 [V. S., J. C., J. S., R. A., D. I. S.]; Millennium Predictive Medicine, Cambridge, Massachusetts 02139 [A. S., S. K., J. Li.]; and Corning, Acton, Massachusetts 01720 [J. Le.]

ABSTRACT

To identify novel tumor suppressor genes involved in ovarian carcinogenesis, we generated four down-regulated suppression subtraction cDNA libraries from two early-stage (stage I/II) and two late-stage (stage III) primary ovarian tumors, each subtracted against cDNAs derived from normal ovarian epithelial cell brushings. Approximately 600–700 distinct clones were sequenced from each library. Comparison of down-regulated clones obtained from early- and late-stage tumors revealed genes that were unique to each library which suggested tumor-specific differences. We found 45 down-regulated genes that were common in all four libraries. We also identified several genes, the role of which in tumor development has yet to be elucidated, in addition to several under expressed genes, the potential role of which in carcinogenesis has been described previously (Bagnoli *et al.*, Oncogene, *19:* 4754–4763, 2000; Yu *et al.*, Proc. Natl. Acad. Sci. USA, *96:* 214–219, 1999; Mok *et al.*, Oncogene, *12:* 1895–1901, 1996). The differential expression of a subset of these genes was confirmed by semiquantitative reverse transcription-PCR using glyceraldehyde-3-phosphate dehydrogenase (GAPDH) as control in a panel of 15 stage I and 15 stage III tumors of mixed histological subtypes. Chromosomal sorting of library sequences revealed that several of the genes mapped to known regions of deletion in ovarian cancer. Loss of heterozygosity (LOH) analysis revealed multiple genomic regions with a high frequency of loss in both early- and late-stage tumors. To determine whether loss of expression of some of the genes corresponds to loss of an allele by LOH, we used a microsatellite marker for one of the novel genes on 8q and have shown that loss of expression of this novel gene correlates with loss of an allele by LOH. In conclusion, our analysis has identified down-regulated genes, which map to known as well as novel regions of deletions and may represent potential candidate tumor suppressor genes involved in ovarian cancer.

INTRODUCTION

Each year approximately 16,000 American women succumb to ovarian cancer, the deadliest of all gynecological malignancies (1). Because ovarian cancer is frequently asymptomatic in its early stages, 75% of patients have advanced-stage disease at the time of diagnosis. However, if the disease is caught in an early stage, the five-year survival rate jumps to 92%, whereas the anticipated 5-year survival for patients with advanced stage disease is less than 20%. If stage I disease is a precursor of late-stage ovarian cancer, as is the case with many other tumor types, identifying molecular alterations in early-stage tumors should provide insights into developing strategies for early detection.

There are several PCR-based approaches to analysis of gene expression changes including mRNA DD-PCR[3] (2, 3), RNA fingerprinting by arbitrary primed-PCR (4, 5), and RDA (6–8). In RDA, several rounds of subtractions are needed. In addition, RDA does not resolve the problem of the wide differences in abundance of individual RNA species. Whereas DD-PCR and arbitrary primed-PCR are potentially faster methods of identifying expression differences between two populations, both of these methods have high levels of false positives and are biased for high-copy-number mRNAs. SSH (9–11) has the distinct advantage over other PCR-based techniques in that SSH is used to selectively amplify target cDNA fragments (differentially expressed) while simultaneously suppressing nontarget DNA amplification and generating a library of differentially expressed sequences. The normalization step equalizes the abundant cDNAs within a target population, and the subtraction step excludes the common sequences between the driver and tester populations.

In this study, we report on down-regulated genes identified from two early- and two late-stage primary ovarian tumors subtracted against normal ovarian epithelial cell brushings. Collectively our studies demonstrate that (*a*) several genes, identified in the SSH libraries as down-regulated genes, map to known regions of deletions in ovarian cancer; and (*b*) LOH analysis revealed novel regions of deletions not previously identified in early-stage tumors.

MATERIALS AND METHODS

Tissue Processing. All of the specimens were snap-frozen in the surgical pathology unit at the Mayo Clinic. The tumor content of the specimens was assessed by H&E-stained sections. Only specimens with >75% tumor content were used for all of the experiments. Twenty normal ovarian epithelial cell brushings from patients without cancer were pooled, and the epithelial nature of these brushings was verified by cytokeratin staining. Only brushings that contained >90% epithelial cell content were used. A majority of patients providing normal ovaries were between 45 and 65 years old and were undergoing incidental oophorectomy at the time of pelvic surgery for other indications. All of the ovaries were examined pathologically and found to be benign. The histology, grade, and stage of each tumor used in SSH library construction, semiquantitative RT-PCR, and LOH studies are listed in Table 1. Tumors were staged according to the criteria proposed by International Federation of Gynecology and Obstetrics.

Cell Culture. Five of seven ovarian-carcinoma cell lines (OV 167, OV 177, OV 202, OV 207, and OV 266) were low-passage primary lines established at the Mayo Clinic (12); SKOV-3 was purchased from American Type Culture Collection (Manassas, VA); OVCAR 5 is a NIH human ovarian cancer cell line (13). All cells were grown according to the supplier's recommendations.

Suppression Subtraction Libraries. Four down-regulated libraries were generated from individual tumors. OV 338 (stage I endometrioid), OV 402 (stage II serous), and two stage III serous tumors (OV 4 and OV 13) were all subtracted against normal ovarian epithelial cell brushings.

Tester and Driver Preparations. Total cellular RNA from primary ovarian tumors (driver) and from 20 pooled normal ovarian epithelial cell brushings (tester) was prepared using Trizol reagent (Life Technologies, Inc., Rockville, MD) followed by purification by RNAeasy kit (Qiagen Inc, Valencia, CA). The integrity of the RNA was assessed by agarose gel electrophoresis. One μg

Received 6/26/01; accepted 11/01/01.

The costs of publication of this article were defrayed in part by the payment of page charges. This article must therefore be hereby marked *advertisement* in accordance with 18 U.S.C. Section 1734 solely to indicate this fact.

[1] Supported by Department of Defense Grant DAMD 17-99-1-9504 (to V. S. and D. I. S.) and by the Mayo Foundation.

[2] To whom requests for reprints should be addressed, at Division of Experimental Pathology, Mayo Clinic/Foundation, 200 First Street SW, Rochester, MN 55905. Phone: (507) 266-2775; Fax: (507) 266-5193; E-mail: shridv@exrch.mayo.edu.

[3] The abbreviations used are: DD-PCR, differential display-PCR; RDA, representational difference analysis; SSH, suppression subtraction hybridization; LOH, loss of heterozygosity; RT-PCR, reverse transcription-PCR; GAPDH, glyceraldehyde-3-phosphate dehydrogenase; HSD3B1, hydroxy-δ-5-steroid dehydrogenase 3β-steroid δ-isomerase 1; EGR1, early growth response 1; EST, expressed sequence tag; NP, nested primer; OSE, ovarian surface epithelial cells.

Table 1 *Tumor cohort*

Histology	Stage	Grade	LOH	Northern	RT-PCR	SSH
Cl Cell[a] OV 106	I	3	–	–	+	–
Cl Cell OV 267	I	3	+	–	+	–
Cl Cell OV 496	I	3	+	–	+	–
Endo OV 51	I	3	+	–	+	–
Endo OV 78	I	3	+	–	+	–
Endo OV 88	I	3	–	–	+	–
Endo OV 105	I	3	+	–	+	–
Endo OV 338	I	3	+	+	+	+
Endo OV 647	I	3	+	+	+	–
Endo OV 684	I	3	+	–	–	–
Serous OV 6	I	3	–	–	+	–
Serous OV 17	I	3	–	–	+	–
Serous OV 20	I	3	–	+	+	–
Serous OV 90	I	3	+	–	+	–
Serous OV 234	I	3	+	–	+	–
Serous OV 363	I	3	–	–	+	–
Serous OV 526	I	3	–	–	+	–
Cl Cell OV 102	II	3	+	–	+	–
Endo OV 296	II	3	+	–	+	–
Serous OV 149	II	3	+	+	+	–
Serous OV 354	II	3	+	–	+	–
Serous OV 401	II	3	–	–	+	–
Serous OV 402	II	3	+	–	+	+
Serous OV 414	II	3	+	–	+	–
Cl Cell OV 176	III	3	+	–	+	–
Cl Cell OV 453	III	3	+	–	–	–
Cl Cell OV 623	III	3	+	–	–	–
Endo OV 93	III	3	+	+	+	–
Endo OV 110	III	3	+	–	+	–
Endo OV 259	III	3	+	–	+	–
Serous OV 4	III	3	+	+	+	+
Serous OV 11	III	3	+		+	–
Serous OV 13	III	3	+	+	+	+
Serous OV 16	III	3	+	–	+	–
Serous OV 29	III	3	+	–	+	–
Serous OV 150	III	3	+	–	+	–
Serous OV 167	III	3	+	–	+	–
Serous OV 182	III	3	+	–	+	–
Serous OV 206	III	3	+	–	+	–
Serous OV 208	III	3	+	–	+	–
Serous OV 461	III	3	+	–	+	–
Serous OV 472	III	3	–	–	+	–
Serous OV 97	IV	3	+	–	+	–

[a] Cl Cell, clear cell; +, tumors in which the specific analysis was performed; Endo, endometrioid.

of total RNA was then used for first- and second-strand cDNA synthesis in a 10-μl reaction volume using Smart II oligonucleotides and cDNA synthesis (CDS) primer (Clontech, Palo Alto, CA) following the manufacturer's instructions. The concentration of reverse-transcribed cDNA was adjusted to 25 ng/μl. The resulting cDNAs were amplified, and the cycle number was optimized for each sample after amplification with PCR primer (5′-AAGCAGTGGTAACAACGCAGAGT-3′). For cycle optimization, aliquots of the PCR reactions were removed after 15, 18, 21, and 24 cycles of amplifications. The resulting products were resolved on a 1.5% agarose gel, and optimum cycle number was chosen after southern hybridization with GAPDH and transferrin receptor genes as probes. For most samples, the optimum cycle numbers were between 17 and 19 cycles of amplification. The reaction was scaled up to generate 3 μg of double stranded cDNAs. The resulting cDNA was precipitated, washed with 70% ethanol, dissolved in 40 μl of deionized water, and digested with *Rsa*I in a 50-μl reaction mixture containing 100 units of enzyme (Boeringher Mannheim, Indianopolis, IN) for 3 h. The blunt-ended cDNAs were then purified using PCR purification columns (Promega, Madison, WI). The driver cDNAs from primary tumors were adjusted to 300 ng/μl in a final 7-μl volume. Fifty ng of digested double-stranded tester (normal ovarian epithelial cell brushings) cDNA was ligated in two separate reactions with 2 μl of adapter 1 (10 μM) and adapter 2 (10 μM; provided in the kit), respectively, and 1.0 unit of T4 DNA ligase (Life Technologies, Inc.) in a 10-μl total volume with buffer supplied by the manufacturer. After ligation, 1 μl of 0.2 M EDTA was added and the samples were heated at 75°C for 5 min to inactivate the ligase and stored at −20°C.

Subtractive Hybridization. SSH was performed between tester and driver mRNA populations using the PCR-select cDNA subtraction kit (Clontech) according to the manufacturer's recommendations. Two μl of driver double-stranded cDNA (150–200 ng/μl) was added to each of two tubes containing one μl of adapter-1 and adapter-2 ligated tester cDNA (10 ng) with 1× hybridization buffer in a total volume of 4 μl. The solution was overlaid with 10 μl of mineral oil and the cDNAs were denatured (1.5 min, 98°C) and allowed to anneal for 8–9 h at 68°C. After the first hybridization, the two samples were combined and an additional heat-denatured driver (300 ng) in 1× hybridization buffer was added. The sample was allowed to hybridize for another 16 h at 68°C. The final hybridization reaction was diluted with 200 μl of dilution buffer provided by the manufacturer, heated at 68°C for 7 min, and stored at −20°C.

PCR Amplification. For each subtraction, two PCR amplifications were performed. The primary PCR reaction in 25 μl contained 1 μl of subtracted cDNA, 1 μl of PCR primer1 (10 μM, 5′-CTAATACGACTCACTATGGGC-3′), and 0.5 μl each of 50× Advantage cDNA polymerase mix (Clontech) and 10 mM dNTP mix. The cycling parameters were 75°C for 7 min, followed by 27 cycles at 94°C for 30 s, 68°C for 30 s, and 72°C for 2 min. The amplified products were diluted 10-fold with deionized water and 2 μl were used in the secondary PCR reactions with NP1 and NP2 primers (provided in the kit). The cycling conditions were the same as in the primary PCR amplification, except the reactions were in a 50-μl volume for 11 cycles only, with a final extension cycle for 7 min at 68°C. The subtraction efficiency was determined by both PCR and-Southern based methods as instructed by the manufacturer.

Cloning and Analysis of the Subtracted cDNAs. Products from the secondary PCRs were inserted into PCR2.1-TOPO TA cloning kit (Invitrogen, Carlsbad, CA) following manufacturer's instructions. Prior to ligation, the subtracted cDNA mix was incubated for 1 h at 72°C with dATP and AmpliTaq DNA polymerase (Perkin-Elmer Cetus, Foster City, CA) to ensure that most of the cDNA fragments contained "A" overhangs. Approximately 100 ng of PCR-amplified cDNA were ligated into 50 ng of vector without further purification. Two μl of ligated products (10 ng of vector and 50 ng of cDNAs ligated in 10-μl volume) were transformed into 40 μl of DH10B cells by electroporation (Bio-Rad, Hercules, CA). Routinely, 50- and 200-μl aliquots of the transformed cells (grown in 1 ml of medium) were plated onto 150-mm Luria-Bertani/agar plates containing 100 μg/ml of ampicillin, with 100 μM isopropyl-1-thio-β-D-galactopyranoside (IPTG) and 50 μg/ml 5-bromo-4-chloro-3-indolyl-β-D-galactopyranoside (X-Gal) to discriminate white from blue colonies. The transformation efficiency was 2–4 × 10^6 colonies/μg of DNA.

Hybridization and Screening for Differentially Expressed Transcripts. The differential hybridization was performed initially on 96 randomly picked clones to determine subtraction efficiency. The inserts in the plasmid were amplified using NP-1 and NP-2 primers provided in the kit. The PCR conditions were 94°C for 4 min followed by 30 cycles of 94°C for 30 s, 60°C for 30 s, and 72°C for 2 min, followed by a final extension at 72°C for 5 min. The products of the PCR reactions were resolved on a 2% agarose gel run in duplicate. After Southern blotting of the amplified inserts onto Hybond N membranes (Amersham, Piscataway, NJ). The membranes were stained with methylene blue in 0.2× SSC and visualized to ensure complete transfer of all of the products. The blots were then hybridized with *Rsa*I-digested cDNA probes (reverse Northern). Fifty ng of *Rsa*I-digested tester and driver cDNAs were labeled using random primer labeling kit (Stratagene, LA Jolla, CA) with 50 μCi of [^{33}P]dCTP following manufacturer's instructions. Equal counts (1–2 × 10^7 cpm/μl) of the cDNA probes from normal and tumor tissues were heat-denatured and used to probe duplicate blots. Hybridization was performed at stringent conditions in 0.5 M Na_2PO_4 (pH 7.2), 7% SDS at 65°C. The next day, the filters were washed twice in 2× SSC, 0.5% SDS at 68°C, then once in 0.1% SSC, 0.1% SDS at 68°C, and exposed to phosphorimager screens overnight. The signal intensity of each spot in the membranes was compared between tester and driver hybridized duplicates. cDNA fragments displaying differential expression levels of >1.8-fold or higher were selected to estimate the efficiency of the differential hybridization.

Approximately 600–700 unique clones from each of the four libraries were successfully sequenced with M13 forward primer using an ABI Prism dye terminator cycle sequencing in the sequencing core at Millennium Predictive Medicine, Cambridge, MA. Sequences were compared with the National Center for Biotechnology Information sequence database using the BLAST program.

Semiquantitative RT-PCR. Fifty to 100 ng of reverse-transcribed cDNAs were used in a multiplex reaction with a pair of gene-specific primers and GAPDH forward (5′-ACCACAGTCCATGCCATCAC-3′) and reverse prim-

ers (5′-TCCACCACCCTGTTGCTTGTA-3′), which yield a 450-bp product. The PCR reaction mixes contained 50 mM Tris-HCl (pH 8.3), 1.5 mM $MgCl_2$, 400 μM gene-specific primers, 50 μM each of the GAPDH primers, and 0.5 units of Taq polymerase (Promega, Madison, WI), in a 12.5-μl reaction volume. The conditions for amplification were as follows: 94°C for three min, then 29 cycles of 94°C for 30 s, 50–62°C for 30 s depending on the gene-specific primers being tested, and 72°C for 30 s in a Perkin-Elmer-Cetus 9600 Gene-Amp PCR system. The products of the reactions were resolved on a 1.6% agarose gel. Band intensities were quantified using the Gel Doc 1000 photo-documentation system (Bio-Rad, Hercules, CA) and its associated software.

The following gene-specific primers were used: for CTSK, (forward) F-GGA GAT ACT GGA CAAC CCA CTG and (reverse) R-CCA ACT CCC TTC CAA AGT GC; for PAI1, F-AAT CGC AAG GCA CCT CTG AG and R-GAT CTG GTT TAC CAT CTT TT; for cyclin D2, F-AGC TGC TGT GCC ACG AGG T and R-ACT GGC ATC CTC ACA GGT C; for FGF7, F-TAA TGC ACA AAT GGA TAC and R-ATT GCC ATA GGA AGA AAG; for EGR1, F-GAC ACC AGC TCT CCA GCC TGC and R-GGA AGG GCT TCT GGT CTG GGG; for SPARC, F-CCA CTG AGG GTT CCC AGC AC and R-GGA AAC ACG AAG GGG AGG GT; for decorin, F-CCT GGT TGT GAA AAT ACA TGA and R-TGA CAT TAA CAA GAT TTT GCC; for THBS2, F-TGG TCA CCA GGA CAA AGA CAC and R-ATC CTG CCA GCA AGC TGA CA; for ITM2A, F-CGC AGC CCG AAG ATT CAC TAT G and R-CTT ATT ACC AAG GAC ACT CTA TCT; for PEG3, F-CGG AGA ACT GTG AGA AGC TCG TC and R-GGT GGG GCT AGG CTA GAA GG.

Northern Blot Analysis. Fifteen μg of total RNA was fractionated on 1.2% formaldehyde agarose gels and blotted in 1× SPC buffer [10 mM sodium phosphate (pH 6.8), 1 mM CDTA (Sigma Chemical Co., St. Louis, MO)] onto Hybond N membranes (Amersham, Piscataway, NJ). The control small ribosomal protein S9, (*RPS9*) and gene-specific probes were labeled using the random primer labeling system (Life Technologies, Inc., Gaithersburg, MD) and purified using spin columns (TE-100) from Clontech. Filters were hybridized at 68°C with radioactive probes in a microhybridization incubator (Model 2000, Robbins Scientific, Sunnyvale, CA) for 1–3 h in Express hybridization solution (Clontech, Palo Alto, CA) and washed according to the supplier's guidelines. The primers, F-GCA ACA TGC CAG TGG CCC GG and R-ATC CTC CTC CTC GTC GTC TC for RPS9 yield a 586-bp cDNA fragment, and the conditions for amplification are similar to the semiquantitative RT-PCR conditions described above.

LOH Analysis. Fifteen early- and 18 late-stage tumors of differing histologies (Table 1) were analyzed. The 15 early-stage tumors included 3 clear-cell, and 6 each of endometrioid and serous tumors. The 18 late-stage tumors included 3 clear- cell, 4 endometrioid, and 12 serous tumors. The markers (Research Genetics, Huntsville, AL) used in this study are listed in Table 1 along with their chromosomal locations. Two new microsatellite markers, one near Methylation Controlled J protein on 13q14.1 (14) and another marker within BAC CIT-B-470f8 on 19q14.3 (AC006115) are: *MCJ*-NF-5′-GATTGACCACAGTCTTATCT-3′ and *MCJ*-18–5′-TAA-GAGGTCTACTCATTGCTCAC-3′, and 19-F-5′-GCACCTGGCCCA-ACTGTAAC-3′ and 19R-5′-CCAGCTGCTGGCTCACCTT-3′, respectively. The individual oligonucleotides were synthesized in the Mayo Molecular Technology Core at the Mayo Clinic, Rochester, MN. The PCR reaction mix contained: 50 ng of genomic DNA, 50 mM KCl, 10 mM Tris-HCl (pH 8.3), 1.5 mM $MgCl_2$, 200 μM concentration of each primer, 0.05 μl of [^{32}P]dCTP (10 μCi/μl), and 0.5 units of Taq polymerase (Promega, Madison, WI) in a 10-μl reaction volume. The conditions for amplification were: 94°C for two min, then 30 cycles of 94°C for 30 s, 52–57°C for 30 s, and 72°C for 30 s in a Perkin-Elmer-Cetus 9600 Gene-Amp PCR system in a 96-well plate. PCR products were denatured and run on 6% polyacrylamide sequencing gels containing 8 M urea. The gels were dried and autoradiographed for 16–24 h and scored for LOH. Multiple exposures were used before scoring for LOH. Allelic imbalance indicative of LOH was scored when there was more than 50% loss of intensity of one allele in the tumor sample with respect to the matched allele from normal tissue. The evaluation of the intensity of the signal between the different alleles was determined by visual examination by two independent viewers (V. S. and J. S.).

RESULTS

In an attempt to identify novel tumor suppressor genes in ovarian cancer, we generated down-regulated cDNA libraries from two early-stage (stages I and II; OV 338 and OV 402) and two late-stage (stage III; OV 4 and OV 13) tumors subtracted against normal ovarian epithelial cell brushings. The libraries were monitored at each stage of library construction to ensure that the clones generated from each of the four libraries truly reflected differentially expressed sequences. The subtraction efficiency was determined by both Southern- and PCR-based protocols. Fig. 1, *A* and *B* show the subtraction efficiency of libraries OV 402 (*panel 1*) and OV 4 (*panel 2*) by Southern- and PCR-based methods (Fig. 1*B*), respectively. We estimated a 60- to 70-fold enrichment of the differentially expressed genes in all four libraries. This was confirmed with the Southern-based analysis, in which we saw a complete subtraction of GAPDH in the subtracted cDNAs (Fig. 1*A*).

We evaluated the differential expression of genes in each of the libraries by hybridizing tester and driver cDNAs to randomly amplify 96 cloned inserts by colony PCR. PCR products were resolved in duplicate. Care was taken to ensure equal loading of the PCR products onto 2% agarose gels to allow direct comparison of hybridization signal intensities (Fig. 2*A*). After transfer of the PCR products onto nylon membranes, we performed reverse Northern analyses to identify differentially expressed transcripts. The cDNA probes used for hybridization were restricted with *Rsa*I to minimize background hybridization. Faint signals representing rare transcripts could easily be distinguished with this approach (Fig. 2*B*). After densitometric analysis of each of the corresponding bands hybridized with tester and driver cDNAs, the percentage of these clones that showed the expected differential hybridization was 70–80%.

We sequenced ~2000 randomly picked clones from each of the four libraries. After consolidating for clones that appeared more than once in the libraries, we estimated that there were ~600 distinct clones sequenced from each of the four libraries.

Analysis of SSH Library Genes. To discern the differences in gene expression in early- *versus* late-stage tumors, we compared the genes in each of the libraries to one another to verify how many of the

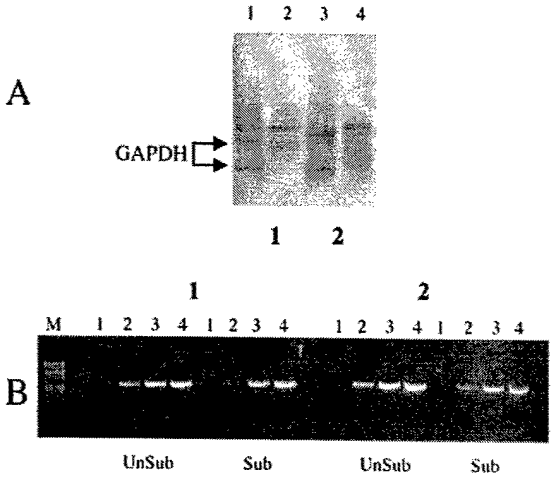

Fig. 1. *A*, Southern analysis: equal amounts of unsubtracted and subtracted cDNAs were fractionated on 2% agarose gel, blotted, and hybridized with [^{33}P]dCTP-labeled GAPDH. *Along bottom of image*: *1*, OV 402 library; *2*, OV 4 library. *Lanes 1* and *3*, unsubtracted cDNAs; *Lanes 2* and *4*, subtracted cDNAs. *B*, PCR-based analysis: 10 ng of unsubtracted (*Unsub*) and subtracted (*Sub*) cDNAs were amplified with GAPDH primers as described in "Materials and Methods." *Uppermost numbers*, *1*, OV 402 library; *2*, OV 4 library. *Lanes 1–4*, products after 18, 23, 28, and 32 cycles of GAPDH amplification; *M*, 100-bp ladder.

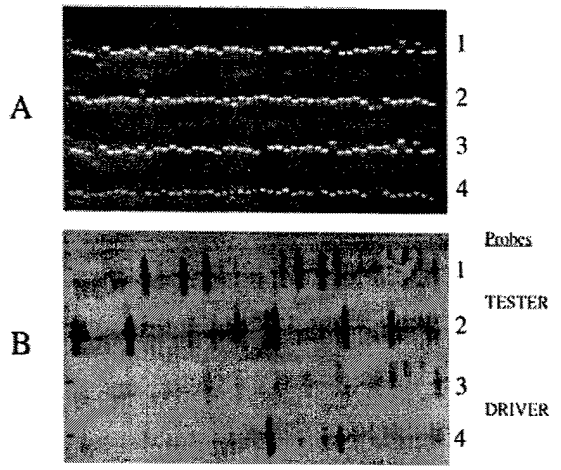

Fig. 2. *A*, products of colony PCR resolved on a 2% agarose gel. The gels were stained with ethidium bromide and photographed to ensure equal loading. Rows 1 and 3 and 2 and 4 are duplicates. *B*, duplicate filters hybridized with double-stranded P^{33}-tester (*rows 1* and *2*) and -driver (*rows 3* and *4*) cDNAs of equal specificity under the same conditions as described in "Materials and Methods."

differentially expressed genes were in common among these four libraries. Of the 600 or so distinct clones in each library, 45 genes were common to all four libraries (Table 2). These potentially represent genes that may consistently be down-regulated in both early- and late-stage ovarian tumors. Similar comparison of genes that were isolated from any three of four libraries revealed 80 common genes. There were 130 common genes in the two early-stage tumors. Sixty of these 130 genes were also present in one of the two late-stage tumors. A similar kind of analysis comparing sequences in the two late-stage libraries revealed that there were 210 genes that were common between them. Only 55 of 210 genes were also identified in either one of the two libraries generated from early-stage tumors.

Because we had randomly picked the clones for sequencing, we validated the differential expression of 20 genes ranging from clones that were highly represented to those that were infrequently occurring in the libraries to ensure that the sequences generated truly represented differentially expressed genes between normal and tumor cells. Initially, seven ovarian tumor cell lines were used for validation by semiquantitative RT-PCR with GAPDH as control. The expression profile of these genes in tumor cell lines was compared with short-term cultures of normal ovarian epithelial cells. Several of these genes showed complete loss of expression in a number of cell lines (Fig. 3*A*; Table 3). For example, *HSD3B1* (15), which was represented by only two clones in each of the four libraries, showed complete loss of expression in all of the seven tested cell lines (Table 4). However, *PAI1* (16), which appeared several times (100–140) in each of the two late-stage libraries, showed complete loss of expression in only two of seven cell lines. We also tested the differential expression of these genes in 20 early (I/II)-stage and 16 late (III/IV)-stage primary tumors of mixed histological subtypes by semiquantitative RT-PCR comparing them with normal epithelial cell brushings. The 20 early-stage tumors included 5 clear cell, 6 endometrioid, and 9 serous tumors. The late-stage tumors included 1 clear cell, 4 endometrioid, and 11 serous tumors (Table 1). Fig. 3*B* shows the results of this analysis for *PAI1* (16), *ITM2A* (17), *FGF7* (18), *PEG3* (19), and a novel gene on 8q.

In addition we tested the expression of *HSD3B1* and *PRSS11*, a serine protease with an insulin-like growth-factor-binding domain (20), in cell lines and primary tumors by Northern analysis (Fig. 4, *A* and *B*). *HSD3B1* showed complete loss of expression in all of the cell lines and the primary tumors. *PRSS11* showed complete loss of expression in four of seven cell lines in three of eight primary tumors. Lower levels of *PRSS11* expression was also detected in four of eight primary tumors. Control probe *RPS9* was hybridized to the cell line and primary tumor blots to indicate equal loading of RNA.

Chromosomal Sorting of SSH Genes. Genes from each of the four libraries were sorted based on their chromosomal positions. Several of the common genes identified in three or all four libraries mapped to known regions of deletions in ovarian cancer (21–24). For example, *ARHI* (*NOEY2*), a well-characterized imprinted tumor suppressor gene, with a reported LOH in 40–50% of ovarian cancer cases maps to 1p31 (25). In addition, *caveolin 1* (26), on 7q31.1–31.2, was identified in all four libraries that maps to a known region of deletion in ovarian cancer (27). Table 4 lists additional genes mapping to specific chromosomal regions of deletions in ovarian cancer. Of interest are chromosomal bands 5q31–32, 10q11, and 10q25.3–26.2, because several of the down-regulated genes, isolated from these bands, were common to three, or were in all four, of the libraries. The 5q31–32 genes are *catenin* (28), *FGF1* (29), *HDAC3* (30), *selenoprotein P, plasma1* (*SEPP1*; Ref. 31), testican (*SPOCK*; 32), *transcription elongation factor B* (*SIII*) *polypeptide-like* (*TCEB1L*; Ref. 33), *transforming growth factor*, β-induced, M_r 68,000 (*TGFβ1*); Ref. 34), *CDC23*, (35) *EGR1* (36), and *osteonectin* (*SPARC*; Ref. 37). Down-regulated genes from chromosomal band 10q11.2 and 10q25.3–26.2

Table 2 *Common down-regulated genes in all four libraries*
The unigene cluster identifications (IDs) and gene descriptions are included.

Cluster ID	Cluster title
Hs. 195851	Actin, α 2, smooth muscle
Hs. 180952	Actin, γ 1
Hs. 75442	Albumin
Hs. 4	Alcohol dehydrogenase 2, β polypeptide
Hs. 87268	Annexin, A8
Hs. 182183	Caldesmon
Hs. 83942	Cathepsin K
Hs. 74034	Caveolin 1
Hs. 169756	Complement component, 1 s subcomponent
Hs. 78065	Complement component 7
Hs. 76053	DEAD/H box polypeptide 5 (RNA helicase, M_r 68,000)
Hs. 76152	Decorin
Hs. 58419	DKFZP586L2024 protein
Hs. 181165	Eukaryotic translation elongation factor 1, α 1
Hs. 2186	Eukaryotic translation elongation factor 1, γ 1
Hs. 62954	Ferritin, heavy polypeptide 1
Hs. 89552	Glutathione *S*-transferase A2
Hs. 5662	G protein, β polypeptide 2-like 1
Hs. 83381	Guanine nucleotide binding protein 11
Hs. 3297	H. sapiens Uba80, mRNA for ubiquitin
Hs. 180532	Heat shock, M_r 90,000 protein 1, α
Hs. 158675	Heat shock factor binding protein 1
Hs. 155376	Hemoglobin, β
Hs. 75445	Hevin
Hs. 103391	IGFBP5
Hs. 38586	HSD3B1
Hs. 825	HSD3B2
Hs. 182187	IGF2
Hs. 107169	Insulin-like growth factor binding protein 5
Hs. 17109	Integral membrane protein 2A
Hs. 184914	KIAA0471-myosin heavy chain
Hs. 181357	Laminin receptor 1 (M_r 67,000, ribosomal protein SA)
Hs. 173714	MORF-related gene X
Hs. 153837	Myeloid cell nuclear differentiation antigen
Hs. 1255	Nuclear receptor subfamily 2, group F, member 2
Hs. 74615	PDGF, α polypeptide
Hs. 75111	PRSS11
Hs. 194695	Ras homolog gene family, member 1 (NOEY2)
Hs. 184108	Ribosomal protein L21
Hs. 180946	Ribosomal protein L5
Hs. 217493	Ribosomal protein S6
Hs. 151604	Ribosomal protein S8
Hs. 82448	Selectin L
Hs. 3314	Selenoprotein P, plasma, 1-histidine rich
Hs. 56306	Small proline-rich protein A
Hs. 46158	ESTs
Hs. 182643	Transcription factor B (SIII), polypeptide 1-like
Hs. 2064	Vimentin

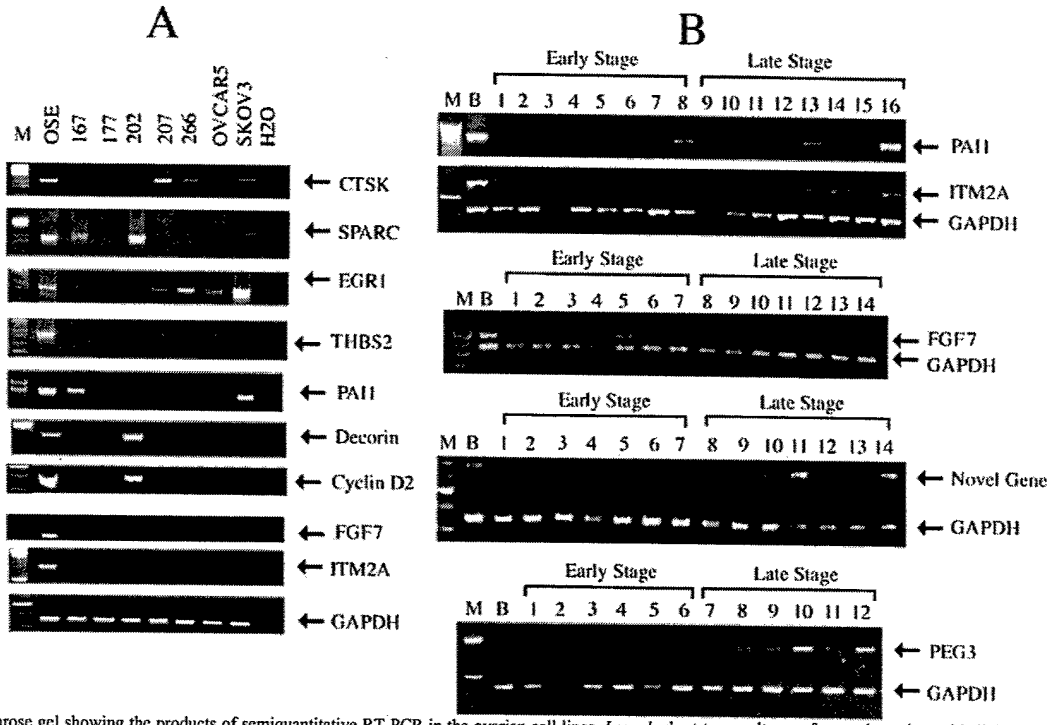

Fig. 3. *A*, agarose gel showing the products of semiquantitative RT-PCR in the ovarian cell lines. *Lane 1*, short-term cultures of normal ovarian epithelial cells (OSE 54); *Lane 2*, OV 167; *Lane 3*, OV 177; *Lane 4*, OV 202; *Lane 5*, OV 207; *Lane 6*, OV 266; *Lane 7*, OVCAR 5; *Lane 8*, SKOV 3; *Lane 9*, water control. Probes: *CTSK*, cathepsin K; *SPARC*; *EGR1*; *THBS2*, thrombospondin 2; *PAI1*, plasminogen activator inhibitor 1; *decorin*; *cyclin D2*; *FGF7*, fibroblast growth factor 7; *ITM2A*, integral membrane protein 2A; and *GAPDH*. *B*, agarose gel showing the products of the result of semiquantitative RT-PCR resolved on a 1.6% agarose gel. *Along top of the figure*, tumor sample numbers; *above top of the tumor numbers*, the staging information for these tumors. *Lane M*, 100-bp ladder; *Lane B*, normal epithelial cell brushings. *Panel 1*, *PAI1*, plasminogen activator inhibitor 1; *Panel 2*, *ITM2A*, integral membrane protein 2A; *Panel 3*, *FGF 7*, fibroblast growth factor 7; *Panel 4*, A novel gene; *Panel 5*, PEG3 and GAPDH .

that were identified from all four libraries were *annexin A8* (*ANXA8*; Ref. 38) and *PRSS11* (39), respectively. Other genes such as *nuclear receptor coactivator 4* (*ELE1*, 10q11.2; Ref. 40), *proteoglycan, secretory granule* (*PRG1*, 10q22.1; Ref. 41), *vinculin* (*VCL*, 10q22.1–23; Ref. 42), *lipase A* (*LIPA*, 10q23.3; Ref. 43), and *protein phosphatase regulatory (inhibitor) subunit 5* (*PPP1R5*, 10q23–24; Ref. 44) were identified only from the two late-stage libraries, OV 4 and OV 13.

LOH Analysis of Chromosomal Regions 1p, 6q, 7q, 8p, 9p, 10q, 13q, 17p, and 19q in Stage I/II and Stage III/IV tumors. Because many of the genes identified from the SSH libraries mapped to known regions of deletions in ovarian cancer, we analyzed a set of early- and late-stage tumors for LOH in regions of the genome to which some of the down-regulated genes mapped. The chromosomal locations of the markers and the potential down-regulated genes (identified in the SSH libraries) mapping to these regions are listed in Table 5. Fig. 5 shows the overall LOH profile obtained. Down-regulated genes mapping to chromosomal regions of loss identified from the libraries are *HSD3B1*, *EGR1*, *serum glucocorticoid kinase* (*SGK*; Ref. 45), and *forkhead* (*Drosophila*) *homologue 1* (*rhabdomyosarcoma*; *FRKH*; Ref. 46) mapping to 1p12–13, 5q31.1–31.2, 6q23.3, and 13q14.1, respectively. The approximate positions of these genes in relation to the markers of their respective chromosomes are also shown (Fig. 5). The chromosome 1p11–13 and 6q 23.3 markers showed a higher frequency of loss in late stage-tumors compared with early-stage tumors. Other markers on chromosomes 8, 9, and 10 also showed more losses in high-stage tumors. However, two markers on 5q31 and 13q14.1 and a marker within the BAC CIT-B-470f8 100-kb distal to the *PEG3* locus on 19q13.4 had a higher frequency of LOH in early- compared with late-stage tumors. Markers *D1S440, D1S534*, *D6S377*, and *D19S572* showed no LOH in early-stage tumors. To test whether loss, and/or lower levels, of expression of a gene corresponded to a region of loss, we used a microsatellite repeat present within intron 2 of a novel gene on 8q that was identified in this study to determine the frequency of LOH in these tumors. This marker showed 50% loss both in low- and high-stage tumors (Table 5; Fig. 5). Fig. 6 shows the pattern of LOH of this marker in ovarian tumors with the loss of expression of this gene. For example, as shown in Fig. 6, there was a direct correlation between lower levels of expression of this gene and loss of an allele by LOH (tumor numbers 684 and 208). In tumor with complete loss of expression and deletion of one of the alleles by LOH (tumor number 182), the remaining allele could be inactivated either by hypermethylation or by transcriptional inactivation as a result of other mechanisms. Tumors without LOH (tumors numbers 13 and 234) showed no loss of expression, as evidenced by semiquantitative RT-PCR.

Thus our LOH analysis revealed known and novel regions of loss to which down-regulated genes identified from the SSH libraries map, lending support to the strength of the SSH technique to identify genes with low levels of expression in tumors. Some of these genes could potentially represent candidate tumor suppressor genes involved in ovarian carcinogenesis.

DISCUSSION

This is the first report of down-regulated genes in SSH libraries generated from primary ovarian tumors. The concept of identifying differentially expressed genes has been used before in techniques such as DD-PCR and RDA. The strength of the SSH library is in the technique's ability to identify low-abundance transcripts. Although some of the genes identified from these libraries were also identified as down-regulated genes by transcriptional profiling of the same

Table 3 *Chromosomal localization of down-regulated genes from SSH libraries*

Chromosome	Down-regulated genes
1p12-13	*Hydroxy-δ-5-steroid dehydrogenase, 3 β- and steroid δ-isomerase 2*
1p12-13	Hydroxy-δ-5-steroid dehydrogenase, 3 β- and steroid δ-isomerase 1
1p31	Ras homolog gene family, member I
1q21	Cathepsin K (pycnodysostosis)
1q21-q22	Small proline-rich protein 2A
2q33-36	Insulin-like growth factor binding protein 5
2q33	Aldehyde oxidase 1
3p21.3	Ras homolog gene family, member A
4q12	Insulin-like growth factor binding protein 7
4q21.2	Alcohol dehydrogenase 2 (class I), β polypeptide
5q31	Selenoprotein P, plasma, 1
5q31	Early growth response 1
5q31	Secreted protein, acidic, cysteine-rich (osteonectin)
6p12.2	Glutathione S-transferase A2
6q23.3	Serum/glucocorticoid regulated kinase
6q27	Thrombospondin 2
7p15-13	Inhibin, β A (activin A, activin AB α polypeptide)
7q21.3-22	Plasminogen activator inhibitor, type I
7q31.1-31.2	Caveolin 1, caveolae protein, M_r 22,000
8p22-p21.3	Platelet-derived growth factor receptor-like
8q21	Novel gene
9p21	Ribosomal protein S6
9q11-q22	Annexin A1
10q24.3	Cytochrome P450, subfamily XVII (steroid 17-α-hydroxylase)
10q25.3-q26.2	Protease, serine, 11 (IGF binding)
11p15.5	Hemoglobin, β
11p15.5	Insulin-like growth factor 2 (somatomedin A)
12p13	Cyclin D2
12q23	Decorin
13q14.1	Forkhead (Drosophila) homolog 1 (rhabdomyosarcoma)
13q14.3	Integral membrane protein 2B
14q32.1	Protease inhibitor 1 (anti-elastase), α-1-antitrypsin
14q22-q24	Butyrate response factor 1 (EGF-response factor 1)
15q15-q21.1	Fibroblast growth factor 7 (keratinocyte growth factor)
15q15	Thrombospondin 1
16q13-q21	Matrix metalloproteinase 2 (gelatinase A, M_r 72,000)
16q24.2-q24.3	Cadherin 13, H-cadherin (heart)
17	ESTs
19q13.4	Paternally expressed gene 3
22q12.3	Tissue inhibitor of metalloproteinase 3
Xq13.3-Xq21.2	Integral membrane protein 2A
Xq21.1	ESTs

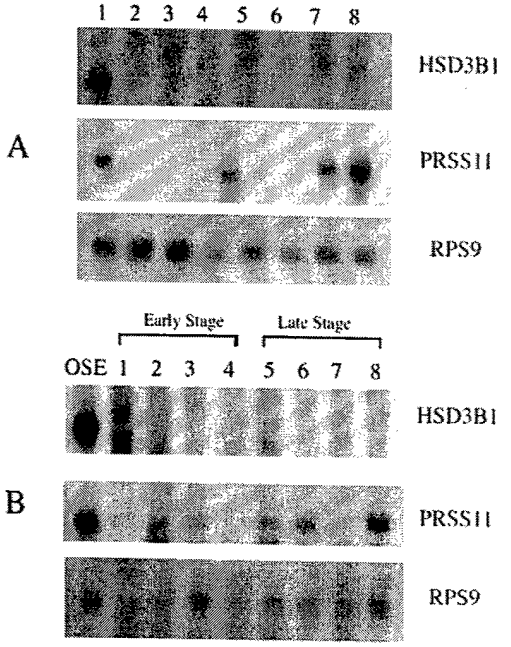

Fig. 4. Autoradiograph showing the Northern hybridization results with probes *HSD3B1* and *PRSS11*. *RPS9*, ribosomal protein S9. *A*, *cell lines*: OSE; *Lane 1*, OV167; *Lane 2*, OV 177; *Lane 3*, OV 202; *Lane 4*, OV 207; *Lane 5*, OV 266; *Lane 6*, OVCAR 5; *Lane 7*, SKOV3. *B*, primary tumors: *Lanes 1–4*, early-stage tumors; *Lanes 5–8*, late-stage tumors. The staging information for the primary tumors is listed in Table 1.

tumors (47), we identified several known and unknown genes of very low abundance only in the SSH libraries.

Analysis of the differentially expressed sequences from early and late tumors allowed us to compare the library sequences to one another. In the four SSH libraries, we identified several genes the function of which in carcinogenesis is known and others with no known roles in cancer. Some of the common genes, such as *tissue plasminogen activator inhibitor 1*, *SPARC*, *caveolin1*, and *NOEY2* have been demonstrated by others (16, 25, 26) to be differentially regulated in tumors. The potential tumor-associated function of genes such as *aldehyde oxidase*, *HSD3B1* and 2, *ITM2A*, *alcohol dehydrogenase 2* (48), *PRSS11*, and *PEG3* have not previously been linked with ovarian cancer. In addition, the function of several novel ESTs and genes identified from these libraries remain to be determined.

Table 4 *Results of semiquantitative RT-PCR analysis of down-regulated genes in ovarian cancer cell lines*

Genes	OSE	OV 167	OV 177	OV 202	OV 207	OV 266	OVCAR 5	SKOV 3	Chromosomal location
HSD3B1	+	–	–	–	–	–	–	–	1p13
CTSK	++	weak	–	–	–	–	–	–	1q21
IGFBP5	+	–	–	+	–	–	ND	ND	2q33-36
Hevin	+	–	–	–	–	–	–	–	4
SEPP1	+	+	+	–	–	+	+	+	5q31
TCEB1L	+	–	+	+	+	+	+	+	5q31
EGR1	+	weak	–	–	weak	+	weak	++	5q31
SPARC	+	–	–	weak	–	–	–	–	5q31
FGF1	+	–	–	–	+	–	–	+	5q31
Testican	+	–	+	+	+	–	+	–	5q31
THBS2	++	weak	–	–	–	–	–	–	6q27
PAI1	++	+	–	–	weak	weak	weak	+	7q21
Novel gene	+	+	–	+	–	–	–	–	8q21
PRSS11	++	–	–	+	–	–	+	+	10q25
Cyclin D2	+	–	–	+	–	–	–	–	12p13
Decorin	++	–	–	++	–	–	–	–	12q21.3
FGF7	+	–	–	+	–	–	–	–	15q15-21.1
PEG3	+		++	++	–	–	–	–	19q13.4
ITM2A	++	–	–	–	+	–	–	–	Xq13.3-21.1
Novel gene	+	–	–	–	–	–	–	–	Xq22

[a] +, presence of a product; –, Absence of a product; weak, presence of a weak product; ND, not determined.

Table 5 *Markers used for LOH analysis and % LOH in early- and late-stage tumors*

The numbers in parentheses are the number of tumors with LOH/total number of informative tumors.

Markers	% LOH in early-stage tumors	% LOH in late-stage tumors	Cytogenetic band location	Down-regulated genes from SSH libraries
D1S189	27 (4/15)	26 (5/17)	1p13.1	
D1S440	0 (0/13)	19 (3/16)	1p12	
D1S453	14 (2/14)	29 (5/17)	1p12	
D1S2863	27 (3/11)	29 (5/17)	1p12	*HSD3B1*
D1S534	0 (0/10)	22 (4/18)	1p11.2	
D1S514	14 (2/14)	33 (6/18)	1p11.2	
D5S396	50 (6/12)	50 (8/16)	5q31.1	*EGR1, SPARC*
D5S500	50 (5/10)	38 (5/13)	5q31.2	
D5S476	28 (2/7)	50 (6/12)	5q31.2	
D5S2119	30 (3/10)	25 (2/8)	5q31.2	
D6S311	0 (0/8)	54 (6/11)	6q23.1	*SGK*
D6S977	18 (2/11)	46 (6/13)	6q23.3	
D6S1008	10 (1/10)	37.5 (6/16)	6q25	
D7S1805	25 (2/8)	64 (7/11)	7q36	
D8S258	18 (2/11)	37.5 (6/16)	8p21	*PDGFRL 8q Novel Gene*
8q NG	50 (6/12)	50 (4/8)	8q	
D9S259	36 (5/14)	44 (8/18)	9p21	
D10S215	9 (1/11)	20 (3/15)	10q23.1	*LIPA, Actin α 2 smooth muscle (ACTA2)*
D10S574	21 (3/15)	17 (3/18)	10q23.3	
D17S1868	50 (4/8)	23 (3/13)	17q21.1	
D13S263	67 (6/9)	50 (9/18)	13q14.1	
MCJ[a]	62 (5/8)	46 (8/15)	13q14.1	*FKHR*
D19S180	17 (2/12)	28 (5/18)	19q13.3	
D19S572	0 (0/15)	14 (2/17)	19q13.3	
PEG3[a]	33 (4/12)	19 (3/16)	19q13.4	*PEG3*
D19S254	42 (5/12)	53 (9/17)	19q13.4	
D19S926	23 (3/13)	50 (8/16)	19q13.4	

[a] Primers are listed in the "Materials and Methods" section.

Some of these same genes have been identified as down-regulated genes by other techniques such as cDNA microarray analysis (47, 49) and DD-PCR (25).

It is a well-accepted concept that functional inactivation of both the alleles is a prerequisite for a tumor suppressor gene to be defined as such. The loss of expression of a gene could be caused by the deletion of both alleles (homozygous deletions), or deletion of one of the alleles and inactivation of the other allele either by inactivating mutations or by hypermethylation (50, 51) and/or by altered activity of a transcriptional repressor (52).

However, chromosomal sorting of ~600 genes and ESTs from each of the libraries revealed some interesting trends. Many of the genes identified from the SSH libraries were already mapped to known regions of deletions in ovarian cancer (21–24, 53, 54). We wanted to determine whether some of the known and novel genes identified from this screen would also map to regions of loss in ovarian cancer.

As evidenced in the LOH analysis, several of these coincided with regions of deletions observed in ovarian cancer. We identified several genes mapping to 5q31–32 in the SSH libraries. Of interest is *EGR1*, which has recently been identified as a down-regulated gene in ovarian cancer by cDNA microarray analysis (49). Two markers in the region, *D5S396* and *D5S500*, showed a high frequency of LOH in early-stage tumors not previously seen. *SPARC*, an acidic, cysteine-rich component of the extracellular matrix, is directly regulated by progesterone and dexamethasone and indirectly by cytokines (55). Mok *et al.* transfected the full length *SPARC* into SKOV3 cells and

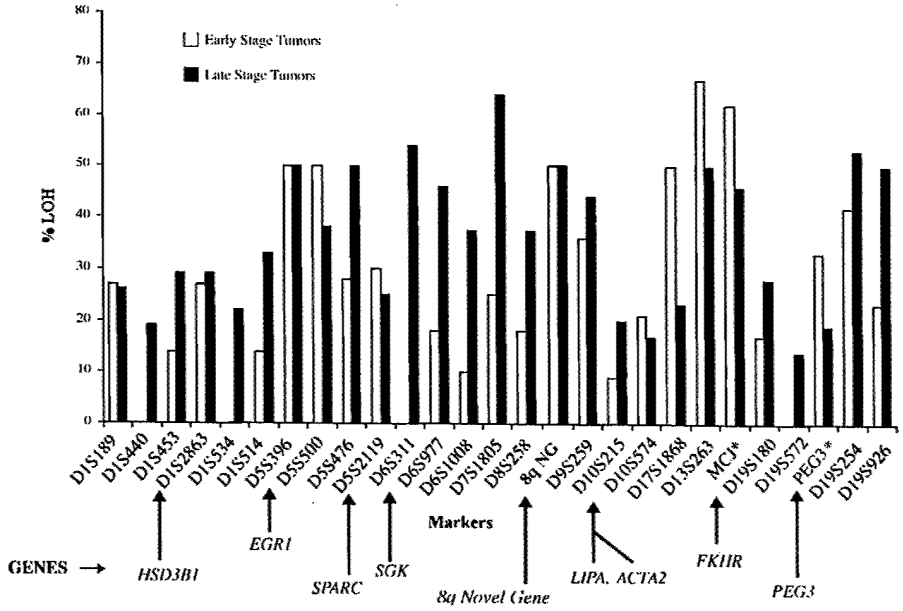

Fig. 5. Histogram of the results of LOH with the markers tested. □, early stage; ■, late stage. *% LOH* (on Y axis), frequency of LOH with specific markers. *Arrows*, approximate positions of these genes in relation to the markers on their respective chromosomes.

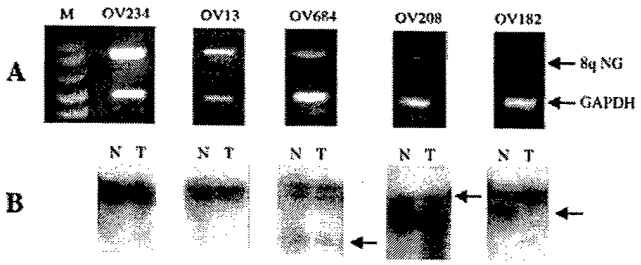

Fig. 6. *On top of the figure* for both *A* and *B*, tumor sample numbers. *A*, agarose gel showing the products of semiquantitative RT-PCR resolved on a 1.6% agarose gel. *M*, 1-kb-plus ladder; the top band is the product of amplification with novel gene (*8q NG*) primers. Bottom band is the product of amplification with GAPDH primers F (forward) and R (reverse). *B*, autoradiograph of LOH results of corresponding tumor samples with intron 2-associated microsatellite marker. *N*, normal DNA; *T*, tumor DNA; *arrow*, loss of the allele in the tumor.

showed both a reduced growth rate in cells expressing SPARC and a reduced ability of these cells to form tumors in nude mice, which lent support to *SPARC* as a tumor suppressor. *SPARC* was identified as a down-regulated gene in all four libraries from 5q31. Serum glucocorticoid kinase on 6q23.3, another region of deletion (23), was recently shown by Brunet *et al.* (56) to act in concert with Akt in phosphorylating forkhead transcription factor, *FKHRL1*. This phosphorylation event leads to the activation of the phosphatidylinositol 3-kinase cascade. Bagnoli *et al.* (52) have shown a reciprocal negative regulation of α folate receptor (αFR) and caveolin 1 (Cav-1, on 7q31.1) proteins providing evidence for a new mechanism of *Cav-1* silencing in ovarian cancer. As indicated above, comparison of some of the down-regulated genes identified from the libraries corresponded with chromosomal regions of loss identified from the LOH studies. A marker 100 kb distal to paternally expressed gene 3 on 19q13.4 that was identified in all four libraries showed a higher frequency of deletion in low-stage compared with high-stage tumors. This is the first report of such a high frequency of deletion (33%) in early-stage tumors in this region. Combining genomic with expression-based analysis, we were able to identify novel regions of loss in ovarian cancer. We have identified several known and novel genes, including ESTs, whose functions in cancer have yet to be discerned. These genes could potentially lead to the identification of candidate tumor suppressor genes involved in ovarian cancer.

However, not all of the down-regulated genes in these libraries could potentially represent tumor suppressor genes. This is essentially true for ribosomal genes. Other investigators also have reported the loss of expression of several ribosomal genes (Cancer Genome Anatomy Project-Digital Differential Display) in cancer and yet the functional consequence of loss of expression of these genes have not been directly linked to tumor suppression. Although some of the genes such as *ARHI, caveolin 1*, and *SPARC* that map to regions of deletions in ovarian cancer have known tumor-suppressing functions, for other genes, neither the mechanistic basis for the loss nor the functional consequence of such a loss is known. One of the novel genes identified in this screen showed 50% LOH in both early- and late-stage tumors. Using a microsatellite marker associated with this gene, we were able to correlate the loss and/or lower levels of expression of this gene with the loss of an allele by LOH.

The data from the SSH library analysis revealed that there were many genes that were differentially expressed in both early- and late-stage tumors. Genes identified in only one library could potentially indicate tumor-specific differences. We do not yet know what changes are critical in an early-stage tumor to progress to a more malignant tumor. The genes identified from the SSH libraries are all based on expression differences. This technique cannot detect gross genomic changes, including chromosomal rearrangements or the mutator phenotype (57), unless they result in concomitant changes in transcript levels of genes. However, one very important epigenetic phenomenon, namely, methylation (58, 59), has been associated with changes in the levels of gene expression. Evidence seems to indicate that methylation changes are early events in carcinogenesis leading to the possibility that the majority of the genes inactivated in early-stage tumors could be hypermethylated. Some of the genes isolated in this screen have been reported by others to be inactivated by hypermethylation in ovarian cancer (60, 61). For example, two of the down-regulated genes identified from chromosomal band 12p13 from the library sequences such as cyclin D2 (62) and complement component 1 subcomponent (63) do not map to known regions of deletion in ovarian cancer. These genes could be inactivated by methylation. The inactivation of cyclin D2 by methylation in Burkitt's lymphoma (62) and breast cancer (64) has previously been reported. Transcriptional inactivation can also result because of aberrant regulation of factors.

In conclusion, we have identified several known and several novel genes that are down-regulated both in early- and in late-stage tumors. Several of these genes were later mapped to the regions of loss by LOH analysis. However, we do not rule out the possibility that loss of expression of some of these genes could also be attributable to decreased transcriptional inactivation or through promoter hypermethylation. Thus, combining expression- and genomic-based analyses has provided us with novel regions of alterations in ovarian cancer not previously reported. We are currently pursuing the cloning and characterization of some of the novel genes identified from these libraries to address the functional roles of these genes in ovarian cancer.

ACKNOWLEDGMENTS

We acknowledge Dr. Kimberly Kalli, Mayo Clinic, Rochester, MN, for providing the cells from the short-term cultures of OSEs.

REFERENCES

1. Landis, S. H., Murray, T., Bolden, S., and Wingo, P. A. Cancer statistics, 1999. CA Cancer J. Clin., *49:* 8–31, 1999.
2. Liang, P., and Pardee, A. B. Differential display of eukaryotic messenger RNA by means of the polymerase chain reaction. Science (Wash. DC), *257:* 967–971, 1992.
3. Liang, X., Zhuang, G., and Fang, Q. The secretion and receptor gene of insulin-like growth factor-I quantitative expression in ovarian stroma in polycystic ovarian syndrome patients. Chung Hua Fu Chan Ko Tsa Chih, *32:* 582–585, 1997.
4. Rothschild, C. B., Brewer, C. S., and Offden, D. W. DD/AP-PCR: combination of differential display and arbitrarily primed PCR of oligo(dT) cDNA. Anal. Biochem., *245:* 48–54, 1997.
5. Peinado, M. A., Malkhosyan, S., Velazquez, A., and Perucho, M. Isolation and characterization of allelic losses and gains in colorectal tumors by arbitrarily primed polymerase chain reaction. Proc. Natl. Acad. Sci. USA, *89:* 10065–10069, 1992.
6. Lin, H., Pizer, E. S., and Morin, P. J. A frequent deletion polymorphism on chromosome 22q13 identified by representational difference analysis of ovarian cancer. Genomics, *69:* 391–394, 2000.
7. Yuan, L., Shan, J., De Risi, D., Broome, J., Lovecchio, J., Gal, D., Vinciguerra, V., and Xu, H. P. Isolation of a novel gene, *TSP50*, by a hypomethylated DNA fragment in human breast cancer. Cancer Res., *59:* 3215–3221, 1999.
8. Watson, J. E., Gabra, H., Taylor, K. J., Rabiasz, G. J., Morrison, H., Perry, P., Smyth, J. F., and Porteous, D. J. Identification and characterization of a homozygous deletion found in ovarian ascites by representational difference analysis. Genome Res., *9:* 226–233, 1999.
9. Ye, Z., and Connor, J. R. Identification of iron responsive genes by screening cDNA libraries from suppression subtractive hybridization with antisense probes from three iron conditions. Nucleic Acids Res., *28:* 1802–1807, 2000.
10. Diatchenko, L., Lau, Y. F., Campbell, A. P., Chenchik, A., Moqadam, F., Huang, B., Lukyanov, S., Lukyanov, K., Gurskaya, N., Sverdlov, E. D., and Siebert, P. D. Suppression subtractive hybridization: a method for generating differentially regulated or tissue-specific cDNA probes and libraries. Proc. Natl. Acad. Sci. USA, *93:* 6025–6030, 1996.
11. Diatchenko, L., Lukyanov, S., Lau, Y. F., and Siebert, P. D. Suppression subtractive hybridization: a versatile method for identifying differentially expressed genes. Methods Enzymol., *303:* 349–380, 1999.
12. Conover, C. A., Hartmann, L. C., Bradley, S., Stalboerger, P., Klee, G. G., Kalli, K. R., and Jenkins, R. B. Biological characterization of human epithelial ovarian

carcinoma cells in primary culture: the insulin-like growth factor system. Exp. Cell Res., *238:* 439–449, 1998.
13. Hamilton, T. C., Young, R. C., and Ozols, R. F. Experimental model systems of ovarian cancer: applications to the design and evaluation of new treatment approaches. Semin. Oncol., *11:* 285–298, 1984.
14. Shridhar, V., Bible, K. C., Staub, J., Avula, R., Lee, Y. K., Kalli, K., Huang, H., Hartmann, L. C., Kaufmann, S. H., and Smith, D. I. Loss of expression of a new member of the DNAJ protein family confers resistance to chemotherapeutic agents used in the treatment of ovarian cancer. Cancer Res., *61:* 4258–4265, 2001.
15. Morissette, J., Rheaume, E., Leblanc, J. F., Luu-The, V., Labrie, F., and Simard, J. Genetic linkage mapping of HSD3B1 and HSD3B2 encoding human types I and II 3 β-hydroxysteroid dehydrogenase/δ5-δ4-isomerase close to D1S514 and the centromeric D1Z5 locus. Cytogenet. Cell Genet., *69:* 59–62, 1995.
16. Bajou, K., Noel, A., Gerard, R. D., Masson, V., Brunner, N., Holst-Hansen, C., Skobe, M., Fusenig, N. E., Carmeliet, P., Collen, D., and Foidart, J. M. Absence of host plasminogen activator inhibitor 1 prevents cancer invasion and vascularization. Nat. Med., *4:* 923–928, 1998.
17. Kirchner, J., and Bevan, M. J. ITM2A is induced during thymocyte selection and T cell activation and causes down-regulation of CD8 when overexpressed in CD4(+)CD8(+) double positive thymocytes. J. Exp. Med., *190:* 217–228, 1999.
18. Jacquemier, J., Sun, Z. Z., Penault-Llorca, F., Geneix, J., Devilard, E., Adelaide, J., and Birnbaum, D. FGF7 protein expression in human breast carcinomas. J. Pathol., *186:* 269–274, 1998.
19. Kim, J., Bergmann, A., and Stubbs, L. Exon sharing of a novel human zinc-finger gene, *ZIM2*, and paternally expressed gene 3 (*PEG3*). Genomics, *64:* 114–118, 2000.
20. Zumbrunn, J., and Trueb, B. Localization of the gene for a serine protease with IGF-binding domain (PRSS11) to human chromosome 10q25.3-q26.2. Genomics, *45:* 461–462, 1997.
21. Allan, G. J., Cottrell, S., Trowsdale, J., and Foulkes, W. D. Loss of heterozygosity on chromosome 5 in sporadic ovarian carcinoma is a late event and is not associated with mutations in APC at 5q21–22. Hum. Mutat., *3:* 283–291, 1994.
22. Cliby, W., Ritland, S., Hartmann, L., Dodson, M., Halling, K. C., Keeney, G., Podratz, K. C., and Jenkins, R. B. Human epithelial ovarian cancer allelotype. Cancer Res., *53:* 2393–2398, 1993.
23. Shridhar, V., Staub, J., Huntley, B., Cliby, W., Jenkins, R., Pass, H. I., Hartmann, L., and Smith, D. I. A novel region of deletion on chromosome 6q23.3 spanning less than 500 Kb in high-grade invasive epithelial ovarian cancer. Oncogene, *18:* 3913–3918, 1999.
24. Bicher, A., Ault, K., Kimmelman, A., Gershenson, D., Reed, E., and Liang, B. Loss of heterozygosity in human ovarian cancer on chromosome 19q. Gynecol. Oncol., *66:* 36–40, 1997.
25. Yu, Y., Xu, F., Peng, H., Fang, X., Zhao, S., Li, Y., Cuevas, B., Kuo, W. L., Gray, J. W., Siciliano, M., Mills, G. B., and Bast, R. C., Jr. NOEY2 (*ARHI*), an imprinted putative tumor suppressor gene in ovarian and breast carcinomas. Proc. Natl. Acad. Sci. USA, *96:* 214–219, 1999.
26. Engelman, J. A., Zhang, X. L., and Lisanti, M. P. Genes encoding human caveolin-1 and -2 are co-localized to the *D7S522* locus (7q31.1), a known fragile site (FRA7G) that is frequently deleted in human cancers. FEBS Lett., *436:* 403–410, 1998.
27. Huang, H., Reed, C. P., Mordi, A., Lomberk, G., Wang, L., Shridhar, V., Hartmann, L., Jenkins, R., and Smith, D. I. Frequent deletions within FRA7G at 7q31.2 in invasive epithelial ovarian cancer. Genes Chromosomes Cancer, *24:* 48–55, 1999.
28. Bugert, P., Von Knobloch, R., and Kovacs, G. Duplication of two distinct regions on chromosome 5q in non-papillary renal-cell carcinomas. Int. J. Cancer, *76:* 337–340, 1998.
29. Crickard, K., Gross, J. L., Crickard, U., Yoonessi, M., Lele, S., Herblin, W. F., and Eidsvoog, K. Basic fibroblast growth factor and receptor expression in human ovarian cancer. Gynecol. Oncol., *55:* 277–284, 1994.
30. Wen, Y. D., Perissi, V., Staszewski, L. M., Yang, W. M., Krones, A., Glass, C. K., Rosenfeld, M. G., and Seto, E. The histone deacetylase-3 complex contains nuclear receptor corepressors. Proc. Natl. Acad. Sci. USA, *97:* 7202–7207, 2000.
31. Holben, D. H., and Smith, A. M. The diverse role of selenium within selenoproteins: a review. J. Am. Diet. Assoc., *99:* 836–843, 1999.
32. Charbonnier, F., Perin, J. P., Mattei, M. G., Camuzat, A., Bonnet, F., Gressin, L., and Alliel, P. M. Genomic organization of the human *SPOCK* gene and its chromosomal localization to 5q31. Genomics, *48:* 377–380, 1998.
33. Conaway, J. W., Bradsher, J. N., Tan, S., and Conaway, R. C. Transcription factor SIII: a novel component of the RNA polymerase II elongation complex. Cell. Mol. Biol. Res., *39:* 323–329, 1993.
34. Cardillo, M. R., Yap, E., and Castagna, G. Molecular genetic analysis of TGF-β1 in ovarian neoplasia. J. Exp. Clin. Cancer Res., *16:* 49–56, 1997.
35. Zhao, N., Lai, F., Fernald, A. A., Eisenbart, J. D., Espinosa, R., Wang, P. W., and Le Beau, M. M. Human *CDC23*: cDNA cloning, mapping to 5q31, genomic structure, and evaluation as a candidate tumor suppressor gene in myeloid leukemias. Genomics, *53:* 184–190, 1998.
36. Du, B., Fu, C., Kent, K. C., Bush, H., Jr., Schulick, A. H., Kreiger, K., Collins, T., and McCaffrey, T. A. Elevated egr-1 in human atherosclerotic cells transcriptionally represses the transforming growth factor-β type II receptor. J. Biol. Chem., *275:* 39039–39047, 2000.
37. Brown, T. J., Shaw, P. A., Karp, X., Huynh, M. H., Begley, H., and Ringuette, M. J. Activation of SPARC expression in reactive stroma associated with human epithelial ovarian cancer. Gynecol. Oncol., *75:* 25–33, 1999.
38. Liu, D., Rudland, P. S., Sibson, D. R., Platt-Higgins, A., and Barraclough, R. Expression of calcium-binding protein S100A2 in breast lesions. Br. J. Cancer, *83:* 1473–1479, 2000.
39. Hu, S. I., Carozza, M., Klein, M., Nantermet, P., Luk, D., and Crowl, R. M. Human HtrA, an evolutionarily conserved serine protease identified as a differentially expressed gene product in osteoarthritic cartilage. J. Biol. Chem., *273:* 34406–34412, 1998.
40. Klugbauer, S., Demidchik, E. P., Lengfelder, E., and Rabes, H. M. Molecular analysis of new subtypes of ELE/RET rearrangements, their reciprocal transcripts and breakpoints in papillary thyroid carcinomas of children after Chernobyl. Oncogene, *16:* 671–675, 1998.
41. Mattei, M. G., Perin, J. P., Allicl, P. M., Bonnet, F., Maillet, P., Passage, E., Mattei, J. F., and Jolles, P. Localization of human platelet proteoglycan gene to chromosome 10, band q22.1, by *in situ* hybridization. Hum. Genet., *82:* 87–88, 1989.
42. Mulligan, L. M., Gardner, E., Telenius, H., and Ponder, B. A. Complementary physical and genetic techniques map the vinculin (*VCL*) gene on chromosome 10q. Genomics, *13:* 1347–1349, 1992.
43. Anderson, R. A., and Sando, G. N. Cloning and expression of cDNA encoding human lysosomal acid lipase/cholesteryl ester hydrolase. Similarities to gastric and lingual lipases. J. Biol. Chem., *266:* 22479–22484, 1991.
44. Permana, P. A., Luczy-Bachman, G., and Bogardus, C. Protein targeting to glycogen/PPP1R5: screening of coding and flanking genomic regions for polymorphisms and association analysis with insulin action in Pima Indians. Biochem. Biophys. Res. Commun., *258:* 184–186, 1999.
45. Brennan, F. E., and Fuller, P. J. Rapid upregulation of serum and glucocorticoid-regulated kinase (*sgk*) gene expression by corticosteroids *in vivo*. Mol. Cell. Endocrinol., *166:* 129–136, 2000.
46. Davis, R. J., Bennicelli, J. L., Macina, R. A., Nycum, L. M., Biegel, J. A., and Barr, F. G. Structural characterization of the *FKHR* gene and its rearrangement in alveolar rhabdomyosarcoma. Hum. Mol. Genet., *4:* 2355–2362, 1995.
47. Shridhar, V., Lee, J., Pandita, A., Iturria, S., Avula, R., Staub, J., Morrissey, M., Calhoun, E., Sen, A., Kalli, K., Keeney, G., Roche, P., Cliby, W., Lu, K., Schmandt, R., Mills, G. B., Bast, R. C., Jr., James, C. D., Couch, F. J., Hartmann, L. C., Lillie, J., and Smith, D. I. Genetic analysis of early- *versus* late-stage ovarian tumors. Cancer Res., *61:* 5895–5904, 2001.
48. Yokoyama, A., Muramatsu, T., Omori, T., Yokoyama, T., Matsushita, S., Higuchi, S., Maruyama, K., and Ishii, H. Alcohol and aldehyde dehydrogenase gene polymorphisms and oropharyngolaryngeal, esophageal and stomach cancers in Japanese alcoholics. Carcinogenesis (Lond.), *22:* 433–439, 2001.
49. Welsh, J. B., Zarrinkar, P. P., Sapinoso, L. M., Kern, S. G., Behling, C. A., Monk, B. J., Lockhart, D. J., Burger, R. A., and Hampton, G. M. Analysis of gene expression profiles in normal and neoplastic ovarian tissue samples identifies candidate molecular markers of epithelial ovarian cancer. Proc. Natl. Acad. Sci. USA, *98:* 1176–1181, 2001.
50. Yakicier, M. C., Legoix, P., Vaury, C., Gressin, L., Tubacher, E., Capron, F., Bayer, J., Degott, C., Balabaud, C., and Zucman-Rossi, J. Identification of homozygous deletions at chromosome 16q23 in Aflatoxin B1 exposed hepatocellular carcinoma. Oncogene, *20:* 5232–5238, 2001.
51. Watanabe, T., Nakamura, M., Yonekawa, Y., Kleihues, P., and Ohgaki, H. Promoter hypermethylation and homozygous deletion of the *p14ARF* and *p16INK4a* genes in oligodendrogliomas. Acta Neuropathol., *101:* 185–189, 2001.
52. Bagnoli, M., Tomassetti, A., Figini, M., Flati, S., Dolo, V., Canevari, S., and Miotti, S. Downmodulation of caveolin-1 expression in human ovarian carcinoma is directly related to α-folate receptor overexpression. Oncogene, *19:* 4754–4763, 2000.
53. Sato, N., Tsunoda, H., Nishida, M., Morishita, Y., Takimoto, Y., Kubo, T., and Noguchi, M. Loss of heterozygosity on 10q23.3 and mutation of the tumor suppressor gene *PTEN* in benign endometrial cyst of the ovary: possible sequence progression from benign endometrial cyst to endometrioid carcinoma and clear cell carcinoma of the ovary. Cancer Res., *60:* 7052–7056, 2000.
54. Watson, R. H., Neville, P. J., Roy, W. J., Jr., Hitchcock, A., and Campbell, I. G. Loss of heterozygosity on chromosomes 7p, 7q, 9p and 11q is an early event in ovarian tumorigenesis. Oncogene, *17:* 207–212, 1998.
55. Mok, S. C., Chan, W. Y., Wong, K. K., Muto, M. G., and Berkowitz, R. S. SPARC, an extracellular matrix protein with tumor-suppressing activity in human ovarian epithelial cells. Oncogene, *12:* 1895–1901, 1996.
56. Brunet, A., Park, J., Tran, H., Hu, L. S., Hemmings, B. A., and Greenberg, M. E. Protein kinase SGK mediates survival signals by phosphorylating the forkhead transcription factor FKHRL1 (FOXO3a). Mol. Cell. Biol., *21:* 952–965, 2001.
57. Loeb, K. R., and Loeb, L. A. Significance of multiple mutations in cancer. Carcinogenesis (Lond.), *21:* 379–385, 2000.
58. Jones, P. A., and Laird, P. W. Cancer epigenetics comes of age. Nat. Genet., *21:* 163–167, 1999.
59. Robertson, K. D., and Jones, P. A. DNA methylation: past, present and future directions. Carcinogenesis (Lond.), *21:* 461–467, 2000.
60. Luo, R. Z., Peng, H., Xu, F., Bao, J., Pang, Y., Pershad, R., Issa, J. P., Liao, W. S., Bast, R. C., Jr., and Yu, Y. Genomic structure and promoter characterization of an imprinted tumor suppressor gene *ARHI*. Biochim. Biophys. Acta, *1519:* 216–222, 2001.
61. Kawakami, M., Staub, J., Cliby, W., Hartmann, L., Smith, D. I., and Shridhar, V. Involvement of H-cadherin (CDH13) on 16q in the region of frequent deletion in ovarian cancer. Int. J. Oncol., *15:* 715–720, 1999.
62. Sinclair, A. J., Palmero, I., Holder, A., Peters, G., and Farrell, P. J. Expression of cyclin D2 in Epstein-Barr virus-positive Burkitt's lymphoma cell lines is related to methylation status of the gene. J. Virol., *69:* 1292–1295, 1995.
63. Leytus, S. P., Kurachi, K., Sakariassen, K. S., and Davie, E. W. Nucleotide sequence of the cDNA coding for human complement C1r. Biochemistry, *25:* 4855–4863, 1986.
64. Evron, E., Umbricht, C. B., Korz, D., Raman, V., Loeb, D. M., Niranjan, B., Buluwela, L., Weitzman, S. A., Marks, J., and Sukumar, S. Loss of cyclin D2 expression in the majority of breast cancers is associated with promoter hypermethylation. Cancer Res., *61:* 2782–2787, 2001.

GENES, CHROMOSOMES & CANCER 34:406–415 (2002)

Transcriptional Profiling Reveals That Several Common Fragile-Site Genes Are Downregulated in Ovarian Cancer

Stacy R. Denison,[1] Nicole A. Becker,[1] Matthew J. Ferber,[2] Leslie A. Phillips,[1] Kimberly R. Kalli,[3] John Lee,[4] Jim Lillie,[4] David I. Smith,[1]* and Viji Shridhar[1]

[1]Division of Experimental Pathology, Department of Laboratory Medicine and Pathology, Mayo Foundation, Rochester, Minnesota
[2]Biochemistry and Molecular Biology, Mayo Foundation, Rochester, Minnesota
[3]Endocrine Research Unit, Mayo Foundation, Rochester, Minnesota
[4]Millenium Pharmaceuticals, Inc., Cambridge, Massachusetts

Previous transcriptional profiling analysis of 14 primary ovarian tumors identified approximately 12,000 genes as decreased in expression by at least twofold in one or more of the tumors sampled. Among those genes were several known to be mapped to common fragile sites (CFSs), some of which had previously been shown to exhibit a loss of expression in ovarian carcinoma. Therefore, we selected a subset of genes to determine whether they localized within CFSs. Of the 262 genes that were downregulated at least twofold in 13 of 14 tumors, 10 genes were selected based on the following criteria: localization to a CFS band; documented aberrations in at least one malignancy; and feasibility of scoring breakage at the specific CFS. Fluorescence in situ hybridization analysis was performed using bacterial artificial chromosome clones encompassing portions of the genes to determine the position of the genes relative to their corresponding CFSs. Nine genes were determined to localize within seven previously uncloned CFSs. Semiquantitative reverse-transcription/polymerase chain reaction analysis of the cell lines and primary ovarian tumors validated the downregulation of seven of the 10 genes. We identified portions of seven uncloned CFSs and provide data to suggest that several of the genes mapping within CFSs may be inactivated in ovarian cancer.

INTRODUCTION

Present in virtually all individuals, the common fragile sites (CFSs) are chromosomal loci at which gaps/breaks and rearrangements are visualized when cells are challenged under appropriate tissue culture conditions. Hypotheses have suggested that CFSs are causally related to cancer. Initially, the evidence supporting a relationship between CFSs and cancer was the observation that many CFSs localized within cytogenetic bands were frequently altered or rearranged during cancer development (Yunis, 1983; Hecht and Glover, 1984; Hecht and Sutherland, 1984; Yunis and Soreng, 1984). Since that initial observation, regions of chromosomal fragility have also been shown to be associated with gene amplification as well as sites of preferential viral integration (Wilke et al., 1996; Coquelle et al., 1997; Mishmar et al., 1998; Thorland et al., 2000). However, these data did not conclusively demonstrate a link between CFSs and cancer development. Therefore, in an attempt to determine the role that the CFSs play in cancer development, a substantial effort has been made to clone and characterize the CFSs, to characterize the genes that localize within these fragile regions, and to determine the role that these genes may play in tumorigenesis and cancer progression.

To date, five of the 87 currently recognized CFSs have been cloned and characterized [FRA3B (3p14.2), FRA7G (7q31.2), FRA7H (7q32.3), FRA16D (16q23.2), and FRAXB (Xp22.3)] (Wilke et al., 1996; Huang et al., 1998; Mishmar et al., 1998; Krummel et al., 2000; Mangelsdorf et al., 2000; Paige et al., 2000; Arlt et al., 2002). Many of these CFSs have been associated with a cancer-specific chromosomal rearrangement, a region of high loss of heterozygosity (LOH) in one or more tumor types, and/or a site of viral integration (Wilke et al., 1996; Huang et al., 1998; Mishmar et al., 1998; Smith et al., 1998; Krummel et al., 2000;

Supported by: National Cancer Institute; Grant number: CA48031; Department of Defense; Grant number: DAMD-99-1-9504; Mayo Clinic Cancer Center Ovarian Cancer Working Group.

*Correspondence to: Dr. David I. Smith, Director of the Cancer Genetics Program, Mayo Clinic Cancer Center, Division of Experimental Pathology, Mayo Foundation, 200 First Street SW, Rochester, MN 55905.

Received 16 November 2001; Accepted 28 January 2002
DOI 10.1002/gcc.10084

Mangelsdorf et al., 2000; Paige et al., 2001). In addition, chromosomal deletions involving all five of these fragile sites have been observed in several different cancer types (Inoue et al., 1997; Huang et al., 1998; Smith et al., 1998; Mimori et al., 1999; Mangelsdorf et al., 2000; Paige et al., 2001; Arlt et al., 2002). These observations initiated the search for genes located within these breakage regions that were potential targets for alterations. A total of eight genes, the fragile histidine triad gene (*FHIT*, FRA3B), caveolin-1 and -2 (*CAV1* and *CAV2*, FRA7G), *TESTIN* (FRA7G), the WW domain containing the oxidoreductase gene (*WWOX*, FRA16D), and *GSI*, *TLR5A*, and the steroid sulfatase genes (*STS*, FRAXB), have been identified within these fragile regions (Ohta et al., 1996; Engelman et al., 1998; Bednarek et al., 2001; Tatarelli et al., 2000; Arlt et al., 2002). Several of these genes have been shown to have a loss of expression (LOE) in a variety of different tumor types including lung, breast, and ovarian cancer (Lee et al., 1998; Smith et al., 1998; Tatarelli et al., 2000). Two of these genes, *FHIT* and *WWOX*, have been shown to act functionally as tumor suppressors (Ohta et al., 1996; Siprashvili et al., 1997; Bednarek et al., 2001).

Transcriptional profiling is a powerful technique for the identification of a large number of genes that are aberrantly regulated during cancer development. Utilizing transcriptional profiling technology, 14 primary ovarian tumors (seven early and seven late stage) were analyzed previously to identify genes that were downregulated in ovarian cancer (Shridhar et al., 2001). Analysis of the 14 tumors identified approximately 12,000 genes, including several known CFS genes, as downregulated by ≥ twofold in at least one of the 14 tumors sampled. Prior analyses of *FHIT*, *WWOX*, and *CAV1* had also indicated the downregulation of these genes during ovarian cancer development (Mandai et al., 1998; Manning et al., 1999; Bagnoli et al., 2000; Ozaki et al., 2001; Paige et al., 2001). Therefore, we selected a subset of 10 genes to determine whether genes located within CFSs were inactivated in ovarian cancer. Using selective criteria, which limited analysis to genes found in CFSs that had been implicated previously as playing a role in cancer, 10 genes were selected from the 262 genes downregulated in at least 13 of the 14 tumors analyzed (Shridhar et al., 2001). Fluorescence in situ hybridization (FISH) analysis of bacterial artificial chromosome (BAC) clones identified as spanning portions of these 10 genes indicated that nine of the 10 were contained within CFSs. As a result, portions of seven previously uncloned CFSs were identified and the genes within them localized relative to their specific CFS. LOE analysis of the nine CFS genes confirmed that six were downregulated in primary ovarian tumors. Therefore, not only have portions of seven uncloned CFSs been identified, but also our data suggest that many of the genes within CFSs may be inactivated during ovarian tumorigenesis and/or cancer development.

MATERIALS AND METHODS

Transcriptional Profiling

For a detailed description of the tumor processing and selection, the RNA isolation and labeling, the cDNA microarray, and the image analysis and data recovery, see Shridhar et al. (2001).

Clone Selection

For each of the 10 genes, gene-specific primers were designed using Oligo 6.4 software (Molecular Biology Insights, Cascade, CO) and utilized for polymerase chain reaction (PCR) screening of the CITB Human BAC DNA Library (Release IV; Research Genetics, Huntsville, AL) (Table 1). Clones were then obtained from Research Genetics and grown according to the manufacturer's specifications. The protocol for the isolation of the BAC clones is available upon request.

Localization of Clones

Metaphase chromosomes were obtained from blood cultures established from 1 ml of whole blood and 9 ml of Chang Media PB (Irvine Scientific, Santa Ana, CA). Cultures were incubated at 37°C in 5% CO_2 for 72 hr and inoculated with 0.2 ml of a 0.2 μM (0.4 μM final concentration) aphidicolin (APC) solution approximately 24 hr before harvest. For those CFSs that were low expressing, 500 μl of 50 mM (2.5 mM final concentration) caffeine was added to the culture medium 4 hr prior to harvest, to increase the observed breakage at those particular loci. Cell harvest and metaphase preparations were performed using routine cytogenetic techniques.

For each BAC clone, 1 μg of purified DNA was labeled with biotin-16-dUTP (Boehringer/Roche, Indianapolis, IN) by nick translation, precipitated, and hybridized to the APC-treated metaphase cells according to the protocol of Verma and Babu (1995). Probe detection was accomplished using minor modifications of the manufacturer's protocol (Ventana Medical Systems, Tucson, AZ), and the chromosomes were subsequently counterstained

TABLE 1. Downregulated Genes Selected for Further Analysis Using FISH and/or Semiquantitative RT-PCR*

Gene	Image clone	Accession no.	Band	CFS	BAC primers	Clone	RT primers
NOEY2	345680	W72033	1p31	FRA1C	5′-AGGACCGCCTTCCAATTTTT-3′ 5′-TTTCTTTTTCCCAGGCCAGA-3′	15D15	5′-GCTTTGGCTCCAAGGAAC-3′ 5′-GGGCTCACATGATTATGCAC-3′
RGS4	429349	AA007419	1q21	FRA1F	5′-CCCGATGTTTGGAATGAAAT-3′ 5′-AATGGCTCTGGGCTATATGC-3′	112M12	5′-TGAGGAGTGCAAAAGATATG-3′ 5′-GAGAATTAGGCACACTGAGG-3′
FHIT	—	XM043137	3p14.2	FRA3B	—	—	5′-GGCCAACATCTCATCAAG-3′ 5′-TTTCCTCCTCTGATCTCC-3′
PDGFRA	52096	H23235	4q12	FRA4B	5′-ATGCTAAATGTGTAATAATGTA-3′ 5′-TTACTTTGTTCTCTATGCTC-3′	574J21	5′-CAAATGAAAATGAAAAGGTTG-3′ 5′-TAATCTCCACTGTCTTTCACC-3′
FST	434768	AA701860	5p14; 5q11	FRA5E; Hecht et al., 1988	5′-TTTCAAGGTTGGGAGAGG-3′ 5′-GCTTTACTTCCAGTAGCACACC-3′	326J12	5′-TACAGGACCGAACTGAGC-3′ 5′-GCTTTGATACACTTTCCC-3′
IGF2R	67055	T70421	6q26	FRA6E	5′-GTCGGGCCAGAACAAG-3′ 5′-AGGGCAACGATCACCATTCA-3′	421P10	5′-ATTGTCCAGTGCGGGCCATC-3′ 5′-CCCAGGGTTTTCCCACACAG-3′
PLG	875979	T73187	6q26	FRA6E	—[a]	81D8	5′-AAGGAGAGCCTCTGGATGAC-3′ 5′-AGGTCTGTGGGGAGAAGTGG-3′
SLC22A3	127120	R08121	6q26	FRA6E	—[a]	81D8	5′-CAGAGACAGTGGATGATG-3′ 5′-GCTTCTTTGTTAAACTGG-3′
CAV1	—	XM057981	7q31.2	FRA7G	—	—	5′-ATGTGATTGCAGAACCAG-3′ 5′-CAACTTGGAACTTGAAATTG-3′
CAV2	—	NM001233	7q31.2	FRA7G	—	—	5′-TTGTTTGTCTGTTTTTACTCTG-3′ 5′-ATGAAGTTTACCTTGTGGG-3′
TESTIN	—	?	7q31.2	FRA7G	—	—	5′-TTTCACCATGTTAGCCAG-3′ 5′-ATTTGATATATCCATGGACAG-3′
PSAP	291255	N72215	10q21-22	FRA10C; FRA10D	5′-ATCTGCCTGAATGTAACCTG-3′ 5′-AACTTCATGTCCTGCTGG-3′	31K4	5′-TATGCTGAAGGACAATGC-3′ 5′-ATCAGACTTTGCTGGGAC-3′
TSG101	123087	R02529	11p15	FRA11C; FRA11D; FRA11E	5′-TCTCTGATACCAGCTGGAG-3′ 5′-AGTCCCAACATTCAGCAC-3′	296P21	5′-TCTCTGATACCAGCTGGAG-3′ 5′-AGTCCCAACATTCAGCAC-3′
TPM1	341328	W58092	15q22.1	FRA15A	5′-AACACAGTGTGCTTAGTCAG-3′ 5′-TGGACAGAGTTCTACATTGTAC-3′	368M11	5′-AAGATGAGCTGGTGTCAC-3′ 5′-GTCATATCGTTGAGAGCG-3′
WWOX	—	NM016373	16q23.2	FRA16D	—	—	5′-GGGGAGACAAATCTCAGAAC-3′ 5′-TACAATGTGAAAGCAAGAGAA-3′

*The possible band location(s) as identified by UniGene (band), potential CFS, gene-specific BAC clone (clone), and the gene-specific primers for BAC slection and RT analysis are provided for each of the genes analyzed.

[a]BAC primers not designed as BACs were identified by the Sanger Centre.

TABLE 2. FISH Localization of Downregulated Genes Relative to their Respective Common Fragile Site

Gene	Band	FS	Breakage[a]			LOE cell lines (tumors)	Position relative to FS
			Centromeric	Crossing	Telomeric		
NOEY2	1p31	FRA1C	12	0	13	100% (100%)	Within
RGS4	1q21	FRA1F	20	0	0	85.7% (100%)	Off; centromeric
PDGFRA	4q12	FRA4B	0	1	19	100% (100%)	Telomeric end
FST	5q11	Hecht et al., 1988	19	0	1	57.1% (0%)	Centromeric end
IGF2R	6q26	FRA6E	18	0	2	57.1% (100%)	Centromeric end
PLG	6q26	FRA6E	16	0	6	0% (0%)	Within
SLC22A3	6q26	FRA6E	—[b]	—[b]	—[b]	85.7% (100%)	Within
PSAP	10q22	FRA10D	13	0	8	37% (35.7%)	Within
TSG101	11p15.1	FRA11C	13	2	5	42.9% (100%)	Within
TPM1	15q22.1	FRA15A	11	2	7	85.7% (100%)	Within

[a]The number and position (centromeric/crossing/telomeric) of observed hybridization signals relative to each particular common fragile site.
[b]*PLG* and *SLC22A3* localize to the same BAC; therefore, the counts for *SLC22A3* are identical to that of *PLG* (Table 1).

with 4′-6-diamidino-2-phenylindole (DAPI; Vector Laboratories, Burlingame, CA). A Zeiss Axioplan 2 fluorescence microscope (Zeiss, Thornwod, NY) and the IPLab Spectrum P software (Scanalytics Inc., Fairfax, VA) were used for photomicroscopy. The cytogenetic location of each individual clone was established by DAPI banding (Table 2). The position of the clone relative to the fragile site was determined from the analysis of a minimum of 20 APC-treated metaphase cells with breakage at that particular fragile site. A BAC was considered to be crossing the fragile site if the hybridization signal was observed on both sides of the breakage, or was observed proximal to the fragile site (centromeric) in one metaphase cell and distal (telomeric) to the fragile site in a different metaphase cell.

Semiquantitative Reverse Transcription/Polymerase Chain Reaction (RT-PCR)

Normal ovarian surface epithelial (OSE) cells were collected following oophorectomy for reasons unrelated to gynecological malignancy, and were used as either uncultured brushings or grown as short-term cultures as described by Kruk et al. (1990). Only OSE cultures between passages two and five with epithelial morphology and uniform cytokeratin staining were utilized. Total RNA was extracted from normal ovarian epithelial brushings, short-term cultured normal OSE, seven ovarian tumor-derived cell lines [Mayo cell lines: OV167, OV177, OV202, OV207, OV266 (Conover et al., 1998), SKOV3, and OVCAR5], and 14 primary ovarian tumors (stages 1–4) using Trizol reagent (GibcoBRL, Rockville, MD) according to the manufacturer's specifications. Approximately 5 μg of total RNA from each sample was treated with RNase-free DNase for 30 min at 37°C, and the DNase was inactivated by incubation of the reaction for 10 min at 90°C. The DNase-treated RNA was reverse-transcribed according to the manufacturer's protocol (GibcoBRL).

Unique primers (Table 2) were designed for all 10 genes by use of the Oligo 6.4 software (Molecular Biology Insights) and used in a multiplex reaction with *GAPDH* (5′-ACCACAGTCCATGCCATCAC-3′, 5′-TCCACCACCCTGTTGCTTGTA-3′; 450-bp product), β-tubulin (5′-GCATCAACGTGTACTACAA-3′, 5′-TACGAGCTGGTGGACTGAGA-3′; 454-bp product), or β2-microglobulin primers (5′-AGCTGTGCTCGCGCTACTCTCTC-3′, 5′-GTGTCGGATTGATGAAACCCAGACAC-3′; 140-bp product) as an internal control. The PCR reaction consisted of reverse-transcribed cDNA, 50 mM KCl, 10 mM Tris–HCl (pH 8.3), 1.5 mM $MgCl_2$, 400 μM concentration of forward and reverse primers for the specific genes, 50 μM concentration of the control primer, and 0.1 U *Taq* polymerase (Promega, Madison, WI). Amplification conditions were 95°C for 3 min, 28 cycles of 95°C for 30 sec, 55–67°C for 30 sec, and 72°C for 30 sec, and a final extension at 72°C for 10 min.

RESULTS

Based on the data provided by Shridhar et al. (2001), 10 genes were selected from a total of 262 genes that were downregulated by at least twofold in at least 13 of the 14 primary ovarian tumors analyzed. Genes were selected if the cytogenetic location, determined by the UniGene database, was within a band known to contain a CFS. Additional criteria included the localization of the gene to a known region of LOH in one or more tumor types or a documented loss of gene expression in at

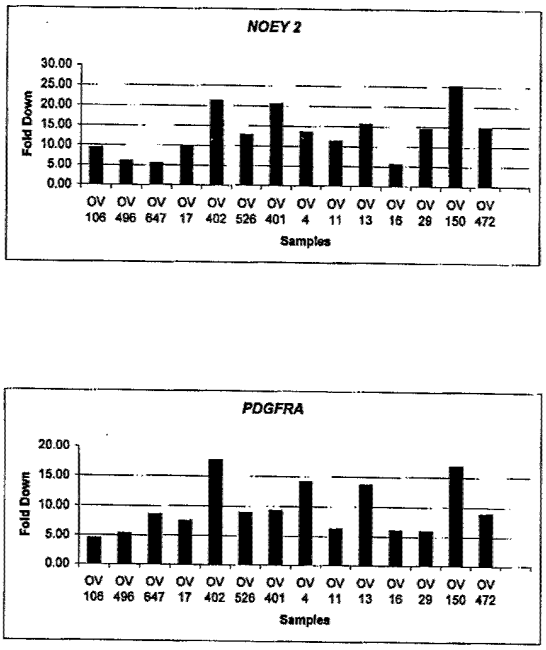

Figure 1. Representative examples of expression profiles obtained from transcriptional profiling of 14 primary ovarian tumors. The decreased expression levels of the tumor compared to levels of normal ovarian surface epithelial brushings (fold down) are provided for each of the tumors sampled.

least one type of cancer. Finally, genes were selected based on the ease of scoring breakage at the CFS of interest. Ease of scoring was evaluated by whether the possible CFS had a relatively high frequency of breakage and could be easily discerned from neighboring CFSs. Using these criteria, we selected 10 genes for FISH and semiquantitative RT-PCR analysis: *RAS* homolog gene family, member 1 (*NOEY2*); regulator of G-protein signaling 4 (*RGS4*); platelet-derived growth factor receptor, alpha polypeptide (*PDGFRA*); follistatin (*FST*); mannose 6 phosphate/insulin-like growth factor receptor II (*IGF2R*); plasminogen (*PLG*); solute carrier family 22, member 3 (*SLC22A3*); prosaposin (*PSAP*); tumor susceptibility gene 101 (*TSG101*); and tropomyosin 1, alpha (*TPM1*) (Table 1).

Figure 1 shows the expression levels of two of the 10 genes, *NOEY2* and *PDGFRA*, analyzed in the ovarian tumors, compared to normal OSE. Table 1 lists the Image clone and GenBank accession numbers, cytogenetic localization, and the CFS(s) located within that region for each of the 10 genes.

FISH analysis of the 10 genes required the identification of BAC clones that contained a portion of the gene to be analyzed. For eight of the 10 genes (*NOEY2, RGS4, PDGFRA, FST, IGF2R, PSAP, TPM1,* and *TSG101*), a gene-specific BAC clone was identified by screening of the CITB Human BAC DNA Library (Release IV; Research Genetics) with gene-specific primers (Table 1). By use of the Sanger Centre database (www.sanger.ac.uk.; Cambridge, UK), a single BAC clone was identified as encompassing portions of both the *SLC22A3* and *PLG* genes (Table 1). Confirmation for the presence of portions of *SLC22A3* and *PLG* in BAC 81D8 was established by PCR (data not shown). Therefore, a total of nine BACs were identified and hybridized to APC-induced metaphase chromosomes to determine the position of the genes relative to their respective CFSs (Table 1, Fig. 2).

For any CFS for which there were CFSs located in neighboring bands, inverse-DAPI banding was used to ensure that the breakage was occurring in the CFS of interest. FISH analysis of the nine BACs determined that nine of the 10 genes were localized within CFS regions (Table 2). A gene was determined to localize within a CFS region if the BAC, containing portions of that gene, hybridized proximal to the site of APC-induced decondensation/breakage in some metaphase cells and distal in others. *RGS4* was the only gene that did not localize to a CFS; *RGS4* maps centromeric to FRA1F (1q21). BACs containing a portion of each of the remaining nine genes mapped to the following CFSs: FRA1C (*NOEY2*), FRA4B (*PDGFRA*), 5q11 [a CFS described by Hecht et al. (1988) that was never given an FRA designation; *FST*], FRA6E (*IGF2R, PLG,* and *SLC22A3*), FRA10D (*PSAP*), FRA11C (*TSG101*), and FRA15A (*TPM1*) (Table 2). Table 2 lists the observed counts (centromeric/crossing/telomeric) for each gene/BAC. Based on the proportion of hybridization signals observed as centromeric, crossing, or telomeric to the region of breakage, the position of the gene relative to its respective fragile site could be determined (Table 2). Three of the genes (*FST, IGF2R,* and *PDGFRA*) localized to the ends of their respective CFSs, centromeric for *FST* and *IGF2R* and telomeric for *PDGFRA*, with counts of 19/0/1, 18/0/2, and 0/1/19, respectively. The six remaining CFS genes localized within the centers of their respective fragile sites as they hybridized with approximately equal frequency proximal and distal to the region of decondensation/breakage within each of the respective sites (Table 2).

To confirm whether the 10 genes were downregulated in ovarian cancer, we analyzed all of the genes by semiquantitative RT-PCR on cDNAs generated from tumor-derived cell lines and primary tumors and tested for decreased expression

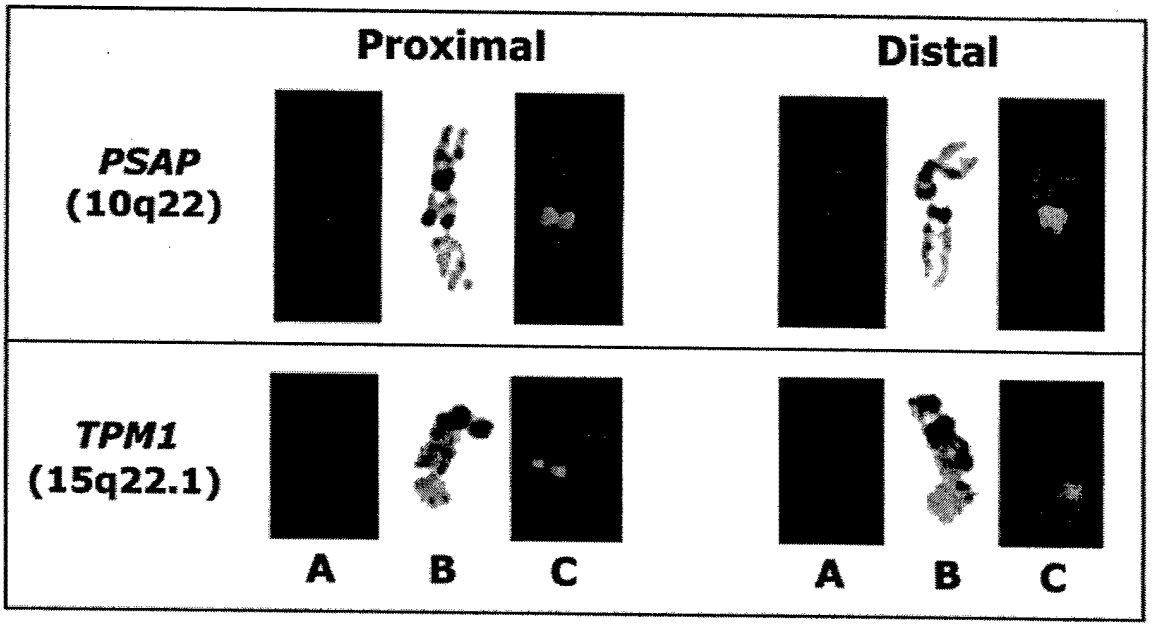

Figure 2. Depiction of FISH clones obtained for *PSAP* and *TPM1* and determined to be crossing FRA10D and FRA15A, respectively. For each APC-induced break analyzed, the presence of breakage at 10q22 (FRA10D) and 15q22.1 (FRA15A) was initially scored from a DAPI-counterstained image (**A**). Breakage was confirmed as mapping to the region of interest by inverted DAPI bands (**B**). Both centromeric and telomeric hybridization signals for the FITC-labeled BAC clone are provided (**C**).

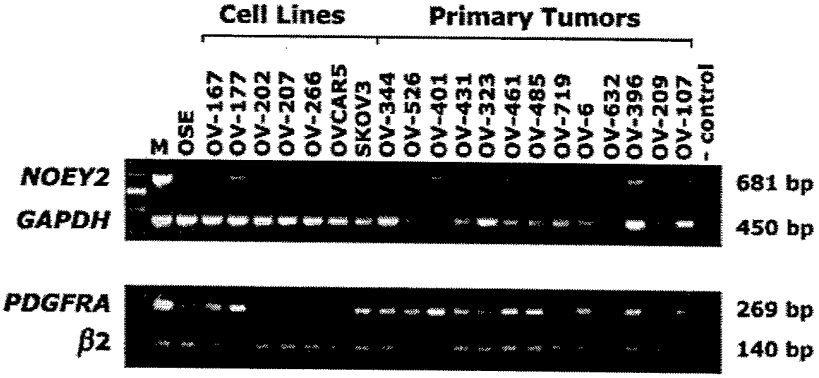

Figure 3. Semiquantitative RT-PCR analysis for two of the 10 genes (*NOEY2* and *PDGFRA*) selected for analysis in this study. The expression levels for both genes were analyzed in short-term cultured normal ovarian surface epithelium (OSE), seven tumor-derived ovarian cell lines (OV166, OV177, OV202, OV207, OV266, OVCAR5, and SKOV3), and 13 primary ovarian tumors. *GAPDH* and β2 primers were used as internal controls. A negative H_2O control (−) and a marker ladder (M) are also provided.

levels. Initially, all 10 genes were tested on cDNA obtained from normal OSE brushings, to ensure that each gene was expressed in normal OSE. Analysis of the 10 genes confirmed the expression of each in normal OSE (data not shown). Expression levels for all the genes were then analyzed in 14 primary ovarian tumors (stages 1–4) and seven tumor-derived cell lines and compared to the expression level in the short-term culture of OSE (Fig. 3, Table 2). Unique primers for each of the 10 genes were initially used in a multiplex reaction with an internal control primer. To ensure that there was no preferential amplification of the control primer in the multiplex reaction, unique primers for several of the 10 genes were analyzed on the same primary tumor panel and yielded similar results (data not shown). Representative examples of the PCR analysis and the observed expression patterns are provided in Figure 3 and Table 3, respectively.

Expression analysis of the tumor-derived cell line and primary tumor panels determined that eight of the 10 genes showed LOE (i.e., decreased or complete absence of expression) in at least one or more of the samples. However, *IGF2R* and *PLG* did not exhibit LOE in any of the cell lines or primary tumors analyzed. Of the eight genes with LOE, five (*NOEY2*, *RGS4*, *PDGFRA*, *SLC22A3*, and *TSG101*) showed decreased expression, and in some cases complete absence of expression, in the

TABLE 3. Loss of Expression Analysis in Tumor-Derived Cell Lines and Primary Tumors

Cell lines/tumors	*NOEY2*	*RGS4*	*PDGFRA*	*FST*	*IGF2R*	*PLG*	*SLC22A3*	*PSAP*	*TPM1*	*TSG101*
OSE	●[a]	●	●	●	●	●	●	●	●	●
OV167	◍[b]	○[c]	◍	●	●	●	◍	◍	●	●
OV177	◍	○	◍	●	●	●	◍	●	●	◍
OV202	◍	○	●	○	●	●	◍	◍	●	◍
OV207	◍	◍	◍	○	●	●	◍	●	●	◍
OV266	◍	◍	◍	○	●	●	◍	●	○	◍
OVCAR5	○	●	◍	○	●	●	●	◍	○	◍
SKOV3	○	○	◍	●	●	●	◍	●	○	◍
% downregulated	100.0	85.7	85.7	57.1	0.0	0.0	85.7	42.9	42.9	85.7
344	◍	◍	◍	●	●	●	◍	●	○	◍
526	○	◍	◍	●	●	●	◍	●	○	○
401	○	◍	◍	●	●	●	◍	●	○	◍
431	◍	◍	●	●	●	●	◍	●	○	◍
323	○	◍	◍	●	●	●	N/A	●	○	◍
461	○	◍	◍	●	●	●	○	●	○	○
485	◍	◍	◍	●	●	●	○	N/A	◍	◍
426	○	◍	◍	●	●	●	◍	●	○	○
719	○	○	◍	●	●	●	○	◍	○	◍
6	◍	◍	◍	●	●	●	○	◍	○	◍
632	○	◍	◍	●	●	●	○	N/A	○	◍
396	◍	◍	◍	●	●	●	◍	◍	○	◍
209	○	◍	◍	●	●	●	◍	●	○	◍
107	◍	◍	◍	●	●	●	○	◍	○	◍
% downregulated	100.0	100.0	92.9	0.0	0.0	0.0	100.0	33.3	100.0	100.0

[a]Normal expression.
[b]Reduced expression.
[c]Complete absence of expression.

majority (≥85.7%) of the cell lines and primary tumors analyzed (Fig. 3).

RT-PCR analysis of the cell lines determined that the remaining three genes showed LOE in at least one of the cell lines. The numbers of cell lines exhibiting LOE were three (42.9%) for *PSAP* and *TPM1* and four (57.1%) for *FST* (Fig. 3, Table 3). Semiquantitative RT-PCR analysis of the primary ovarian tumors determined that only *PSAP* and *TPM1* showed LOE in one or more of the tumors sampled; *FST* did not exhibit any LOE in any of the 14 tumors. The number of tumors that had LOE were three (33.3%) for *PSAP* and 14 (100%) for *TPM1* (Table 3).

To determine whether the five previously identified CFS genes (*FHIT, CAV1, CAV2, TESTIN,* and *WWOX*) also showed LOE in our panel of cell lines and primary tumors, we designed unique primers for each gene and used them in semiquantitative RT-PCR analysis. *FHIT, CAV1, CAV2,* and *WWOX* each showed LOE in at least one of the cell lines tested, whereas *TESTIN* showed normal expression levels compared to that of short-term culture OSE (Fig. 4). When analyzed on the primary tumor panel, all five genes exhibited downregulation (Fig. 4). The percentage of tumors exhibiting LOE ranged from 21.4% (*TESTIN*) to 78.6% (*FHIT*) (Fig. 4).

DISCUSSION

There are considerable data suggestive of a causal relationship between CFSs and cancer; however, the evidence is limited to data obtained from only five CFSs (FRA3B, FRA7G, FRA7H, FRA16D, and FRAXB). The cloning and characterization of these five CFSs and the genes localizing within them, however, have generated significant interest in the potential role of CFSs in tumorigenesis and/or cancer progression. One such observation is that several of the genes localizing within the cloned CFSs (*FHIT, CAV1, TESTIN,* and *WWOX*) exhibit LOE in a variety of different tumor types (Lee et al., 1998; Smith et al., 1998; Tatarelli et al., 2000; Paige et al., 2001). Based on this observation, we selected 10 genes, determined by transcription profiling to be downregulated in primary ovarian tumors and localizing to chromosomal bands containing a CFS, to determine whether genes located within CFSs were inactivated during the development of ovarian cancer.

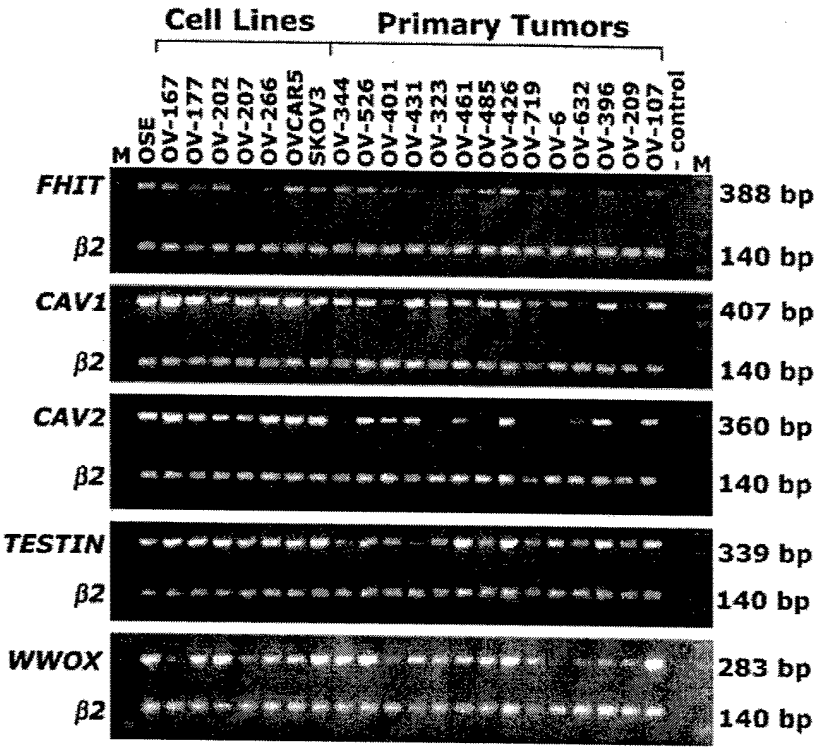

Figure 4. Semiquantitative RT-PCR analysis for the five known CFS genes (*FHIT*, *CAV1*, *CAV2*, *TESTIN*, and *WWOX*). The expression levels for these genes were analyzed in short-term culture normal ovarian surface epithelium (OSE), seven tumor-derived ovarian cell lines (OV166, OV177, OV202, OV207, OV266, OVCAR5, and SKOV3), and 14 primary ovarian tumors. β2 microglobulin primers were used as an internal control for each primer set. A negative H_2O control (−) and a marker ladder (M) are also provided.

FISH analysis of the 10 genes established that nine (90%) localized within seven different CFSs (Table 2); three of the genes (*IGF2R*, *SLC22A3*, and *PLG*) were all derived from the same chromosomal band (6q26) and were determined to map within the CFS FRA6E. As a result, BACs have been identified that cross a portion of the previously uncloned CFSs mapping to 1p31 (FRA1C), 4q12 (FRA4B), 5q11 (Hecht et al., 1988), 6q26 (FRA6E), 10q22 (FRA10D), 11p15.1 (FRA11C), and 15q22 (FRA15A). Only *RGS4* mapped outside a CFS region. The complete cloning and characterization of these CFSs, however, will require the definition of both the centromeric and telomeric ends for each of these CFSs; this work is ongoing in our laboratory.

Transcriptional profiling, though considered to be a powerful technique for identifying aberrantly regulated genes, can result in the identification of numerous false positives (Mills et al., 2001). To validate the expression profiles provided by the microarray analysis, we confirmed the expression levels for all 10 genes by semiquantitative RT-PCR analysis of a panel of seven ovarian cancer cell lines and 14 primary tumors. RT-PCR analysis of the cell line/tumor panels indicated that seven of the 10 genes (70%) were downregulated in one or more of the cell lines and primary tumors analyzed (Fig. 3, Table 3). There was no direct correlation between genes that were downregulated and those that were localized within CFSs. Three of the genes that mapped within a CFS (*FST*, *IGF2R*, and *PLG*) did not show LOE, and *RGS4*, the gene located outside FRA1F, did exhibit LOE in both the cell line and primary tumor panels (Table 3). Six of the nine (66.7%) CFS genes, however, exhibited LOE in the primary tumors analyzed, therefore suggesting that several CFS genes are inactivated in ovarian cancer.

LOE analysis of the five known CFS genes (*FHIT*, *CAV1*, *CAV2*, *WWOX*, and *TESTIN*) has indicated that *FHIT*, *CAV1*, and *WWOX* are downregulated in ovarian tumors (Mandai et al., 1998; Manning et al., 1999; Bagnoli et al., 2000; Paige et al., 2001). Expression analysis on primary ovarian tumors was not previously performed for either *CAV2* or *TESTIN*. We therefore analyzed the expression levels for *FHIT*, *CAV1*, *CAV2*, *WWOX*, and *TESTIN* on the ovarian cell line and primary tumor panels (Fig. 4). All five genes were identified as being downregulated in at least one of the primary ovarian tumors analyzed. The percentage of tumors exhibiting LOE ranged from 21.4% (*TESTIN*) to 78.6% (*FHIT*). Therefore, the majority of the 15

CFS genes (13/15) are downregulated in primary ovarian tumors, indicating that CFS genes may play a role in the development and/or progression of ovarian cancer. Additionally, these data provide further evidence supporting the hypothesis that CFSs and the genes contained within them are causally related to cancer.

The data provided in this study also suggest that genes mapping within the same CFS may exhibit different expression patterns depending on the tumor type. Previous expression analyses of *CAV1* and *CAV2* in lung carcinoma identified an inverse correlation in expression patterns (Racine et al., 1999). *CAV1* was determined to be downregulated in all of the lung cancer cell lines analyzed, but *CAV2* had expression levels similar to those of normal bronchial epithelial cells (Racine et al., 1999); *TESTIN* expression levels have not been examined in lung carcinoma. In this study, all three genes (*CAV1*, *CAV2*, and *TESTIN*) exhibited LOE in the primary ovarian tumors, 28.6, 57.1, and 21.4%, respectively (Fig. 4). These data indicate that the expression levels for CFS genes may be dependent on the tumor type. This is further supported by the observation that the three FRA6E genes *IGF2R*, *SLC22A3*, and *PLG* also exhibited alternative expression patterns. Although *SLC22A3* was validated as exhibiting LOE in ovarian tumors, the expression levels for *IGF2R* and *PLG* were normal compared to that of normal OSE. The expression levels for *IGF2R*, *PLG*, and *SLC22A3* have not been compared in any other tumor types. Nevertheless, if the instability within the CFSs were solely responsible for gene inactivation, LOE would be expected for all the genes within the region. Therefore, these data would suggest that, although the genes are located within the same CFS region, there might be a selection pressure for the loss of specific genes, but not of others.

Additionally, the data provided in this study indicate that a number of currently recognized tumor-suppressor genes not only map within CFS regions but also may play a role in the development and/or progression of ovarian cancer. Three of the nine genes identified in this study as localizing within CFSs (*NOEY2*, *IGF2R*, and *TSG101*) have already been determined to be putative tumor-suppressor genes (De Souza et al., 1995; Li et al., 1997; Sun et al., 1997; Oates et al., 1998; Yu et al., 1999; Kong et al., 2000; Luo et al., 2001). LOE has been documented for *NOEY2* in breast and ovarian carcinomas (Yu et al., 1999) and *IGF2R* in breast, hepatocellular, and lung carcinomas (De Souza et al., 1995; Oates et al., 1998; Kong et al., 2000). In the case of *TSG101*, aberrant transcripts have been identified in both breast and prostate cancer (Li et al., 1997; Sun et al., 1997). The identification of these genes as downregulated in primary ovarian tumors by transcriptional profiling suggests that some of these genes may be functioning as tumor suppressors, as has already been demonstrated for *FHIT* (Ohta et al., 1996; Siprashvili et al., 1997). Localization of *NOEY2*, *IGF2R*, and *TSG101* to CFSs, in addition to the previously localized candidate tumor-suppressor genes *FHIT*, *CAV1*, *WWOX*, and *TESTIN* (Ohta et al., 1996; Siprashvili et al., 1997; Tatarelli et al., 2000; Liu et al., 2001; Paige et al., 2001), also suggests that CFSs may preferentially harbor tumor-suppressor genes.

ACKNOWLEDGMENTS

We thank Gwen Callahan for providing the tissue samples. This work was supported, in part, by National Cancer Institute Grant CA48031 and Department of Defense Grant DAMD-99-1-9504 (both to D.I.S.).

REFERENCES

Arlt MF, Miller DE, Beer DG, Glover TW. 2002. Molecular characterization of FRAXB and comparative common fragile site instability in cancer cells. Genes Chromosomes Cancer 33:82–92.

Bagnoli M, Tomassetti A, Figini M, Flati S, Dolo V, Canevari S, Miotti S. 2000. Downmodulation of caveolin-1 expression in human ovarian carcinoma is directly related to alpha-folate receptor overexpression. Oncogene 19:4754–4763.

Bednarek AK, Laflin KJ, Daniel RL, Liao Q, Hawkins KA, Aldaz CM. 2000. WWOX, a novel WW domain-containing protein mapping to human chromosome 16q23.3–24.1, a region frequently affected in breast cancer. Cancer Res 60:2140–2145.

Conover CA, Hartmann LC, Bradley S, Stalboerger P, Klee GG, Kalli KR, Jenkins RB. 1998. Biological characterization of human epithelial ovarian carcinoma cells in primary culture: the insulin-like growth factor system. Exp Cell Res 238:439–449.

Coquelle A, Pipiras E, Toledo F, Buttin G, Debatisse M. 1997. Expression of fragile sites triggers intrachromosomal mammalian gene amplification and sets boundaries to early amplicons. Cell 89:215–255.

De Souza AT, Hankins GR, Washington MK, Orton TC, Jirtle RL. 1995. M6P/IGF2R gene is mutated in human hepatocellular carcinomas with loss of heterozygosity. Nat Genet 11:447–479.

Engelman JA, Zhang XL, Lisanti MP. 1998. Genes encoding human caveolin-1 and -2 are co-localized to the D7S522 locus (7q31.1), a known fragile site (FRA7G) that is frequently deleted in human cancers. FEBS Letters 436:403–410.

Hecht F, Glover TW. 1984. Cancer chromosome breakpoints and common fragile sites induced by aphidicolin. Cancer Genet Cytogenet 13:185–188.

Hecht F, Sutherland GR. 1984. Fragile sites and cancer breakpoints. Cancer Genet Cytogenet 12:179–181.

Hecht F, Tajara EH, Lockwood D, Sandberg AA, Hecht BK. 1988. New common fragile sites. Cancer Genet Cytogenet 33:1–9.

Huang H, Qian C, Jenkins RB, Smith DI. 1998. FISH mapping of YAC clones at human chromosomal band 7q31.2: identification of YACs spanning FRA7G within the common region of LOH in breast and prostate cancer. Genes Chromosomes Cancer 21:152–159.

Inoue H, Ishii H, Alder H, Snyder E, Druck T, Huebner K, Croce CM. 1997. Sequence of the FRA3B common fragile region: implications for the mechanism of FHIT deletion. Proc Natl Acad Sci USA 94:14584–14589.

Kong FM, Anscher MS, Washington MK, Killian JK, Jirtle RL. 2000.

M6P/IGF2R is mutated in squamous cell carcinoma of the lung. Oncogene 19:1572–1578.
Kruk PA, Maines-Bandiera SL, Auersperg N. 1990. A simplified method to culture human ovarian surface epithelium. Lab Invest 63:132–136.
Krummel KA, Roberts LR, Kawakami M, Glover TW, Smith DI. 2000. The characterization of the common fragile site FRA16D and its involvement in multiple myeloma translocations. Genomics 69:37–46.
Lee SW, Reimer CL, Oh P, Campbell DB, Schnitzer JE. 1998. Tumor cell growth inhibition by caveolin re-expression in human breast cancer cells. Oncogene 16:1391–1397.
Li L, Li X, Francke U, Cohen SN. 1997. The TSG101 tumor susceptibility gene is located in chromosome 11 band p15 and is mutated in human breast cancer. Cell 88:143–154.
Liu J, Lee P, Galbiati F, Kitsis RN, Lisanti MP. 2001. Caveolin-1 expression sensitizes fibroblastic and epithelial cells to apoptotic stimulation. Am J Physiol Cell Physiol 280:C823–C835.
Luo RZ, Peng H, Xu F, Bao J, Pang Y, Pershad R, Issa JP, Liao WS, Bast RC Jr, Yu Y. 2001. Genomic structure and promoter characterization of an imprinted tumor suppressor gene ARHI. Biochim Biophys Acta 1519:216–222.
Mandai M, Konishi I, Kuroda H, Nanbu K, Matsushita K, Yura Y, Hamid AA, Mori T. 1998. Expression of abnormal transcripts of the FHIT (fragile histidine triad) gene in ovarian carcinoma. Eur J Cancer 34:745–749.
Mangelsdorf M, Ried K, Woollatt E, Dayan S, Eyre H, Finnis M, Hobson L, Nancarrow J, Venter D, Baker E, Richards RI. 2000. Chromosomal fragile site FRA16D and DNA instability in cancer. Cancer Res 60:1683–1689.
Manning AP, Mes-Masson AM, Seymour RJ, Tetrault M, Provencher DM, Tonin PN. 1999. Expression of FHIT in primary cultures of human epithelial ovarian tumors and malignant ovarian ascites. Mol Carcinog 24:218–225.
Mills JC, Roth KA, Cagan RL, Gordon JI. 2001. DNA microarrays and beyond: completing the journey from tissue to cell. Nat Cell Biol 3:E175–E178.
Mimori K, Druck T, Inoue H, Alder H, Berk L, Mori M, Huebner K, Croce CM. 1999. Cancer-specific chromosome alterations in the constitutive fragile region FRA3B. Proc Natl Acad Sci USA 96:7456–7461.
Mishmar D, Rahat A, Scherer SW, Nyakatura G, Hinzmann B, Kohwi Y, Mander-Gutfroind Y, Lee JR, Drescher B, Sas DE, Margalit H, Platzer M, Weiss A, Tsui LC, Rosenthal A, Kerem B. 1998. Molecular characterization of common fragile site (FRA7H) on human chromosome 7 by the cloning of a simian virus 40 integration site. Proc Natl Acad Sci USA 95:8141–8146.
Oates AJ, Schumaker LM, Jenkins SB, Pearce AA, DaCosta SA, Arun B, Ellis MJ. 1998. The mannose 6-phosphate/insulin-like growth factor 2 receptor (M6P/IGF2R), a putative breast tumor suppressor gene. Breast Cancer Res Treat 47:269–281.
Ohta M, Inoue H, Cotticelli MG, Kastury K, Baffa R, Palazzo J, Siprashvili Z, Mori M, McCue P, Druck T, Croce CM, Huebner K. 1996. The *FHIT* gene, spanning the chromosome 3p14.2 fragile site and renal carcinoma-associated t(3;8) breakpoint, is abnormal in digestive tract cancers. Cell 84:587–597.
Paige AJ, Taylor KJ, Stewart A, Sgouros JG, Gabra H, Sellar GC, Smyth JF, Porteous DJ, Watson JE. 2000. A 700-kb map of a region of 16q23.2 homozygously deleted in multiple cancers and spanning the common fragile site FRA16D. Cancer Res 60:1690–1697.
Paige AJW, Taylor KJ, Taylor C, Hillier SG, Farrington S, Scott D, Porteous DJ, Smyth JK, Gabra H, Watson JEV. 2001. WWOX: a candidate tumor suppressor gene involved in multiple tumor types. Proc Natl Acad Sci USA 98:11414–11422.
Racine C, Belanger M, Hirabayashi H, Boucher M, Chakir J, Couet J. 1999. Reduction of caveolin 1 gene expression in lung carcinoma cell lines. Biochem Biophys Res Commun 255:580–586.
Shridhar V, Lee J, Pandita A, Iturria S, Avula R, Staub J, Morrissey M, Calhoun E, Sen A, Kalli K, Keeney G, Roche P, Cliby W, Lu K, Schmandt R, Mills GB, Bast RC Jr, James CD, Couch FJ, Hartmann LC, Lillie J, Smith DI. 2001. Genetic analysis of early- versus late-stage ovarian tumors. Cancer Res 61:5895–5904.
Siprashvili Z, Sozzi G, Barnes LD, McCue P, Robinson AK, Eryomin V, Sard L, Tagliabue E, Greco A, Fusetti L, Schwartz G, Pierotti MA, Croce CM, Huebner K. 1997. Replacement of Fhit in cancer cells suppresses tumorigenicity. Proc Natl Acad Sci USA 94:13771–13776.
Smith DI, Huang H, Wang L. 1998. Common fragile sites and cancer [review]. Int J Oncol 12:187–196.
Sun Z, Pan J, Bubley G, Balk SP. 1997. Frequent abnormalitites of TSG101 transcripts in human prostate cancer. Oncogene 15:3121–3125.
Tatarelli C, Linnenbach A, Mimori K, Croce CM. 2000. Characterization of the human testin gene localized in the FRA7G region at 7q31.2. Genomics 68:1–12.
Thorland EC, Myers SL, Persing DH, Sarkar G, McGovern RM, Gostout BS, Smith DI. 2000. Human papillomavirus type 16 integrations in cervical tumors frequently occur in common fragile sites. Cancer Res 60:5916–5921.
Verma RS, Babu A. 1995. Human chromosomes: principles and techniques, Second Ed. New York: McGraw-Hill. 419 p.
Wilke CM, Hall BK, Hoge A, Paradee W, Smith DI, Glover TW. 1996. FRA3B extends over a broad region and contains a spontaneous HPV16 integration site: direct evidence for the coincidence of viral integration sites and fragile sites. Hum Mol Genet 5:187–195.
Yu Y, Xu F, Peng H, Fang X, Zhao S, Li Y, Cuevas B, Kuo WL, Gray JW, Siciliano M, Mills GB, Bast RC Jr. 1999. NOEY2 (ARHI), an imprinted putative tumor suppressor gene in ovarian and breast carcinomas. Proc Natl Acad Sci USA 96:214–219.
Yunis JJ. 1983. The chromosomal basis of neoplasia. Science 221: 227–236.
Yunis JJ, Soreng AL. 1984. Constitutive fragile sites and cancer. Science 226:1199–1204.

DOI 10.1002/cyto.10042

Cytometry 47:60-62 (2002)

Transcriptional Profiling Develops Molecular Signatures For Ovarian Tumors

David I. Smith

Mayo Clinic Cancer Center, Rochester, Minnesota

Of the cancers unique to women, ovarian cancer has the highest mortality rate. Over 26,000 women are diagnosed with this disease in the U.S. annually, and 60% of those diagnosed will die of the disease. One of the greatest problems with this disease is the lack of strong early warning signs or symptoms resulting in advanced stage at presentation in most women, followed by the outgrowth of chemotherapy-resistant disease in the majority of patients. The 5-year survival for patients with early stage disease ranges from 50-90%, but it is less than 25% for advanced-stage disease. In collaboration with researchers at Millennium Predictive Medicine (Cambridge, MA), the Ovarian Cancer Program of the Mayo Clinic Cancer Center analyzed gene expression in over 50 primary ovarian tumors, as compared with normal ovarian epithelial cells. The technologies utilized included microarray analysis with nitrocellulose filters containing 25,000 arrayed human cDNAs, as well as the construction of subtraction suppression hybridization cDNA libraries and their subsequent sequencing. Our specific focus has been on genes that are underexpressed during the development of ovarian cancer, although this analysis has revealed a large number of consistently up- and down-regulated genes. There were more down-regulated genes in ovarian tumors than up-regulated genes. In addition, the number of genes that had altered expression levels was quite large. For example, we found 409 genes down-regulated at least 5-fold, and 72 genes up-regulated at least 5-fold in 33% of the tumors analyzed. We also observed that most of the expression alterations observed in later stage (Stages III/IV) tumors were also observed in early-stage tumors (Stages I/II). This was corroborated using comparative genomic hybridization analysis on the same tumors that were expression profiled. This analysis revealed that the late-stage tumors had more gene amplification than early-stage tumors, but most regions of change (either increases or decreases) were in common between different stage tumors. We also have verified the altered expression levels of several of these genes using several complementary strategies. Finally, we are taking top candidate genes that are consistently under-expressed in ovarian tumors and attempting to determine their functional role in the development of ovarian cancer. Cytometry 47:60-62, 2002.

OBJECTIVES

Our goal was to analyze gene expression in ovarian tumors to identify genes that are consistently aberrantly regulated during the development of ovarian cancer. We partnered with researchers at Millennium Predictive Medicine (MPMx) to gain access to their high-throughput technologies for constructing and analyzing cDNA microarrays as well as for generating and characterizing subtraction suppression hybridization cDNA libraries. We wanted to compare the expression profiles of low-stage tumors with those of high-stage tumors to determine if genes that were differentially expressed between low- and high-stage tumors gave any insights into the dramatic differences in survival between patients with low-stage versus high-stage disease.

WHAT WE DID

Researchers at MPMx prepared 25K cDNA arrays which contained approximately 18,000 independent genes. High-quality RNA was prepared from over 50 primary ovarian tumors (representing different histologies and stages), radiolabeled and hybridized to the 25K arrays. Gene expression in the tumors was compared with that of noncultured normal ovarian epithelium. To complement the microarray analysis and potentially to identify additional genes, we also performed both differential display analysis (This work only identified 100 differentially expressed genes.) and constructed a number of SSH cDNA libraries that were sequenced and characterized by MPMx.

Ovarian-dedicated arrays containing any aberrantly regulated genes (identified from the microarrays, differential display, or SSH libraries) were then produced, and these are being used currently to analyze a much greater number of primary ovarian tumors. This analysis should

This work was supported by a Program Project Grant obtained from the Department of Defense (D.I. Smith, principal investigator), the Women's Cancer Program, and the Ovarian Cancer Program of the Mayo Clinic Cancer Center.

Correspondence to: David I. Smith, Cancer Genetics Program, Mayo Clinic Cancer Center, Rochester, MN 55905

E-mail:smith.david@mayo.edu

certainly yield a number of consistently over-expressed genes, several of which may make excellent genes for the early detection of ovarian cancer. This analysis also may yield a number of important genes that can differentiate among tumors with different histologies as well as among those with a distinct clinical outcome.

We then used a number of complementary techniques to verify that some of the genes identified were indeed aberrantly expressed in the primary tumors. These included Northern blot and reverse transcriptase polymerase chain reaction (RT-PCR) analyses in a panel of ovarian cancer cell lines followed by RT-PCR analysis with the primary tumors. We found that only 70% of the genes which appeared to be aberrantly expressed as determined by microarray analysis were indeed aberrantly expressed.

One of the greatest problems with this technology for global expression profiling is determining which genes of the hundreds or thousands of aberrantly regulated genes are worthy of study. We have employed functional analysis of several top candidates to demonstrate that aberrant regulation of these genes might have a functional consequence that would promote ovarian tumor development. Genes were reintroduced into ovarian cancer cell lines that were not expressing those genes, and the cell lines were analyzed for changes in growth characteristics, growth in soft agar, and sensitivity to chemotherapeutic agents (as chemoresistance is an important clinical part of the lethality of ovarian cancer).

WHAT WE OBSERVED

The 25K cDNA arrays were used to analyze over 50 primary ovarian tumors. Each tumor was hybridized to duplicate membranes, and the overall reproducibility on these filters was found to be quite high. Gene expression levels in the tumors were compared with noncultured ovarian epithelial cells (from brushings obtained from women without ovarian cancer that were having oophorectomies). We divided gene expression changes into > 2-fold, 5-fold, 10-fold, and 20-fold for both down- and up-regulated genes. Next we determined the proportion of the 50 tumors in which 2-fold, 5-fold, etc., changes in expression occurred. We found that there were many more down-regulated genes than up-regulated genes in ovarian tumors. For example, we found 24 genes that were down-regulated at least 5-fold in all the tumors profiled but only a single gene up-regulated 5-fold in all the samples.

How much of a change in expression is significant and in what proportion of the tumors must that change occur to be worthy of study? This is an important question as there were 5718 genes that were 2-fold down-regulated in at least 20% of the tumors and 4303 up-regulated genes, which is far too many genes to analyze. However, if we opt for the most stringent of criteria (for example, at least a 10-fold change in all of our samples), we find only 9 down-regulated genes and no up-regulated genes. We arbitrarily decided to examine genes that were at least 5-fold down-regulated in > 50% of the tumors analyzed (This is a list of 179 genes.).

The profound difference in survival between patients with early-stage disease as compared with those with late-stage disease suggests that there may be profound differences in gene expression between early- and late-stage disease and that some of these genes may be important in determining these differences. However, when we compared the expression profiles between early- and late-stage disease, we found that most of the genes that are aberrantly expressed in late-stage tumors are also aberrantly expressed in the early-stage tumors. There were indeed differences, and we detected several genes that were only aberrantly expressed in the late-stage tumors as well as several that were only aberrantly expressed in the early-stage tumors. We then used comparative genomic hybridization to analyze the same tumors that were transcriptionally profiled. This analysis revealed that the majority of the chromosomal regions that had either consistent losses or gains in ovarian tumors was common to both early- and late-stage tumors. The one important distinction that we did observe is that gene amplification was very infrequent in early-stage tumors but much more common in late-stage tumors.

Our strategy for verifying that these genes were indeed aberrantly regulated was to first analyze gene expression in a panel of ovarian cancer cell lines. We then tested gene expression in primary ovarian tumors using semi-quantitative RT-PCR analysis. To confirm that the aberrant expression detected was due to changes in the ovarian tumors themselves and not due to changes in contaminating stromal cells or infiltrating lymphocytes, we performed RNA in situ hybridization analysis of a number of our top candidate genes. These analyses revealed that only 70% of the genes determined to be aberrantly regulated from microarray analysis were indeed aberrantly regulated.

Finally we performed functional analysis with several of the consistently under-expressed genes. One gene, which was previously identified using differential display analysis, codes for a protein with a DNAJ domain. This gene, designated MCJ (for methylation-controlled J Protein), was consistently not expressed in ovarian tumors. We determined that this gene's expression is inactivated by loss of one allele (detected by loss of heterozygosity) and methylation of the remaining allele. This gene was introduced again into two ovarian cancer cell lines that did not express the gene, and we found that expression of this gene was associated with enhanced sensitivity to paclitaxel, topotecan, and cisplatin, suggesting that loss of MCJ expression may play a role in the de novo chemoresistance in ovarian carcinoma.

CONCLUSIONS AND FUTURE DIRECTIONS

We have used transcriptional profiling to analyze gene expression in primary ovarian tumors. This analysis has revealed that there are more genes that are down-regulated than up-regulated during the development of ovarian cancer. Surprisingly, most of the aberrantly regulated

genes in late-stage tumors also are aberrantly regulated in early-stage tumors. Indeed, the most profound difference that we observed between early- and late-stage tumors was that gene amplification was common only in late-stage tumors. Currently, a much larger number of primary ovarian tumors (representing all the distinct histologies of ovarian cancer) are being analyzed using arrays containing genes that appeared to be aberrantly regulated on the primary arrays or were identified from differential display or SSH cDNA libraries. This analysis should give us a large list of genes that we will need to examine before choosing a manageable number of genes to be characterized in much greater detail.

Our goal is to determine the number of genetic alterations that underlie the development of ovarian cancer. We also would like to identify the earliest genetic alterations that occur, as this will give much greater insight into the process whereby ovarian cancer develops. This work will generate markers that can be used to distinguish tumors of distinct histologies as well as clinical outcome. Our goal is to use this information to understand better the biology of this disease.

ACKNOWLEDGEMENTS

The author acknowledges all the members of the Ovarian Cancer Program of the Mayo Clinic Cancer Center. Special acknowledgement must go to Dr. Lynn Hartmann, the co-leader who started the Ovarian Program 10 years ago. Dr. Viji Shridhar performed much of the work described above in collaboration with the researchers at Millennium including Dr. Jim Lillie and John Lee.

Loss of hSulf, a Novel Sulfatase That Modulates Heparin Binding Growth Factor Signaling, in Ovarian Carcinoma

Jinping Lai[1], Jeremy Chien[2], Julie Staub[2], Rajeswari Avula[2], Eddie L.Greene[3], Tori A. Mathews[3], David I Smith[2], Scott H Kaufmann[4], Lewis R Roberts[1*], Viji Shridhar[2*#]

Mayo Clinic Cancer Center

Division of Gastroenterology and Hepatology[1]

Department of Experimental Pathology[2]

Department of Nephrology[3]

Department of Molecular Pharmacology and Experimental Therapeutics[4]

Mayo Clinic and Foundation, Rochester, MN 55905

* Both authors equally contributed to this work.

#Correspondence:

Viji Shridhar, Ph.D

Assistant Professor

Mayo Clinic Cancer Center

Division of Experimental Pathology

Mayo Foundation

200 First Street SW

Rochester, MN 55905

Phone (507) 266-2775

FAX (507) 266-5193

E-mail: shridv@exrch.mayo.edu

Summary

The sulfation state of cell surface heparan sulfate proteoglycans (HSPGs) is a determinant of growth factor signaling. Here, we report the identification of hSulf, a member of an evolutionarily conserved family of heparan-specific N-acetyl glucosamine sulfatases, as a down-regulated gene in ovarian carcinomas. Semi-quantitative RT-PCR analysis with overlapping primers flanking the open reading frame revealed complete loss of expression in five of seven ovarian cancer cell lines and complete loss or markedly diminished expression in 25/31 (80%) of primary ovarian tumors. Further analysis demonstrated that hSulf localizes to the cell surface, where it decreases the sulfation state of heparan sulfate glycosaminoglycans (HS-GAGs), diminishes signaling induced by heparin binding growth factors, and facilitates stress-induced apoptosis. Collectively, these observations provide evidence for a unique mechanism by which growth factor signaling is uregulated during ovarian carcinogenesis.

Significance

Emerging data suggests signaling by heparin binding growth factors (HB-GFs) is influenced by the sulfation states of N-acetyl glucosamine residues of heparan sulfate proteoglycans (HSPGs), indicating a regulatory function of the sulfated HSPGs in signal transduction pathways mediated by HB-GFs. In this report, we describe the cloning of a new sulfatase domain containing protein designated hSulf and functional consequences of its loss in ovarian cancer. Our current studies demonstrate that increased expression of hSulf resulted in diminished levels of HSPG sulfation and a consequent attenuation of growth factor signaling mediated by FGF and HB-EGF, that may account for the function of hSulf as a suppressor of tumor growth. These data suggest that loss of expression of hSulf may provide cancer cells a novel mechanism to promote growth factor signaling.

Introduction

In the United States there are 27,000 new cases and 14,000 deaths from ovarian cancer annually (Greenlee et al., 2000). An improved understanding of the genetic alterations associated with the development and progression of this cancer could conceivably allow the development of early detection markers as well as novel therapeutic targets. Although neoplasia involves many processes, the underlying platform for cancer development is deregulated proliferation and suppression of cell death (Green, 1998; Hanahan and Weinberg, 2000). Genes previously implicated in the development of ovarian cancer include *c-myc, EGFR* 1, 2 and 4 (Berchuck et al., 1990; Gilmour et al., 2001; Plowman et al., 1993; Slamon et al., 1989), phosphotidyl inositol 3 kinase (*PI3K*) and its downstream effector *AKT2* (Mills et al., 2001), *p53* (Murphy et al., 1997) and *ARHI* (Yu et al., 1999). LOH studies have delineated several chromosomal regions (6q, 7q, 9p, 11p, 13q, 17p, 17q, 18q, 22 and X) that harbor potential tumor suppressor genes involved in the development of ovarian cancer (Cliby et al., 1993; Colitti et al., 1998; Devlin et al., 1996; Englefield et al., 1994; Gabra et al., 1996; Kerr et al., 1996; Latil et al., 1994; Lu et al., 1997; Shridhar et al., 1999; Yang-Feng et al., 1992). In addition, altered expression of and signaling by growth factors such as FGF, VEGF and HB-EGF is also frequently seen in ovarian cancer (Crickard et al., 1994; Di Blasio et al., 1995; Doldi et al., 1996; Garzetti et al., 1999; Raab and Klagsbrun, 1997; Wang et al., 2002). Thus, the genetic and biochemical changes underlying the development and progression of ovarian cancer are complex.

Several growth factors, including FGF, PDGF, HGF, VEGF and HB-EGF, are known to bind heparin. Signaling by these heparin binding growth factors (HB-GFs) is influenced by the sulfation states of N-acetyl glucosamine residues of heparan sulfate proteoglycans (HSPGs), indicating a regulatory function of the sulfated HSPGs in signal transduction pathways mediated by HB-GFs (Davis-Fleischer and Besner, 1998; Fu et al., 1999; Garzetti et al., 1999; Mishima et al., 1998; Ono et al., 1999; Peifley et al., 1996; Raab and Klagsbrun,

1997). Therefore, enzymes that regulate the sulfation status of heparan sulfate glycosaminglycans (HS-GAGs) may modulate growth factor signaling at the cell surface. Consistent with this notion, Dhoot et al (Dhoot et al., 2001) recently cloned the avian sulfatase Qsulf1and provided indirect evidence that it regulates Wnt signaling through desulfation of the cell surface HSPGs.

In this report, we describe the molecular cloning and function of a new member of the sulfatase domain containing protein family designated hSulf and describe the functional consequences of its loss in ovarian cancer. We previously performed suppression subtraction hybridization analyses (SHH) of two early and late stage tumors subtracted against normal ovarian epithelial brushings. These studies resulted in the identification of several transcripts that are differentially expressed in ovarian cancer (Shridhar et al., 2002). One of these encodes a novel 871 amino acids long polypeptide that contains a highly conserved sulfatase domain. Our current studies demonstrate that decreased expression of hSulf is common in human ovarian cancer, that it results from deletion of one of the hSulf alleles by LOH, and that it results in enhanced signaling by two different heparin binding growth factors, FGF and HB-EGF. These observations identify a previously unidentified strategy used by cancer cells to enhance growth factor signaling.

Materials and Methods

Cell Culture

Five of seven ovarian-carcinoma cell lines (OV167, OV177, OV202, OV207, and OV266) were cell lines established at the Mayo Clinic (Conover et al., 1998), while OVCAR-5 and SKOV-3 were purchased from American Type Culture Collection (Manassas, VA). All cells were grown according to the provider's recommendations.

Drugs and Reagents

Staurosporine (Sigma, St. Louis, MO) and UCN-01 (Drug Synthesis Branch, National Cancer Institute) were dissolved in DMSO at a concentration of 1 mM, stored at –20°C and subsequently diluted with serum free medium before use. In all experiments the concentration of DMSO did not exceed 0.1%. The broad spectrum caspase inhibitor N-(N$^{\alpha}$-benzyloxycarbonylvalinylalanyl) aspartic acid (O-methyl ester) fluoromethylketone [Z-VAD(OMe)-fmk] was dissolved in DMSO and stored at 4°C.

Strategy for Cloning the Gene

BLAST search of the isolated sequence from SSH libraries of early and late stage tumors identified ESTs homologous to KIAA1077 in the dbEST. The homologous ESTs were assembled into a contig with the use of Sequencher 3 (Gene Codes Corp, Ann Arbor, MI) software. Additional 5' sequences not present in KIAA1077 were obtained with electronic walking by assembling overlapping EST sequences in the genome BLAST server. The integrity of the full-length cDNA obtained by this electronic walking was confirmed by PCR analysis using PCR primers flanking each junction between EST clones. The entire cDNA contig was sequenced twice with overlapping primers.

Cloning of Flag (Flg)-tagged N-terminal Sulf (N-Sulf), C terminal Sulf (C-Sulf) and Full-length Sulf (FL-hSulf).

The N terminal portion of hSulf (N-Sulf) containing only the sulfatase domain was amplified using primers NF (5'-ATTGGACCAAATACAATGAAG-3') and NRFlg (ttaagccttgtcatcgtccttgtagtcGAATGTATCACGCCAAAT). The C terminal domain (C-Sulf) was amplified using primers CF (5'- CGTGATACATTCCTAGTGG) and CRFlg (ttaagccttgtcatcgtccttgtagtcACCTTCCCATCCATCCCA) with a stop codon introduced after the epitope tag (lower case letters). The full-length (FL) hSulf was amplified using primers NF and CRFlg using Expand™ Long Template PCR system (Boehringer Mannheim, Indianopolis,). All three products were cloned into GFP Fusion TOPO® TA Expression plasmid (Invitrogen Corp, Carlsbad CA). For generating a FL hSulf GFP fusion construct for immunocytochemistry, the stop codon of CRFlg was not included. cDNAs generated from short-term cultures of normal ovarian surface epithelial cells (OSE) were used as a template for generating PCR products for cloning. The products of each PCR reaction were resolved on a 1.6% agarose gel and purified using a gel extraction kit (Qiagen, Valencia, CA) for cloning into expression vectors.

Establishment of hSulf -Stable Transfectants

Exponentially growing SKOV3 cells in 100 mm dishes were washed with serum free medium, and treated with a mixture of 4 μg of plasmid, 30 μl of LipofectAmine, and 20 μl of Plus reagent. After 3 hr incubation, complete medium with serum was added. G418 (400 μg/ml) was added 24 hours after transfection to select transfectants. Several stable clonal transfectants, hSulf clones #3-9, were subsequently generated. For controls, cells were similarly transfected with vector (pcDNA3.1 GFP) and selected.

Semi-quantitative RT-PCR.

Total RNA was extracted from 7 ovarian cancer cell lines and 31 primary ovarian tumors using the RNeasy mini kit (Qiagen). cDNA synthesis was performed using a Superscript II RNnase H⁻ reverse transcriptase kit (Life Technologies, Bethasda, MD) to transcribe 1-5μg of total RNA with 1μl of 500 μg/ml oligo$(dT)_{12-18}$ primer. 50-100 ng of reverse transcribed cDNA was used in a multiplex reaction with three different primer pairs Sulf-1F (5'-CCACCTTCATCAATGCCTT-3'), Sulf-1R (5'-CCTTGACCAGTCCAAACCTGC-3'), Sulf-2F (5'-CATCATTTACACCGCCGACC), Sulf-2R (5'-CTGCCGTCTCTTCTCCTTC-3'), Sulf-3F (5'-GAGCCATCTTCACCCATTCAA-3'), Sulf-3R (5'-TTCCCAACCTTATGCCTTGGGT-3') and GAPDH-F (5'-ACCACAGTCCATGCCATCAC-3') and GAPDH-R (5'-TCCACCACCCTGTTGCTTGTA-3') in separate reactions to yield 760 bp, 1260 bp and 825 bp products respectively. The PCR reaction mixes contained 50 mM KCl, 10 mM Tris-HCl (pH 8.3), 1.5 mM $MgCl_2$, 400 μM concentration of each primer for hSulf and 50 μM for the GAPDH primers, and 0.5 units of Taq polymerase (Promega) in a 12.5 μl reaction volume. The conditions for amplification were: 94°C for 3 min followed by 29 cycles of 94°C for 30 sec, 58°C for 30 sec, and 72°C for 30 sec in a Perkin Elmer-Cetus 9600 Gene-Amp PCR system. The products of the reaction were resolved on a 1.6% agarose gel and quantified using the Gel Doc 1000 photo documentation system.

LOH Analysis

The 5 pairs of microsatellite markers within the hSulf gene used in this study are listed in Table 1 along with their locations within the hSulf gene. The PCR reaction mix contained: 50 ng of genomic DNA, 50 mM KCl, 10 mM Tris-HCl (pH 8.3), 1.5 mM $MgCl_2$, 200 μM concentration of each primer, 0.05 μl of [P^{32}] CTP (10 μCi/ul) and 0.5 units of Taq polymerase (Promega) in a 10 μl reaction volume. Amplifications were performed as described above

except that annealing was performed at 52-57°C and reactions were run in a 96 well plate. After denaturation, PCR products were run on 6% polyacrylamide sequencing gels containing 8 M urea. Gels were dried, subjected to autoradiography using multiple exposure times, and scored for LOH. Allelic imbalance indicative of LOH as scored when there was more than 50% loss of intensity of one allele in the tumor sample with respect to the matched allele from normal tissue.

Northern Blot

Total RNA (15 µg) was fractionated on 1.2% formaldehyde agarose gels and blotted in 1X SPC buffer (20 mM Na2HPO4, 2 mM CDTA pH6.8) onto Hybond-N membranes (Amersham, Piscataway, NJ). The probes were labeled using the random primer labeling system (Life technologies, Inc.) and purified using spin columns (100 TE) from Clontech. Filters were hybridized at 68 °C with radioactive probes in a hybridization incubator (Model 2000; Robbins Scientific, Sunnyvale, CA) and washed according to the manufacturer's guidelines.

Analysis of Apoptosis

Apoptosis was quantitated using fluorescence microscopy by assessing the nuclear changes indicative of apoptosis (chromatin condensation and nuclear fragmentation) using the DNA binding dye 4',6-diamidino-2-phenylindole (DAPI) dihydrochloride. hSulf transfected SKOV3 cells were seeded in 35-mm plates at a density of 2 x 10^5 cells/well. After incubation at 37 °C for 24 h, the plates were washed and changed to serum-free medium. Staurosporine was added to a final concentration of 1 µM for 5 h. DAPI was then added to each well. After a 20 min incubation at room temperature in the dark, cells were examined by fluorescence microscopy (Nikon Eclipse TE200; Nikon Corp., Tokyo, Japan) using excitation and emission filters of 380 and 430 nm. An individual blinded to the experimental conditions counted at least 300 cells in six different high-power fields for each treatment. Each treatment was repeated at least

three times, performed in triplicate each time. To inhibit apoptosis, the cells were pretreated with 40 μM Z-VAD(OMe)-fmk for 1 h before the addition of staurosporine. The significance of differences between experimental variables was determined using the Student *t* test.

DNA Fragmentation

Parental, vector and stable hSulf clones 3 and 6 were treated with 1 μM staurosporine at 37°C for 5 hours. 5 x 10^5 control or treated cells were harvested with trypsin and centrifuged. DNA was extracted using the Quiagen DNeasy kit. Alqiuots containing 5 μg were resolved on a 1.5% agarose gel containing 0.5 μg/ml ethidium bromide and visualized under UV light.

Flow Cytometry

After treatment with 1 μM staurosporine for 5 h as described above, cells were washed twice in ice cold PBS containing 3% heat-inactivated fetal bovine serum and 0.02% of sodium azide, stained with 7-AAD (50 μg/ml) for 15 min in the dark, resuspended in 500 μl PBS and subjected to flow cytometry on a FACScan analyzer (BD Biosciences, San Jose, CA). After analysis of 10000 events, the percentage of 7-AAD positive cells was determined.

Analysis of Cytosolic Cytochrome c

Parental SKOV3, stable clones of SKOV3-vector, and SKOV3-hSulf clones 3 and 6 were treated with staurosporine as described above, washed in PBS and lysed by incubating for 30 s in lysis buffer consisting of 210 mM D-mannitol, 70 mM sucrose, 10 mM HEPES, 5 mM sodium succinate, 0.2 mM EGTA, 0.15% BSA and 80 μg/ml digitonin. After sedimentation at 12,000 x g for 1 min, the supernatant was diluted with an equal volume of 2 X sample buffer. The protein samples were quantified, resolved on a 12% SDS-PAGE gel, and subjected to immunoblot analysis as described below using anti-cytochrome c (mouse mononclonal; Pharmingen) at a dilution of 1:500.

FGF2, HB-EGF and EGF Treatment and Protein Extraction

To confirm the role of hSulf in HB-GF mediated signaling, vector-transfected and hSulf clones 7 and 8 were serum starved for 8 -12 h, treated with diluent, 1 ng/ml FGF2, 100 ng/ml of HB-EGF (Sigma, St Louis, MO) or 10 ng/ml EGF for the times indicated in individual figures. Following treatment, cells were rinsed with ice cold PBS, scraped from the dishes, lysed at 4°C in Laemelli buffer without bromophenol blue. Protein concentrations were determined with bicinchonic acid (Pierce, Rockford, IL).

Immunoblot

Equal amounts of protein (20 µg/lane) were separated by electrophoresis on a 4-12% Glycine-SDS gel and electrophoretically transferred to nitrocellulose. Blots were washed once with TBS-0.2% Tween 20 (TBST) and blocked with TBST containing 5% non-fat dry milk for 1 h at room temperature. The blocking solution was replaced with a fresh solution containing 1:500 dilution of rabbit anti-phospho42/44MAPK (Cell Signaling Inc, Beverly, MA). After overnight incubation at 4 °C, the blots were washed three times for 10 min each in TBS/0.1% Tween and incubated with horseradish peroxidase- conjugated secondary antibody in 5% milk/TBST at room temperature for 1 h. After washing 3 times in TBST, the proteins were visualized using enhanced chemiluminescence (Amersham, Arlington Heights, IL). The blots were stripped and reprobed with 1:500 dilution of antibody to total MAPK (Cell Signaling Inc), 1:1000 dilution of rabbit sera that recognize EGFR phosphorylated on Tyr 1068 and /or 992, or 1:1000 dilution of rabbit anti EGFR (Cell Signaling Inc, Beverly, MA), and/or 1:1000 dilution of mouse moclonal antibody to actin (Sigma, St Louis, MO).

hSulf Localization

For localization of hSulf, SKOV3 cells seeded on glass cover slips in 6-well plates overnight were transfected with C-terminal GFP-tagged full-length hSulf or GFP expression plasmid as a

control. Twenty-four hours after the transfection, cells were fixed in 4% paraformaldehyde, permeablized with 0.2% Triton X-100, and then mounted with Vectorshield® mounting medium with DAPI. The GFP fusion protein was visualized using a Zeiss LS510 laser scanning confocal microscope. Alternatively, SKOV3 cells were transfected with 4 μg of Flag-tagged hSulf construct, incubated for 24 h, washed with PBS, fixed for 10 min in PBS containing 3.7% formaldehyde and 1% sucrose, washed with 0.1 M glycine in PBS, permeabilized with PBS containing 0.4% Triton X-100 and 2% BSA for 20 min, and washed three times in washing buffer (PBS containing 0.2% bovine serum albumin and 0.1% Triton X-100). After incubation for 1 h at room temp. with anti-EGFR antibody, cells were washed four times with washing buffer, incubated with 1:200 TRITC-conjugated anti-rabbit IgG and 1:200 FITC-conjugated anti-FLAG monoclonal antibody (Sigma) in the dark, washed twice in washing buffer, stained with 0.5 μg/ml DAPI for 5 min, washed twice in PBS, mounted onto slides and viewed with an Axiovert 35 epifluorescence microscope (Carl Zeiss Thornwood, NY) equipped with a 100-W mercury lamp or a confocal microscope (Zeiss LSM-510).

Sulfation State of Cell Surface HS-GAGs

Parental, stable vector and hSulf clones 7, 8, and 9 were grown on cover slips for 24 h, fixed in methanol for 10 min at –20°C, washed with PBS, and incubated with for 1 h at room temp. with 1:30 dilution of primary anti-mouse antibody recognizing native heparan sulfate that includes the N-sulfated glucosamine residue (10E4-mAb Seikagaku America, Falmouth, MA). After washing, cells were stained with FITC-conjugated anti-mouse IgG and examined by laser scanning confocal microscopy as described above.

Results

Isolation and cloning of a novel cDNA containing a highly conserved sulfatase domain

Differential screening of suppression subtraction cDNA libraries generated from primary ovarian tumors subtracted against normal ovarian epithelial cells (Shridhar et al., 2002) identified an EST homologous to KIAA1077 in the genebank database. Examination of the 4834 bp sequence of KIAA1077 in the database revealed that it was a partial cDNA. Once the full-length hSulf was assembled into a contig with the use of Sequencher 3 software, the full-5699 bp cDNA containing a single open reading frame coding for a 871 amino-acid long protein was isolated (GenBank accession number, AF545571). A putative initiation codon occurs within a strong Kozak context (Kozak, 1996; Kozak, 1999) and is preceded by a stop codon. hSulf was mapped to chromosome 8q13.3 based on the Human Genome BLAST server database. This information, combined with PCR analysis, was used to map the 23 exons of hSulf distributed across approximately 250 kb of DNA. The sufatase domain (1230 bases) spans from 3' end of exon 5 (41 bases) to most of exon 13. The translational codon initiates in exon 5 (Fig. 1A). There are 706 bases of 5' UTR and 2377 bases in the 3'UTR. There are five potential polyadenylation signals AATAAA at positions 4170, 4679, 4820, 4824, 5052 and 5678.

The predicted protein encoded by hSulf (KIAA1077) shares extensive sequence homology to rat Sulf (88%) and to a recently identified sulfatase gene in quail embryos (Qsulf1)(81%) (Fig. 1B) as well as 30% and 45% identity to two other sulfatase domain containing proteins, arylsulfatase and N-acetylglucosamine-6 sulfatase, respectively. hSulf was also 62% identitical to KIAA1247, a gene mapping to 20q12-13. The SULF1 gene of *D.melanogaster* and *C.elegans* were two other genes with a high degree of identity to hSulf (59% and 50% respectively). Based on the computer algorithm, Signal PV1.1 at the Centre for

Biological Sequence Analysis website (Nielsen et al., 1997a; Nielsen et al., 1997b), a 22 amino acid long N-terminal signal peptide (MKYSCCALVLAVLGTELLGSLC↓ST) was identified, with the most likely cleavage site (↓) located between positions 22 and 23. Based on TMPRED (Stoffel, 1993) there are two other putative membrane-spanning domains in addition to the signal peptide, one spanning amino acids #69-88 and the other spanning amino acids #754-779 near the C terminus. Figure 1C shows the sulfatase domain alignment of hSulf to other sulfatase domain containing proteins.

Decreased expression of hSulf in ovarian cancer cell lines and primary tumors

To validate the results obtained by SSH analyses, hSulf expression was evaluated in 7 ovarian cancer cell lines and 31 primary ovarian tumors. Semi-quantitative RT-PCR analysis with overlapping hSulf primers spanning the open reading frame (Fig. 2A) and northern blot analysis (Fig. 2B) demonstrated that hSulf expression was lost in 5 of 7 ovarian cancer cell lines and undetectable or markedly diminished expression relative to normal ovarian surface epithelium (OSE), the cell of origin, in > 80% of the primary ovarian tumors (25/31).

hsulf is ubiquitously expressed

Northern blot analysis revealed that hSulf codes for a 5.7 and a smaller 5.5 kb transcript in a tissue restricted manner (Fig. 2C). The smaller transcript is an alternatively spliced form of hSulf with missing exon 20 that shifts the reading frame and codes for a 790 amino acid long protein (data not shown). Expression of hSulf mRNA is higher in small intestine and colon compared to ovary. A smaller transcript is present in the testis. Spleen, thymus and peripheral blood leukocytes do not express hSulf.

LOH analysis of hSulf in primary ovarian tumors

Genomic sequence analysis of hSulf revealed microsatellite markers in the 5' UTR, one each in introns 1 and 2, and two within intron 3. The primers flanking these repeats are shown

in Table 1. Analysis with these markers in 30 primary ovarian tumor samples revealed that LOH ranged from 44-53% with these markers (Figs. 3A and B).

hSulf modulates staurosporine-induced apoptosis

A parental non-expressing primary ovarian carcinoma cell line (SKOV3), vector transfected SKOV3 control and two hSulf expressing stable clones in SKOV3 (#3 and #6) were tested for the expression of hSulf by semiquantitative RT-PCR. Only the two hSulf transfectants expressed hSulf transcript (Insert in Fig. 4A). These clones did not exhibit appreciably different growth properties compared to parental or vector only-transfected cells (data not shown). In an effort to further examine the biological consequences of changes in hSulf expression, the transfectants were treated for 5 h with 1 μM staurosporine, a non-specific kinase inhibitor that broadly induces apoptosis in all cells (Bertrand et al., 1994). As shown in Fig. 4A, no induction of apoptosis is seen in the parental or vector-transfected SKOV3 cell line after staurosporine treatment. Clones stably transfected with hSulf do not exhibit excess apoptosis in the absence of drug treatment, but instead display markedly enhanced caspase-dependent apoptosis when STP is added. Similar results were obtained when we treated the cells with UCN-01 (7-hydroxystaurosporine), a staurosporine analog currently in clinical trials (Sausville et al., 2001; Wang et al., 1996). Examination of cytochrome c release from mitochondria and DNA fragmentation (Fig. 4B) confirmed the results of the morphological assays. Three additional hSulf expressing stable clones gave similar results on treatment with STP and or UCN-01 (Figs. 4C and D). With these three clones, flow cytometry after staining with 7-AAD provided a fourth assay that confirmed the ability of hSulf to modulate staurosporine-induced apoptosis (Fig. 4E).

Sulfatase activity is required to modulate staurosporine-induced apoptosis

To determine whether an intact sulfatase domain is required for hSulf to modulate staurosporine-induced apoptosis, cells were transiently transfected with an antisense construct of hSulf and a mutated sulfatase domain-containing construct of hSulf. Modulation of apoptosis was more pronounced in cells expressing the N-terminal fragment of hSulf, which contains the sulfatase domain, than in cells expressing the C-terminal domain C-Sulf (Fig. 5A). Site directed mutagenesis of the catalytic cysteines C87 and C88 in N-Sulf (mut N-Sulf, Fig. 5B) or the presence of an antisense construct to hSulf (AS, Fig. 5C) attenuated the ability of hSulf to modulate apoptosis, providing evidence that sulfatase activity is required for this modulation.

hSulf is localized to the cell surface

The avian ortholog of hSulf, Qsulf1 was shown to localize to the cell surface through specific interactions of the hydrophilic domain with cell surface components (Dhoot et al., 2001). hSulf, which has a hydrophilic domain homologous to Q Sulf1, also localized to the plasma membrane (Figs. 6A and B), further supporting the possibility that hSulf may modulate growth factor signaling in a manner similar to that observed with Qsulf1. Further analysis (Fig. 6B) demonstrated that tagged hSulf also co-localized with growth factor receptors such as EGFR1 at the cell surface (Fig. 6B).

hSulf expression is associated with decreased levels of sulfated HS-GAGs at the cell surface

To determine whether hSulf expression causes desulfation of cell surface HS-GAGs, cell lines lacking or containing hSulf were stained with an antibody that recognizes native heparan sulfate that includes the N-sulfated glucosamine (Clayton et al., 2001). Parental and vector transfected SKOV3 cells, which do not express hSulf, were compared to three different clones

expressing full-length hSulf. The parental and vector transfected SKOV3 cells showed cell surface staining for N-sulfated glucosamine-containing HS-GAGs, while the cell surface staining was significantly diminished or absent in all three hSulf-expressing clones (Fig. 6C), strongly suggesting that hSulf desulfates HS-GAGs at the cell surface.

hSulf modulates heparin-binding growth factor signaling

N-sulfation and 2-O-sulfation have been shown to be critical for the interaction between HS-GAGs and FGF2, while 6-O-sulfation is required for the interaction between HS-GAGs and FGFR1 in the formation of the FGF2-HSGAG-FGFR1 ternary complex (Lundin et al., 2000; Ornitz, 2000; Padera et al., 1999; Selva and Perrimon, 2001). Conversely, it has been reported that, cells containing GAG chains with reduced sulfation lose their proliferative response to FGF-2 (Delehedde et al., 2002; McKeehan et al., 1998; Ornitz, 2000; Ornitz and Itoh, 2001). These observations, coupled with the demonstration of elevated FGF-2 and FGFR1 in ovarian cancer cells (Crickard et al., 1994; Di Blasio et al., 1993; Valve et al., 2000), prompted us to examine the effect of hSulf on HB-GF signaling.

As a read out for these assays, we focused on events downstream of FGFR occupation. Formation of the FGF2-HSGAG-FGFR ternary complex induces receptor dimerization, the activation of the intracellular FGFR tyrosine kinase (Lepique et al., 2000; Selva and Perrimon, 2001), receptor autophosphorylation, and binding of the adaptor SNT/FRS, which then activates intracellular signaling pathways, including the MAPK pathway (Ornitz and Itoh, 2001; Rapraeger et al., 1991). Sustained phosphorylation of p42/ERK1 and 44/ERK2 has been shown to be required for FGF2-induced cell proliferation (Esko, 1992; Rapraeger et al., 1994). We hypothesized that desulfation of HS-GAGs by hSulf could interfere with this signaling. To assess this possibility, parental, vector-transfected and two hSulf expressing stable clones (7 and 8) were serum starved for 8 h before the addition of 1 ng/ml of non-heparinated FGF-2 or

100 ng/ml HB-EGF for 15, 30 and 60 min. Cells not treated with FGF-2 or HB-EGF (0 min) served as controls. Blotting with anti-phosphoERK1/2 antibody revealed that unstimulated parental (not shown) or vector-transfected cells (Fig. 7A, left panel) had readily detectable constitutive phosphorylation of ERK1 and, to a lower extent, ERK2, whereas hSulf-expressing clones had no detectable activation of this pathway (Fig. 7A, 0 min). In addition, FGF-2 induced strong, sustained phosphorylation of both ERK1 and ERK2 lasting >60 min in parental (not shown) and vector-transfected cells (Fig. 7A, left panel), but only transient and much lower levels of phosphorylation in hSulf-expressing clones (Fig. 7A, middle and right panels). Collectively, these results suggest that hSulf not only down-regulates the basal activation of p42/44MAPK, but also inhibits a sustained activation of p42/44MAPK that may be required for cell survival and proliferation.

Further analysis confirmed the role of the sulfatase domain in this modulation of MAP kinase activity. 24 h after transient transfection of SKOV3 cells with vector, wild-type N-Sulf or C87,88A mutant N-Sulf construct, cells were serum starved for 8 h, treated with 1ng/ml FGF2 for 10 min, and analyzed for MAPK phosphorylation. Results of this analysis (Fig. 7B) revealed that mutation of the active site cysteines abolished the ability of N-Sulf to down-regulate FGF2-induced ERK phsophorylation.

hSulf modulates signaling by heparin binding EGF (HB-EGF) and not by heparin independent EGF (EGF)

To determine whether hSulf also modulates other HB-GF signaling, we examined HB-EGF because of its postulated role in ovarian carcinogenesis (Peoples et al., 1995). Over-expression of EGFR 2 and 4, which mediate the effects of heparin independant EGF and HB-EGF respectively, is well documented in ovarian cancer cells (Berchuck et al., 1990; Gilmour et al., 2001; Henzen-Logmans et al., 1992). HB-EGF treatment of vector-transfected cells

again resulted in sustained MAPK pathway stimulation; and hSulf transfection diminished this signaling dramatically (Fig. 7C). To assess whether this attenuation of MAPK signaling reflected the downregulation of receptor auto-activation, the blots were stripped and probed with phosphospecific anti-EGFR anti-sera recognizing two different autophosphorylation sites, Tyr 1068 and Tyr 992. Results of this analysis demonstrated marked decrease in EGFR phosphorylation in hSulf clones 7 and 8 compared to vector transfected cells (Fig. 7D and data not shown).

In order to show that hSulf modulates only the heparin binding growth factor signaling, we treated serum starved cells with 10 ng/ml EGF for 15 min and determined the levels of phospho-ERK1/2. Untreated cells served as controls. There is no difference in ERK phosphorylation in hSulf expressing clones 7 and 8 compared to vector transfected control upon EGF treatment (Fig. 7E), indicating that hSulf modulates signaling by HB-GFs but not heparin-independent growth factors.

Discussion

In this report, we describe the molecular cloning and function of a new member of the sulfatase domain-containing protein family designated as hSulf. Our studies also demonstrate that decreased expression of hSulf is common in human ovarian cancer and results, at least in part, from deletion of one of the alleles by LOH. We investigated the role of hSulf in modulating signaling by two different heparin binding growth factors, FGF and HB-EGF, and show that the abrogation of FGF and HB-EGF signaling is at least partly responsible for the pro-apoptotic effect of hSulf in the presence of chemotherapeutic agents. Recent studies implicated Qsulf1 in the regulation of Wnt signaling and alluded to the possibility that Qsulf1 could also potentially regulate FGF signaling, which is controlled by 6-O sulfation of N acetyl glucosamine in HSPGs (Kamimura et al., 2001; Lundin et al., 2000). Based on the similarity of hSulf to Qsulf1, we hypothesized that inactivation of hSulf may modulate HB-GF signaling in cancer by altering the sulfation status of HS-GAGs. In particular, heparan sulfate proteoglycans (HSPGs) are found at the surface of virtually every cell type, where they act as important biological mediators of cellular events such as proliferation, morphogenesis, adhesion, migration, and apoptosis. The ability of HSPGs to regulate a variety of cellular processes is due both to structural and chemical diversity of the HS-GAG polymer (Liu et al., 2002; Sasisekharan et al., 2002). Several studies have shown that tumor-cell-surface HS-GAGs can promote growth factor signaling and tumor-cell proliferation. By modulating the overall density and the sulfation pattern of their HSPGs, tumor cells have been reported to increase the affinity of their HSPGs for FGF2, as well as for other growth factors. In the present study, we have demonstrated that hSulf is localized to the same compartment as HS-GAGs, namely the cell membrane, and that re-expression of hSulf in hSulf negative cell lines

leads to a desulfated form of HS-GAGs that is probably not able to sustain survival signaling mediated by heparin binding growth factors.

There are several growth factor signaling pathways modulated by HS-GAGs, the best characterized of which is the role of HS-GAGs in FGF2 signaling. FGF2 binds to its receptor and to HSPGs, which act as co-receptors and promote formation of a ternary complex that is essential for cell proliferation and angiogenesis. Sulfation of specific sites on the HS-GAGs is critical for this interaction. The interaction of FGF2 with FGFR and HS-GAGs leads to receptor dimerization, activation and autophosphorylation followed by activation of downstream signaling pathways, including the mitogen-activated protein kinase (MAPK) pathway. The identification of heparin/HS-GAGs as an active and essential component of the FGF/FGFR signaling complex suggests that FGF activity can be modulated by sulfation status of HS-GAGs or enzymes that degrade or synthesize HS-GAGs. Cells deficient in endogenous HS-GAGs are not responsive to FGF, thus directly implicating the involvement of HS-GAGs in the biological action of FGF (Esko, 1992; Rapraeger, 1995).

While the heparin binding FGF2 signaling and its interaction with HS-GAGs are very well characterized, HB-EGF is not as well studied. The interaction of HB-EGF with cell surface HSPGs has been indirectly demonstrated by ability of sodium chlorate, which inhibits sulfation of HS-GAGs, and heparinase, to abrogate HB-EGF signaling (Higashiyama et al., 1993). In a subsequent study it was demonstrated that ^{125}I-HB–EGF binding was diminished in Chinese hamster ovary cells deficient in HSPG (Aviezer and Yayon, 1994). The role of the HB–EGF heparin-binding domain in binding to HSPG has been demonstrated by showing that synthetic peptides corresponding to the heparin-binding domain of HB–EGF inhibit its binding to wild type CHO cells (Thompson et al., 1994) and to an endometrial cancer cell line (Besner et al., 1992).

In the present study we have observed that re-expression of hSulf attenuates MAPK signaling induced by FGF-2 and HB-EGF but not heparin-independent EGF. Using mutant N-Sulf construct with a mutation in the catalytic site as well as a truncation mutant lacking the sulfatase domain, we have also shown that an intact sulfatase domain is required for this down regulation. Results obtained with HB-EGF mediated signaling also showed complete inhibition of phosphorylation at EGFR tyrosine 1068, a direct binding site for the Grb2/SH2 domain (Rojas et al., 1996), and tyrosine 992, direct binding site for the phospholipase C-γ (PLC-γ) SH2 domain (Emlet et al., 1997), when hSulf is re-expressed, suggesting that signaling has been abrogated at the level of the cell surface receptor. Inhibition of HB-EGF-induced EGFR tyrosine phosphorylation at these two sites in hSulf expressing clones provides a potential explanation for the inability of HB-EGF to activate MAPK signaling when hSulf is expressed.

Stimulation of the ERK pathway has previously been shown to inhibit apoptosis (Xia et al., 1995). Consistent with the effect of hSulf on MAPK pathway activation, our studies demonstrate that hSulf expression also modulates apoptosis in ovarian cancer cells. Staurosporine, a prototypic agent for activating the mitochondrial apoptotic pathway (Bertrand et al., 1994; Budihardjo et al., 1999), was chosen for these studies. Staurosporine-induced apoptosis was enhanced by hSulf expression and was more pronounced in cells expressing the sulfatase domain of hSulf (N-Sulf) than in cells hSulf lacking the sulfatase domain (C-Sulf). Site directed mutagenesis of the catalytic site (Cys87,88AA) in N-Sulf attenuates STP induced apoptosis, providing evidence that sulfatase activity is required for the modulation of apoptosis.

Based on these results, we conclude that hSulf is a potent negative regulator of signaling events downstream of heparin binding growth factors that can suppress ERK pathway activation by desulfating critical sulfated moieties in HS-GAGs. Interestingly,

expression of hSulf is undetectable or markedly attenuated in >80% of ovarian cancers relative to normal ovarian surface epithelium, providing a unique mechanism by which cancer cell lines and clinical cancer specimens can upregulate their sensitivity to HB-GFs. The importance of this change, which could affect both proliferation and the apoptotic threshold, to the process of ovarian carcinogenesis and progression merits further investigation.

Acknowledgement

This work was supported by DOD grant DAMD17-99-1-9504 (to V.S., D.I.S, and S.H.K) and a John W Anderson Foundation grant (to V.S) and by the Mayo Foundation.

References

Aviezer, D., and Yayon, A. (1994). Heparin-dependent binding and autophosphorylation of epidermal growth factor (EGF) receptor by heparin-binding EGF-like growth factor but not by EGF. Proc Natl Acad Sci U S A *91*, 12173-12177.

Berchuck, A., Kamel, A., Whitaker, R., Kerns, B., Olt, G., Kinney, R., Soper, J. T., Dodge, R., Clarke-Pearson, D. L., Marks, P., and et al. (1990). Overexpression of HER-2/neu is associated with poor survival in advanced epithelial ovarian cancer. Cancer Res *50*, 4087-4091.

Bertrand, R., Solary, E., O'Connor, P., Kohn, K. W., and Pommier, Y. (1994). Induction of a common pathway of apoptosis by staurosporine. Exp Cell Res *211*, 314-321.

Besner, G. E., Whelton, D., Crissman-Combs, M. A., Steffen, C. L., Kim, G. Y., and Brigstock, D. R. (1992). Interaction of heparin-binding EGF-like growth factor (HB-EGF) with the epidermal growth factor receptor: modulation by heparin, heparinase, or synthetic heparin-binding HB-EGF fragments. Growth Factors *7*, 289-296.

Budihardjo, I., Oliver, H., Lutter, M., Luo, X., and Wang, X. (1999). Biochemical pathways of caspase activation during apoptosis. Annu Rev Cell Dev Biol *15*, 269-290.

Clayton, A., Thomas, J., Thomas, G. J., Davies, M., and Steadman, R. (2001). Cell surface heparan sulfate proteoglycans control the response of renal interstitial fibroblasts to fibroblast growth factor-2. Kidney Int *59*, 2084-2094.

Cliby, W., Ritland, S., Hartmann, L., Dodson, M., Halling, K. C., Keeney, G., Podratz, K. C., and Jenkins, R. B. (1993). Human epithelial ovarian cancer allelotype. Cancer Res *53*, 2393-2398.

Colitti, C. V., Rodabaugh, K. J., Welch, W. R., Berkowitz, R. S., and Mok, S. C. (1998). A novel 4 cM minimal deletion unit on chromosome 6q25.1-q25.2 associated with high grade invasive epithelial ovarian carcinomas. Oncogene *16*, 555-559.

Conover, C. A., Hartmann, L. C., Bradley, S., Stalboerger, P., Klee, G. G., Kalli, K. R., and Jenkins, R. B. (1998). Biological characterization of human epithelial ovarian carcinoma cells in primary culture: the insulin-like growth factor system. Exp Cell Res *238*, 439-449.

Crickard, K., Gross, J. L., Crickard, U., Yoonessi, M., Lele, S., Herblin, W. F., and Eidsvoog, K. (1994). Basic fibroblast growth factor and receptor expression in human ovarian cancer. Gynecol Oncol *55*, 277-284.

Davis-Fleischer, K. M., and Besner, G. E. (1998). Structure and function of heparin-binding EGF-like growth factor (HB-EGF. Front Biosci *3*, d288-299.

Delehedde, M., Lyon, M., Gallagher, J. T., Rudland, P. S., and Fernig, D. G. (2002). Fibroblast growth factor-2 binds to small heparin-derived oligosaccharides and stimulates a sustained phosphorylation of p42/44 MAPKand proliferation of rat mammary fibroblasts. Biochem J *Pt.*

Devlin, J., Elder, P. A., Gabra, H., Steel, C. M., and Knowles, M. A. (1996). High frequency of chromosome 9 deletion in ovarian cancer: evidence for three tumour-suppressor loci. Br J Cancer *73*, 420-423.

Dhoot, G. K., Gustafsson, M. K., Ai, X., Sun, W., Standiford, D. M., and Emerson, C. P., Jr. (2001). Regulation of Wnt signaling and embryo patterning by an extracellular sulfatase. Science *293*, 1663-1666.

Di Blasio, A. M., Carniti, C., Vigano, P., and Vignali, M. (1995). Basic fibroblast growth factor and ovarian cancer. J Steroid Biochem Mol Biol *53*, 375-379.

Di Blasio, A. M., Cremonesi, L., Vigano, P., Ferrari, M., Gospodarowicz, D., Vignali, M., and Jaffe, R. B. (1993). Basic fibroblast growth factor and its receptor messenger ribonucleic acids are expressed in human ovarian epithelial neoplasms. Am J Obstet Gynecol *169*, 1517-1523.

Doldi, N., Bassan, M., Gulisano, M., Broccoli, V., Boncinelli, E., and Ferrari, A. (1996). Vascular endothelial growth factor messenger ribonucleic acid expression in human ovarian and endometrial cancer. Gynecol Endocrinol *10*, 375-382.

Emlet, D. R., Moscatello, D. K., Ludlow, L. B., and Wong, A. J. (1997). Subsets of epidermal growth factor receptors during activation and endocytosis. J Biol Chem *272*, 4079-4086.

Englefield, P., Foulkes, W. D., and Campbell, I. G. (1994). Loss of heterozygosity on chromosome 22 in ovarian carcinoma is distal to and is not accompanied by mutations in NF2 at 22q12. Br J Cancer *70*, 905-907.

Esko, J. D. (1992). Animal cell mutants defective in heparan sulfate polymerization. Adv Exp Med Biol *313*, 97-106.

Fu, S., Bottoli, I., Goller, M., and Vogt, P. K. (1999). Heparin-binding epidermal growth factor-like growth factor, a v-Jun target gene, induces oncogenic transformation. Proc Natl Acad Sci U S A *96*, 5716-5721.

Gabra, H., Watson, J. E., Taylor, K. J., Mackay, J., Leonard, R. C., Steel, C. M., Porteous, D. J., and Smyth, J. F. (1996). Definition and refinement of a region of loss of heterozygosity at 11q23.3-q24.3 in epithelial ovarian cancer associated with poor prognosis. Cancer Res *56*, 950-954.

Garzetti, G. G., Ciavattini, A., Lucarini, G., Pugnaloni, A., De Nictolis, M., Amati, S., Romanini, C., and Biagini, G. (1999). Vascular endothelial growth factor expression as a prognostic index in serous ovarian cystoadenocarcinomas: relationship with MIB1 immunostaining. Gynecol Oncol *73*, 396-401.

Gilmour, L. M., Macleod, K. G., McCaig, A., Gullick, W. J., Smyth, J. F., and Langdon, S. P. (2001). Expression of erbB-4/HER-4 growth factor receptor isoforms in ovarian cancer. Cancer Res *61*, 2169-2176.

Green, D. R. (1998). Apoptotic pathways: the roads to ruin. Cell *94*, 695-698.

Greenlee, R. T., Murray, T., Bolden, S., and Wingo, P. A. (2000). Cancer statistics, 2000. CA Cancer J Clin *50*, 7-33.

Hanahan, D., and Weinberg, R. A. (2000). The hallmarks of cancer. Cell *100*, 57-70.

Henzen-Logmans, S. C., Berns, E. M., Klijn, J. G., van der Burg, M. E., and Foekens, J. A. (1992). Epidermal growth factor receptor in ovarian tumours: correlation of immunohistochemistry with ligand binding assay. Br J Cancer *66*, 1015-1021.

Higashiyama, S., Abraham, J. A., and Klagsbrun, M. (1993). Heparin-binding EGF-like growth factor stimulation of smooth muscle cell migration: dependence on interactions with cell surface heparan sulfate. J Cell Biol *122*, 933-940.

Kamimura, K., Fujise, M., Villa, F., Izumi, S., Habuchi, H., Kimata, K., and Nakato, H. (2001). Drosophila heparan sulfate 6-O-sulfotransferase (dHS6ST) gene. Structure, expression, and function in the formation of the tracheal system. J Biol Chem *276*, 17014-17021.

Kerr, J., Leary, J. A., Hurst, T., Shih, Y. C., Antalis, T. M., Friedlander, M., Crawford, E., Khoo, S. K., Ward, B., and Chenevix-Trench, G. (1996). Allelic loss on chromosome 7q in ovarian adenocarcinomas: two critical regions and a rearrangement of the PLANH1 locus. Oncogene *13*, 1815-1818.

Kozak, M. (1996). Interpreting cDNA sequences: some insights from studies on translation. Mamm Genome *7*, 563-574.

Kozak, M. (1999). Initiation of translation in prokaryotes and eukaryotes. Gene *234*, 187-208.

Latil, A., Baron, J. C., Cussenot, O., Fournier, G., Soussi, T., Boccon-Gibod, L., Le Duc, A., Rouesse, J., and Lidereau, R. (1994). Genetic alterations in localized prostate cancer: identification of a common region of deletion on chromosome arm 18q. Genes Chromosomes Cancer *11*, 119-125.

Lepique, A. P., Forti, F. L., Moraes, M. S., and Armelin, H. A. (2000). Signal transduction in G0/G1-arrested mouse Y1 adrenocortical cells stimulated by ACTH and FGF2. Endocr Res *26*, 825-832.

Liu, D., Shriver, Z., Qi, Y., Venkataraman, G., and Sasisekharan, R. (2002). Dynamic regulation of tumor growth and metastasis by heparan sulfate glycosaminoglycans. Semin Thromb Hemost *28*, 67-78.

Lu, K. H., Weitzel, J. N., Kodali, S., Welch, W. R., Berkowitz, R. S., and Mok, S. C. (1997). A novel 4-cM minimally deleted region on chromosome 11p15.1 associated with high grade nonmucinous epithelial ovarian carcinomas. Cancer Res *57*, 387-390.

Lundin, L., Larsson, H., Kreuger, J., Kanda, S., Lindahl, U., Salmivirta, M., and Claesson-Welsh, L. (2000). Selectively desulfated heparin inhibits fibroblast growth factor- induced mitogenicity and angiogenesis. J Biol Chem *275*, 24653-24660.

McKeehan, W. L., Wang, F., and Kan, M. (1998). The heparan sulfate-fibroblast growth factor family: diversity of structure and function. Prog Nucleic Acid Res Mol Biol *59*, 135-176.

Mills, G. B., Lu, Y., Fang, X., Wang, H., Eder, A., Mao, M., Swaby, R., Cheng, K. W., Stokoe, D., Siminovitch, K., *et al.* (2001). The role of genetic abnormalities of PTEN and the phosphatidylinositol 3-kinase pathway in breast and ovarian tumorigenesis, prognosis, and therapy. Semin Oncol *28*, 125-141.

Mishima, K., Higashiyama, S., Asai, A., Yamaoka, K., Nagashima, Y., Taniguchi, N., Kitanaka, C., Kirino, T., and Kuchino, Y. (1998). Heparin-binding epidermal growth factor-like growth factor stimulates mitogenic signaling and is highly expressed in human malignant gliomas. Acta Neuropathol (Berl) *96*, 322-328.

Murphy, M., McManus, D. T., Toner, P. G., and Russell, S. E. (1997). TP53 mutation in ovarian carcinoma. Eur J Cancer *33*, 1281-1283.

Nielsen, H., Engelbrecht, J., Brunak, S., and von Heijne, G. (1997a). Identification of prokaryotic and eukaryotic signal peptides and prediction of their cleavage sites. Protein Eng *10*, 1-6.

Nielsen, H., Engelbrecht, J., Brunak, S., and von Heijne, G. (1997b). A neural network method for identification of prokaryotic and eukaryotic signal peptides and prediction of their cleavage sites. Int J Neural Syst *8*, 581-599.

Ono, K., Hattori, H., Takeshita, S., Kurita, A., and Ishihara, M. (1999). Structural features in heparin that interact with VEGF165 and modulate its biological activity. Glycobiology *9*, 705-711.

Ornitz, D. M. (2000). FGFs, heparan sulfate and FGFRs: complex interactions essential for development. Bioessays *22*, 108-112.

Ornitz, D. M., and Itoh, N. (2001). Fibroblast growth factors. Genome Biol *2*, REVIEWS3005.

Padera, R., Venkataraman, G., Berry, D., Godavarti, R., and Sasisekharan, R. (1999). FGF-2/fibroblast growth factor receptor/heparin-like glycosaminoglycan interactions: a compensation model for FGF-2 signaling. Faseb J *13*, 1677-1687.

Peifley, K. A., Alberts, G. F., Hsu, D. K., Feng, S. L., and Winkles, J. A. (1996). Heparin-binding epidermal growth factor-like growth factor regulates fibroblast growth factor-2 expression in aortic smooth muscle cells. Circ Res *79*, 263-270.

Peoples, G. E., Blotnick, S., Takahashi, K., Freeman, M. R., Klagsbrun, M., and Eberlein, T. J. (1995). T lymphocytes that infiltrate tumors and atherosclerotic plaques produce heparin-binding epidermal growth factor-like growth factor and basic fibroblast growth factor: a potential pathologic role. Proc Natl Acad Sci U S A *92*, 6547-6551.

Plowman, G. D., Culouscou, J. M., Whitney, G. S., Green, J. M., Carlton, G. W., Foy, L., Neubauer, M. G., and Shoyab, M. (1993). Ligand-specific activation of HER4/p180erbB4, a

fourth member of the epidermal growth factor receptor family. Proc Natl Acad Sci U S A *90*, 1746-1750.

Raab, G., and Klagsbrun, M. (1997). Heparin-binding EGF-like growth factor. Biochim Biophys Acta *1333*, F179-199.

Rapraeger, A. C. (1995). In the clutches of proteoglycans: how does heparan sulfate regulate FGF binding? Chem Biol *2*, 645-649.

Rapraeger, A. C., Guimond, S., Krufka, A., and Olwin, B. B. (1994). Regulation by heparan sulfate in fibroblast growth factor signaling. Methods Enzymol *245*, 219-240.

Rapraeger, A. C., Krufka, A., and Olwin, B. B. (1991). Requirement of heparan sulfate for bFGF-mediated fibroblast growth and myoblast differentiation. Science *252*, 1705-1708.

Rojas, M., Yao, S., and Lin, Y. Z. (1996). Controlling epidermal growth factor (EGF)-stimulated Ras activation in intact cells by a cell-permeable peptide mimicking phosphorylated EGF receptor. J Biol Chem *271*, 27456-27461.

Sasisekharan, R., Shriver, Z., Venkataraman, G., and Narayanasami, U. (2002). Roles of heparan-sulphate glycosaminoglycans in cancer. Nat Rev Cancer *2*, 521-528.

Sausville, E. A., Arbuck, S. G., Messmann, R., Headlee, D., Bauer, K. S., Lush, R. M., Murgo, A., Figg, W. D., Lahusen, T., Jaken, S., *et al.* (2001). Phase I trial of 72-hour continuous infusion UCN-01 in patients with refractory neoplasms. J Clin Oncol *19*, 2319-2333.

Selva, E. M., and Perrimon, N. (2001). Role of heparan sulfate proteoglycans in cell signaling and cancer. Adv Cancer Res *83*, 67-80.

Shridhar, V., Sen, A., Chien, J., Staub, J., Avula, R., Kovats, S., Lee, J., Lillie, J., and Smith, D. I. (2002). Identification of underexpressed genes in early- and late-stage primary ovarian tumors by suppression subtraction hybridization. Cancer Res *62*, 262-270.

Shridhar, V., Staub, J., Huntley, B., Cliby, W., Jenkins, R., Pass, H. I., Hartmann, L., and Smith, D. I. (1999). A novel region of deletion on chromosome 6q23.3 spanning less than 500 Kb in high grade invasive epithelial ovarian cancer. Oncogene *18*, 3913-3918.

Slamon, D. J., Godolphin, W., Jones, L. A., Holt, J. A., Wong, S. G., Keith, D. E., Levin, W. J., Stuart, S. G., Udove, J., Ullrich, A., and et al. (1989). Studies of the HER-2/neu proto-oncogene in human breast and ovarian cancer. Science *244*, 707-712.

Stoffel, K. H. W. (1993). TMbase - A database of membrane spanning proteins segments. Biol Chem *374*, 166.

Thompson, S. A., Higashiyama, S., Wood, K., Pollitt, N. S., Damm, D., McEnroe, G., Garrick, B., Ashton, N., Lau, K., Hancock, N., and et al. (1994). Characterization of sequences within heparin-binding EGF-like growth factor that mediate interaction with heparin. J Biol Chem *269*, 2541-2549.

Valve, E., Martikainen, P., Seppanen, J., Oksjoki, S., Hinkka, S., Anttila, L., Grenman, S., Klemi, P., and Harkonen, P. (2000). Expression of fibroblast growth factor (FGF)-8 isoforms and FGF receptors in human ovarian tumors. Int J Cancer *88*, 718-725.

Wang, J., Luo, F., Lu, J. J., Chen, P. K., Liu, P., and Zheng, W. (2002). VEGF expression and enhanced production by gonadotropins in ovarian epithelial tumors. Int J Cancer *97*, 163-167.

Wang, Q., Fan, S., Eastman, A., Worland, P. J., Sausville, E. A., and O'Connor, P. M. (1996). UCN-01: a potent abrogator of G2 checkpoint function in cancer cells with disrupted p53. J Natl Cancer Inst *88*, 956-965.

Xia, Z., Dickens, M., Raingeaud, J., Davis, R. J., and Greenberg, M. E. (1995). Opposing effects of ERK and JNK-p38 MAP kinases on apoptosis. Science *270*, 1326-1331.

Yang-Feng, T. L., Li, S., Han, H., and Schwartz, P. E. (1992). Frequent loss of heterozygosity on chromosomes Xp and 13q in human ovarian cancer. Int J Cancer *52*, 575-580.

Yu, Y., Xu, F., Peng, H., Fang, X., Zhao, S., Li, Y., Cuevas, B., Kuo, W. L., Gray, J. W., Siciliano, M., *et al.* (1999). NOEY2 (ARHI), an imprinted putative tumor suppressor gene in ovarian and breast carcinomas. Proc Natl Acad Sci U S A *96*, 214-219.

Figure Legends

Figure 1. Schematic representation of genomic structure, open reading frame, and homology alignment of hSulf.

A: Schematic representation of genomic structure of hSulf. The numbered boxes indicate exons; the horizontal lines indicate introns. The coding exons (exons 5-part of exon 23) are indicated by black boxes. The first four exons are non-coding. Sulfatase domain spans exons 5-13, **B**: The open reading frame revealed that hSulf codes for an 871 amino acid long protein with a 22 amino-acid long signal peptide (arrow) and 410 amino acid long sulfatase domain at the N-terminus. **C**: Sulfatase domain homology of hSulf (KIAA1077), rat Sulf, Qsulf, and KIAA1247. The potential key residue cysteine in the active site of the enzyme is boxed.

Figure 2. Expression analysis of hSulf in ovarian cancer.

A: [Upper panel] Agarose gel showing the products with hSulf primers 1 and 2 by semi-quantitative RT-PCR in primary ovarian tumors resolved on a 1.6% agarose gel. Samples are numbered and grouped according to tumor stage. (M) 100 bp ladder, (B) normal ovarian epithelial cell brushings. [Lower panel] Agarose gel showing the products with hSulf primers 1 and 2 by semi-quantitative RT-PCR in short-term cultures of normal ovarian epithelial cells (OSE) and ovarian cancer cell lines. The top band is the product of amplification with hSulf primers 1 and 2. Bottom band is the product of amplification with GAPDH primers F and R. **B:** [Upper panel] Autoradiograph showing the northern hybridization results with hSulf ORF as probe in the same cell lines as in A. [Lower panel] Ethidium bromide stained 18S and 28S RNA of the corresponding samples to show equal loading. **C:** Autoradiograph showing the northern hybridization results on a multiple tissue northern blot (Clontech, Palo Alto, CA) with hSulf ORF as probe. The arrows point to the two different splice forms of hSulf in prostate, ovary, small intestine and colon except testis expresses a tissue specific isoform.

Figure 3. LOH analysis of hSulf in ovarian tumors.

[Upper panel] Histogram showing the % LOH with microsatellite repeats in the introns of hSulf in 33 matched normal/tumor tissue samples. Frequency of LOH with specific markers varied between 40-50%. [Lower panel] LOH in tumors OV182, OV282 and OV305 are shown. The locations of the microsatellites are shown above the panels. Arrow indicates loss of an allele in the corresponding tumor DNA. (N) DNA from normal blood, (T) Tumor DNA, (UI) Uninformative for this locus.

Figure 4. hSulf modulates staurosporine (STP) and UCN-01 induced apoptosis.

A: Comparison of apoptosis in SKOV3 parental, vector and high and low expressing hSulf transfectants clones #6 and #3 respectively. Cell lines were treated with the drugs as described in the Methods section. Percent apoptosis was assessed by DAPI staining using fluorescence microscope. The mean and standard error of three separate experiments are plotted. No induction of apoptosis is seen in the parental or vector transfected SKOV3 cell line after treatment with staurosporine. Stable hSulf transfectants do not have significant apoptosis in the absence of drug treatment, but instead display markedly enhanced caspase-dependent apoptosis when staurosporine is added. The insert in Fig A shows the expression of hSulf in SKOV3 parental, vector and high and low expressing hSulf transfectants clones #6 and #3 by semi-quantitative RT-PCR, (M) 100 bp ladder. **B:** Apoptosis in the hSulf over-expressing clone 6 was confirmed by DNA fragmentation and cytochrome c release from mitochondria to cytosol by western blotting. The blot was stripped and hybridized with mouse monoclonal antibody to ensure equal loading [lower panel]. **C**: Percent apoptosis in three additional hSulf stable clones 7, 8, and 9 after treatment with 1 μM staurosporine or UCN-01 as described before.

Group 1:Untreated cells, Group 2: Treated with 1 μM UCN-01 or in Group 3: with 1 μM staurosporine. Percent apoptosis was measured with DAPI staining. Three hundred cells were counted in triplicates and averaged. All three clones undergo apoptosis in the presence of staurosporine. **D:** Expression of hSulf in OSE, SKOV3 parental, vector and hSulf clones 7, 8 and 9 as determined by semi-quantitative RT-PCR. **E:** Flow cytometry analysis of parental, vector and hSulf expressing clones 7 and 8 by 7AAD staining. [Left panel] no treatment, [Right panel] Treated with 1 μM staurosporine for five hours. The experiment was repeated twice.

Figure 5. Sulfatase activity is required for STP-induced apoptosis in hSulf expressing cells.

A: Comparison of apoptosis in SKOV3 expressing N-Sulf versus C-Sulf. Twenty four hours after transient transfection of N-Sulf, C-Sulf and vector constructs, the cells were treated with 1 μM staurosporine or UCN-01 for 5 h and percent apoptosis was measured with DAPI staining as described before. **B:** Vector, wild-type N-Sulf and Mutated (CC87,88AA) N-Sulf construct were transiently transfected into parental SKOV3 cells and percent apoptosis measured with DAPI staining after 5 h treatment with staurosporine. **C:** Antisense and vector constructs were transiently transfected into hSulf stable clone #6 and percent apoptosis measured with DAPI staining after 5 h treatment with staurosporine. Note the decreased level of apoptosis in C-Sulf transfected cells compared to N-Sulf transfected cells (5A), the attenuation of apoptosis in cells transfected with mutant N-Sulf compared to wild-type N-Sulf construct (5B), and the inhibition of apoptosis in hSulf clone 6 transfected with an antisense construct compared to vector transfected into the stable hSulf clone #6 cells (5C).

Figure 6. hSulf expression, localized to plasma membrane, is associated with decreased levels of sulfated HS-GAGs at the cell surface.

A: Using confocal microscopy, a GFP tagged full-length hSulf was localized to the cell surface [left panel] while control with GFP showed a diffuse localization in the cytoplasm [right panel]. **B:** Co-localization of FLAG tagged hSulf and EGFR to cell membrane detected by mouse monoclonal anti-FLAG antibody (FITC) and rabbit polyclonal anti-EGFR (TRITC). The arrow points to the co-localization of hSulf and EGFR to the cell membrane in the merged panel. **C:** Confocal immunoflourescent images of SKOV3 parental, stable vector and hSulf stable clones 7, 8, and 9, fixed and stained for sulfated HS-GAG using antibody 10E4 (anti-mouse antibody recognizing native heparan sulfate with N-sulfated glucosamine residue). Intense immunostaining with the monoclonal antibody 10E4 in parental and vector transfected cells indicates the presence of sulfated HS-GAGs whereas less intense immunostaining in hSulf expressing clones 7, 8, and 9 suggests decreased level of HS-GAG sulfation.

Figure 7. hSulf modulates heparin-binding growth factor signaling.

A: Western blot analysis of phosphorylated ERK1/2. Cells were treated with 1 ng/ml of FGF-2 for 15, 30 and 60 minutes following 8 hours of incubation in serum free media. Blotting with anti-phosphoERK1/2 antibody revealed a basal level of phosphoERK1/2 in unstimulated cells and a sustained activation of phosphoERK1/2 after FGF2 addition in vector transfectant. In contrast, only transient and much lower levels of phosphorylated ERK1/2 were observed in clones 7 and 8. Additionally, no sustained activation was seen in hSulf clones 7 and 8. The blots were stripped and hybridized with antibody against total MAPK to indicate equal loading [lower panel]. **B:** Activation of phosphoERK1/2 in parental, vector and mutant N-Sulf transfected cells after 15 min incubation with 1 ng/ml FGF-2 [Lanes 2, 4, and 8 in upper

panel]. Note the decreased activation of phosphoERK1/2 in cells transfected with N-Sulf construct in lane 6. The blot was stripped and reprobed with actin to show equal loading [lower panel] **C:** 100 ng/ml of HB-EGF was added for 15 and 60 minutes after 12 h serum starvation. PhosphoERK1/2 is completely down regulated in hSulf expressing clones 7 and 8 compared to vector-transfected clone. **D:** The same blots were stripped and hybridized with anti phosopho-EGF Receptor -Tyr 1068 in the top panel and with antiboby against total EGFR to ensure equal loading and transfer of proteins. **E:** 10 ng/ml of heparin independent EGF was added after 12 h serum starvation and activation of phosphoERK1/2 determined as described in the methods. The blots were stripped and hybridized actin to show equal loading.

Table 1. Primers used in LOH analysis

Sequences	Location within the gene	Product Size	% LOH (# of samples with LOH/ # of informative samples
CA1F-5' CATCTCCATGTCTGAACTTC 3' CA1R-5' ACCTCTTCCTTCAACCTCTG 3'	5' UTR 26 CA Repeats	379 bp	46% (4/9)
CA2F-5' GTCCCTTGTAATGATAATAAG 3' CA2R-5' GAAGACCAAAGTGGCATC 3'	Intron 1 70 CA Repeats	275 bp	47% (7/15)
CA3F-5'GAGTAAGAAGAGATATTGGAG 3' CA3R-5' CCTAGCTGTGTGGATCATTGC 3'	Intron 2 34 CA Repeats	247 bp	53% (9/17)
CA4F-5' CGAACTCCTGACCTCAAGTG 3' CA4R-5' CAGAGGGTGGGTGCAGAGTC 3'	Intron 3-1 40 CA Repeats	212 bp	50% (4/7)
CA5F-5' TAGAATACCTGCACTTCACTG 3' CA5R-5' GAAGACCAAAGTGGCATC 3'	Intron 3-2 44 CA Repeats	193 bp	50% (10/20)

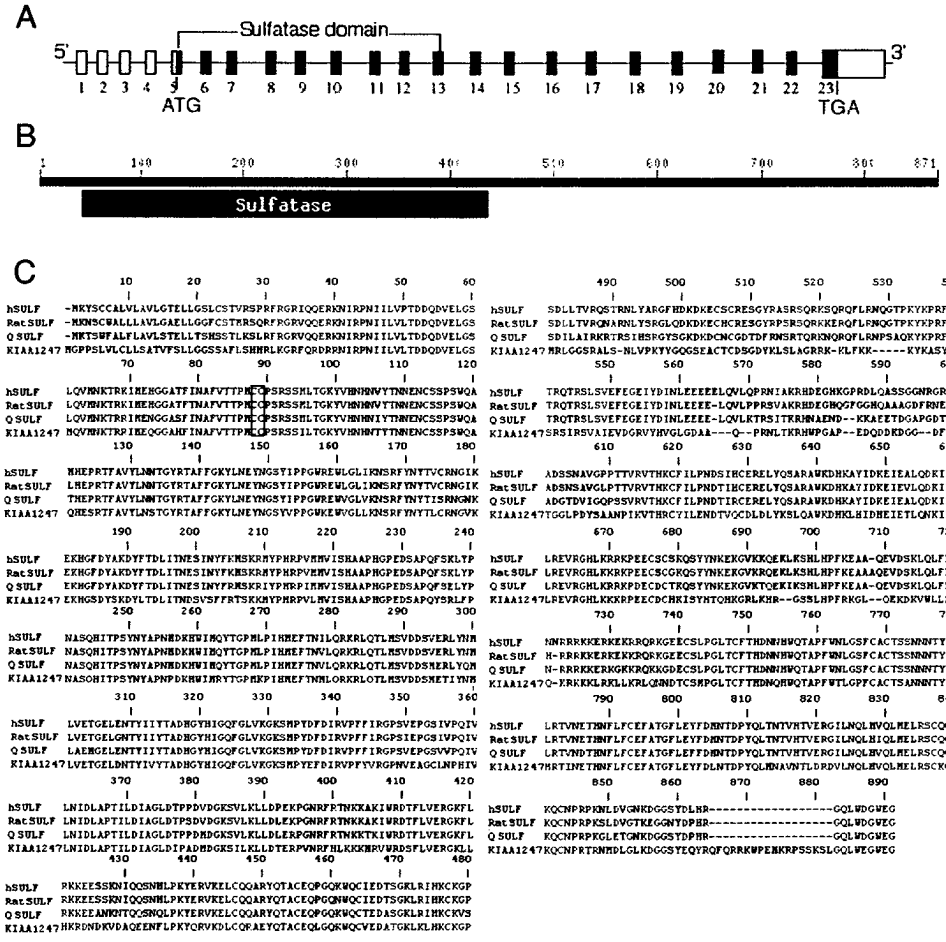
A
Sulfatase domain
5'
3'
1 2 3 4 5 6 7 8 9 10 11 12 13 14 15 16 17 18 19 20 21 22 23
ATG
TGA
B
1 100 200 300 400 500 600 700 800 871
Sulfatase
C
hSULF
RatSULF
QSULF
KIAA1247

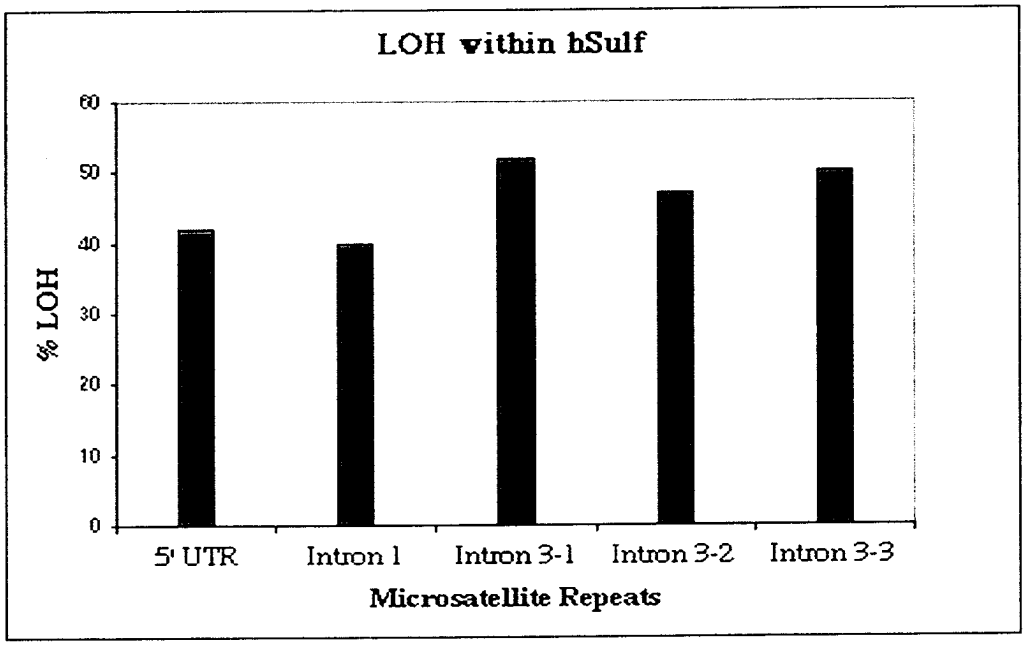
LOH within hSulf
% LOH
60
50
40
30
20
10
0
5' UTR
Intron 1
Intron 3-1
Intron 3-2
Intron 3-3
Microsatellite Repeats

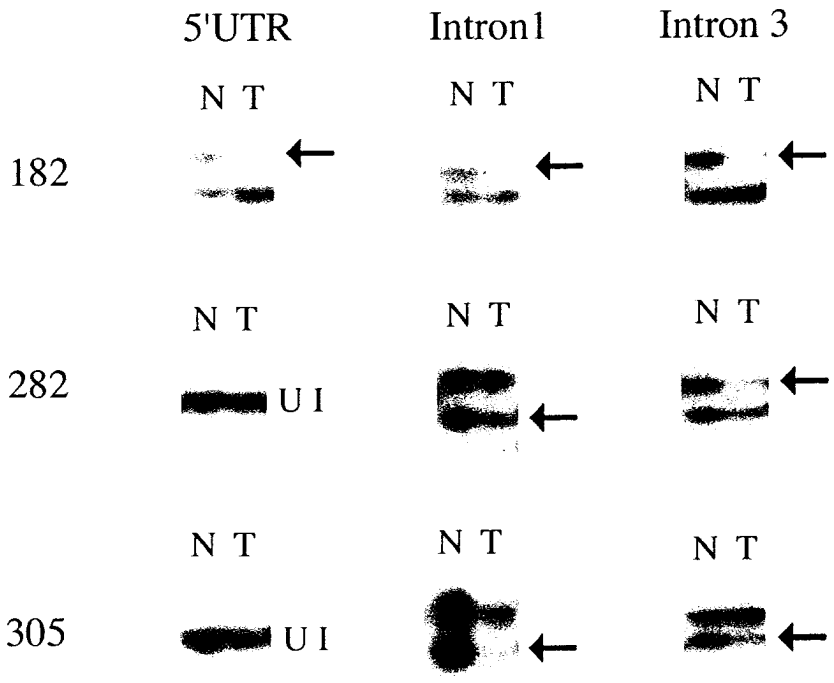
5'UTR
Intron1
Intron 3
N T
N T
N T
182
N T
N T
N T
282
U I
N T
N T
N T
305
U I

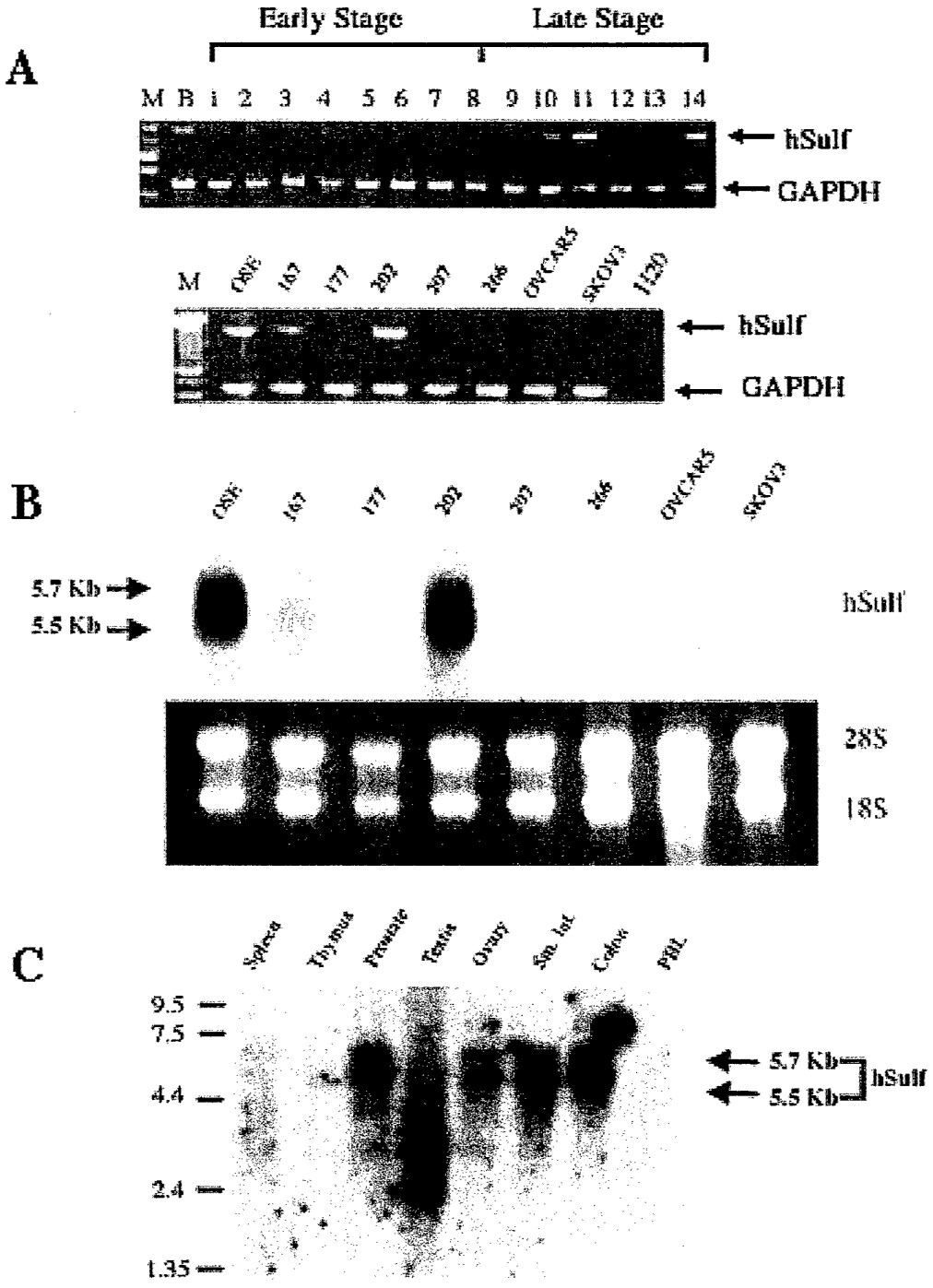
A
Early Stage
Late Stage
M B 1 2 3 4 5 6 7 8 9 10 11 12 13 14
hSulf
GAPDH
M OSE 167 171 202 207 266 OVCAR5 SKOV3 1120
hSulf
GAPDH
B
OSE 167 171 202 207 266 OVCAR5 SKOV3
5.7 Kb
5.5 Kb
hSulf
28S
18S
C
Spleen Thymus Prostate Testis Ovary Sm. Int Colon PBL
9.5
7.5
4.4
2.4
1.35
5.7 Kb
5.5 Kb
hSulf

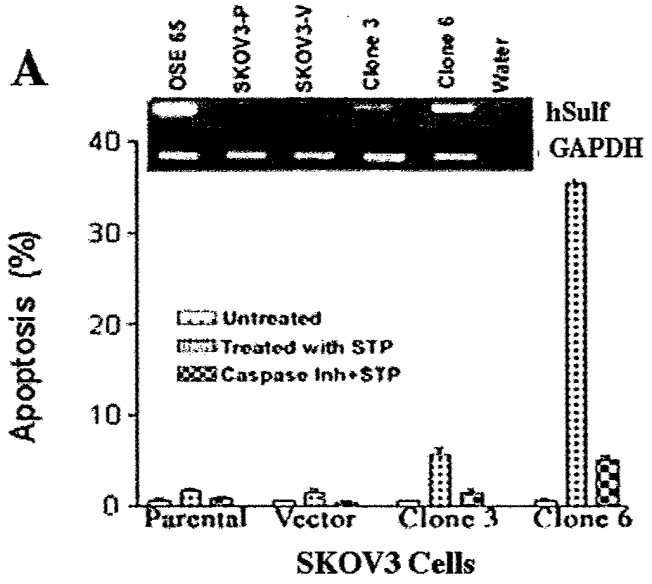
A
OSE 65
SKOV3-P
SKOV3-V
Clone 3
Clone 6
Water
hSulf
GAPDH
Apoptosis (%)
40
30
20
10
0
Untreated
Treated with STP
Caspase Inh+STP
Parental
Vector
Clone 3
Clone 6
SKOV3 Cells

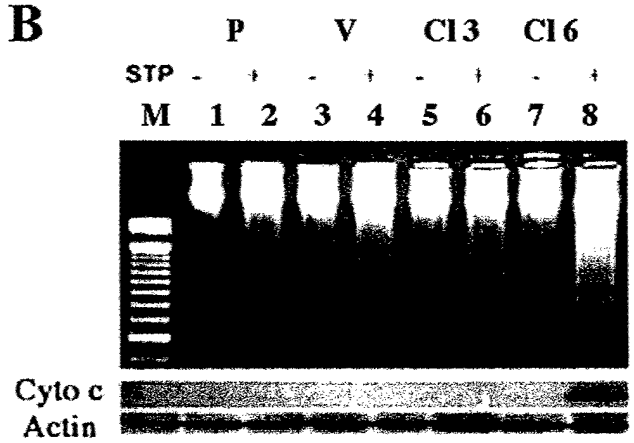
B
P
V
Cl 3
Cl 6
STP - + - + - + - +
M 1 2 3 4 5 6 7 8
Cyto c
Actin

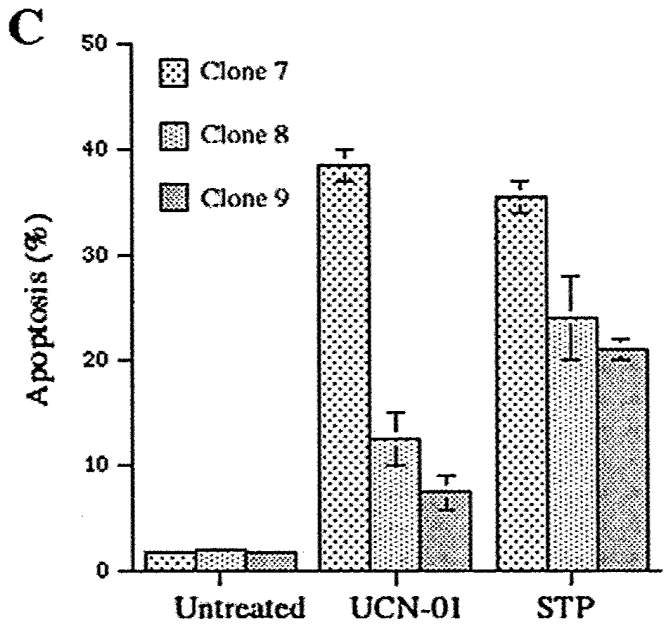
C
Clone 7
Clone 8
Clone 9
Apoptosis (%)
50
40
30
20
10
0
Untreated
UCN-01
STP

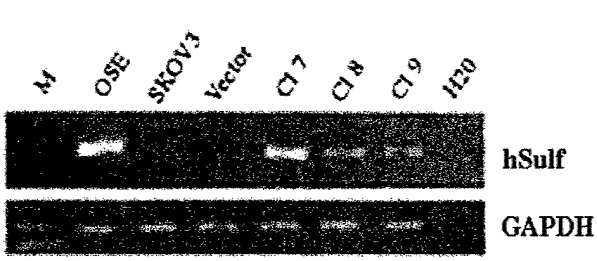
D
M
OSE
SKOV3
Vector
Cl 7
Cl 8
Cl 9
H20
hSulf
GAPDH

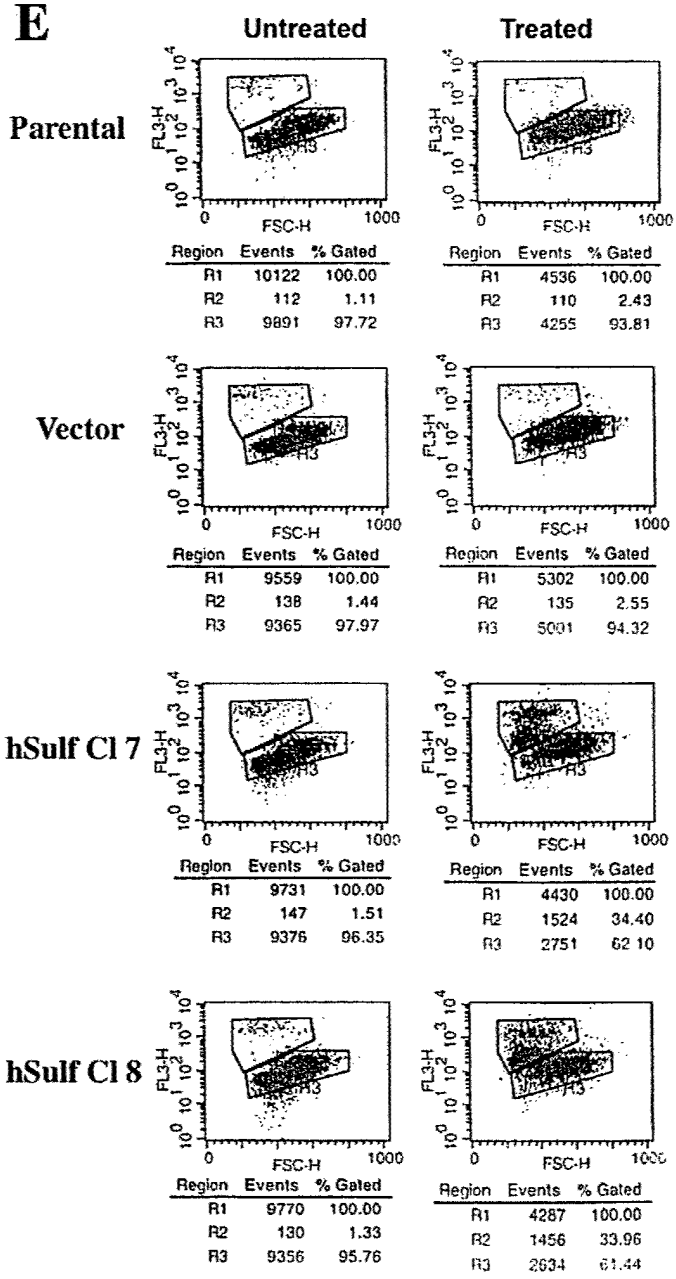
E
Untreated
Treated
Parental
Vector
hSulf Cl 7
hSulf Cl 8
FL3-H
FSC-H
R3
Region Events % Gated
R1 10122 100.00
R2 112 1.11
R3 9891 97.72
R1 4536 100.00
R2 110 2.43
R3 4255 93.81
R1 9559 100.00
R2 138 1.44
R3 9365 97.97
R1 5302 100.00
R2 135 2.55
R3 5091 94.32
R1 9731 100.00
R2 147 1.51
R3 9376 96.35
R1 4430 100.00
R2 1524 34.40
R3 2751 62.10
R1 9770 100.00
R2 130 1.33
R3 9356 95.76
R1 4287 100.00
R2 1456 33.96
R3 2634 61.44

A

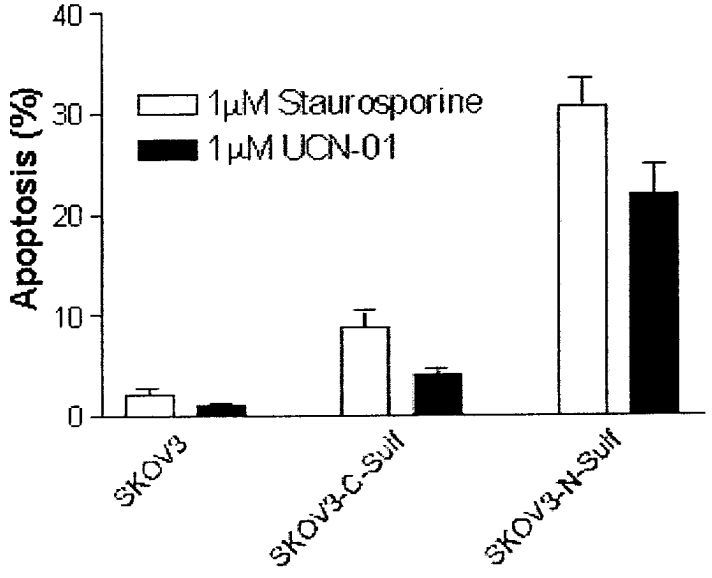
40
30
20
10
0
Apoptosis (%)
1μM Staurosporine
1μM UCN-01
SKOV3
SKOV3-C-Sulf
SKOV3-N-Sulf

B

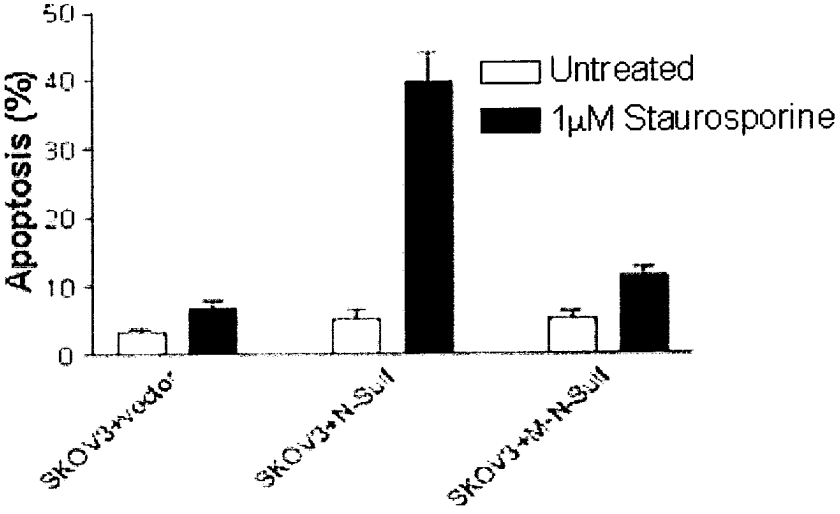
50
40
30
20
10
0
Apoptosis (%)
Untreated
1μM Staurosporine
SKOV3+Vector
SKOV3+N-Sulf
SKOV3+M-N-Sulf

C

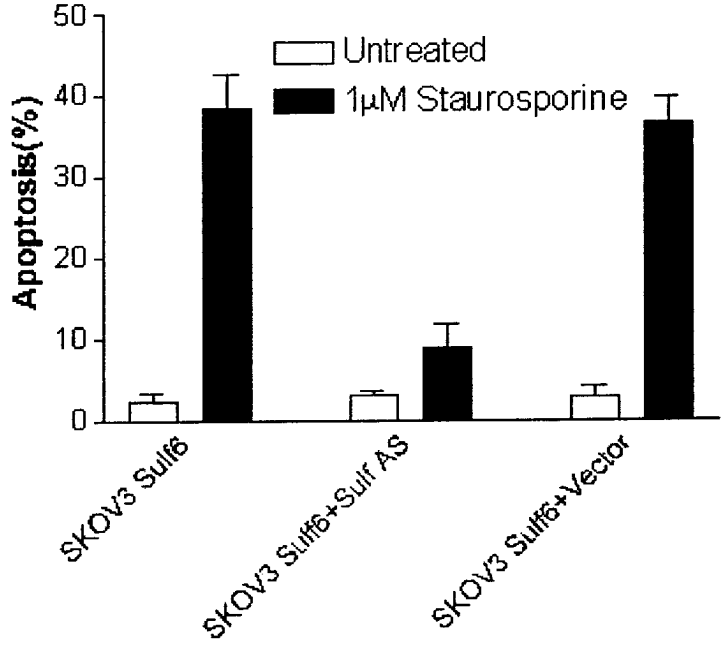
50
40
30
20
10
0
Apoptosis(%)
Untreated
1μM Staurosporine
SKOV3 Sulf6
SKOV3 Sulf6+Sulf AS
SKOV3 Sulf6+Vector

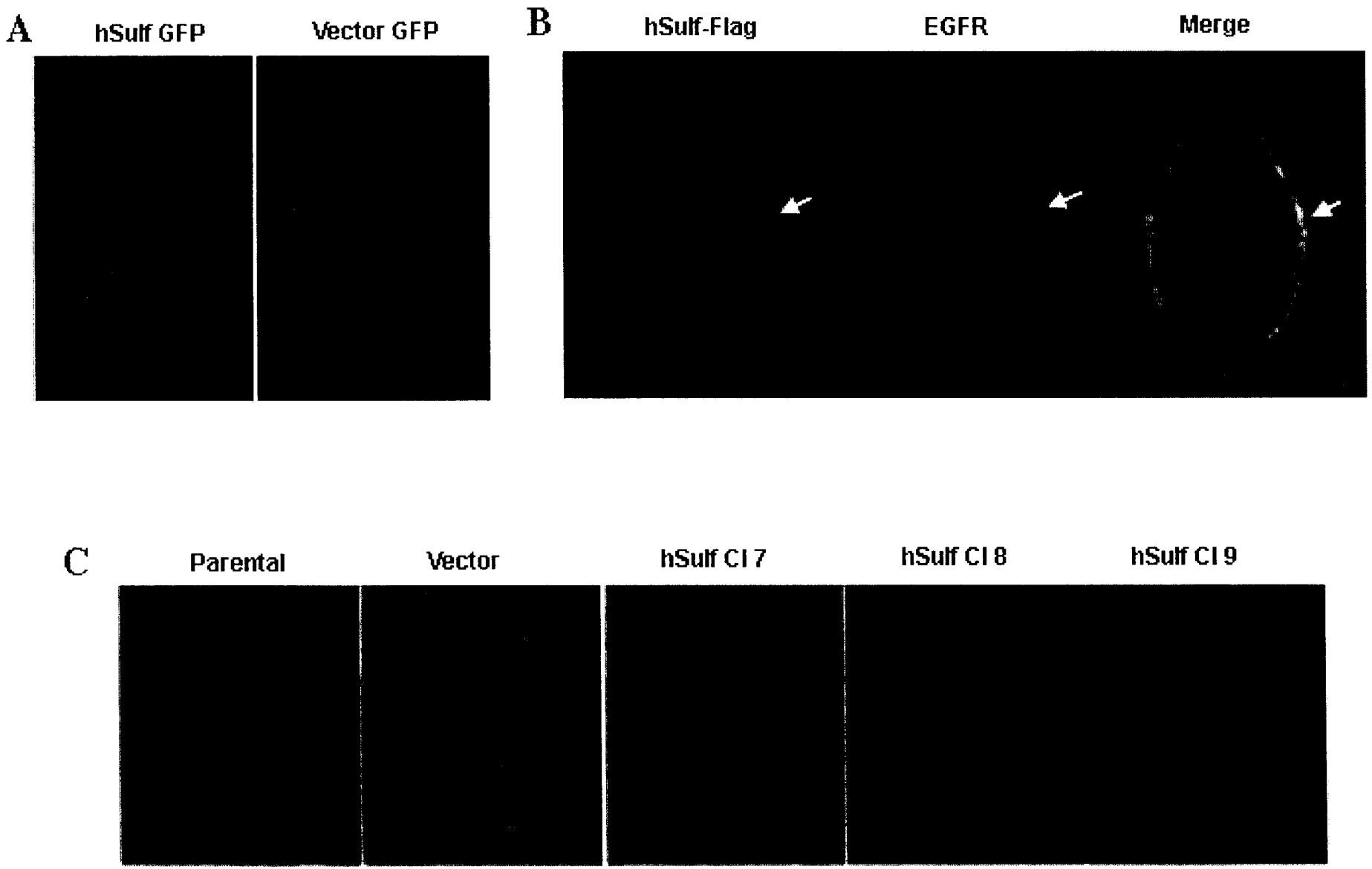
A
hSulf GFP
Vector GFP
B
hSulf-Flag
EGFR
Merge
C
Parental
Vector
hSulf Cl 7
hSulf Cl 8
hSulf Cl 9

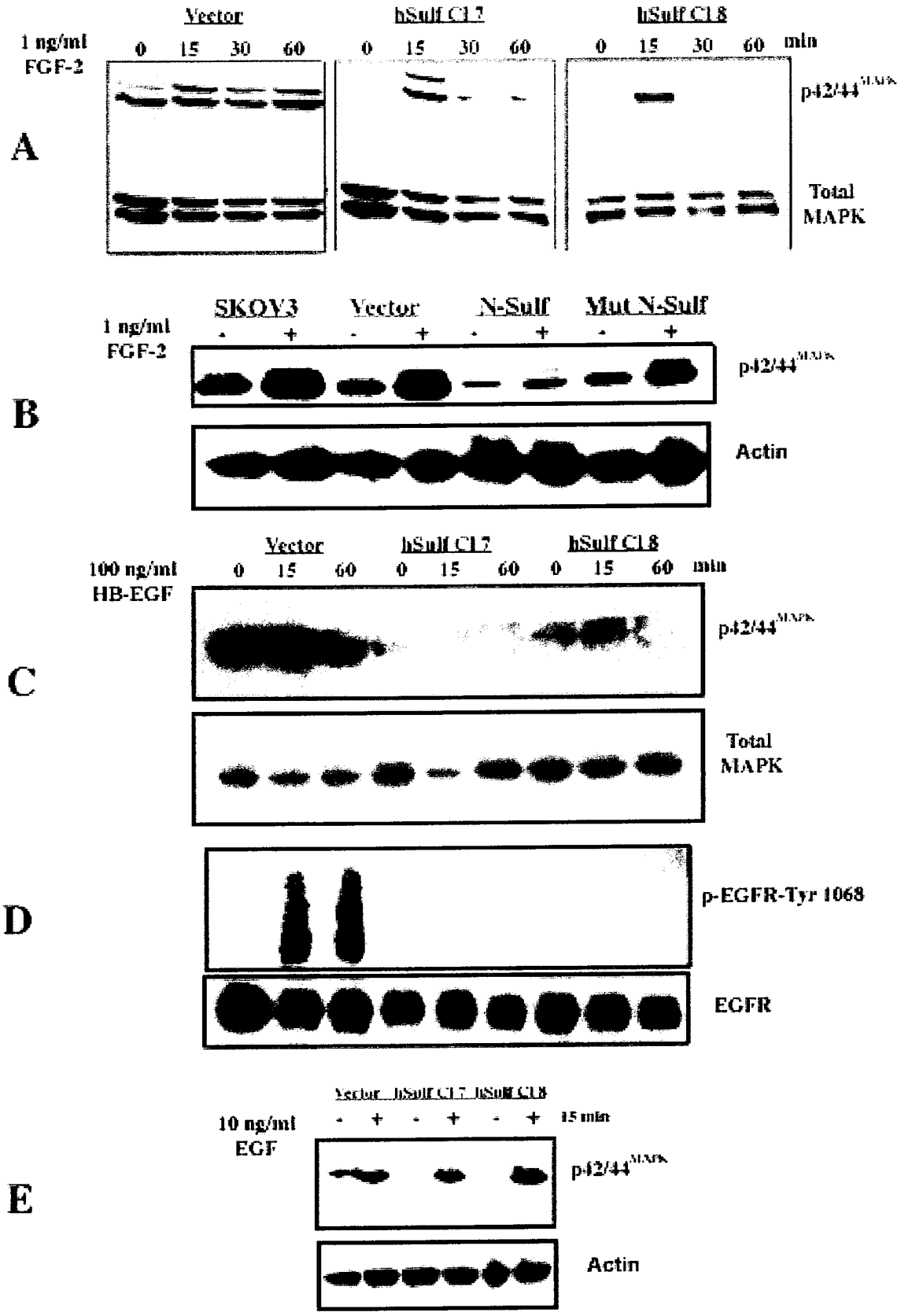
A
Vector
hSulf C17
hSulf C18
1 ng/ml
FGF-2
0 15 30 60 0 15 30 60 0 15 30 60 min
p42/44MAPK
Total
MAPK
B
SKOV3
Vector
N-Sulf
Mut N-Sulf
1 ng/ml
FGF-2
- + - + - + - +
p42/44MAPK
Actin
C
Vector
hSulf C17
hSulf C18
100 ng/ml
HB-EGF
0 15 60 0 15 60 0 15 60 min
p42/44MAPK
Total
MAPK
D
p-EGFR-Tyr 1068
EGFR
E
Vector hSulf C17 hSulf C18
10 ng/ml
EGF
- + - + - + 15 min
p42/44MAPK
Actin

Down-regulation of the Serine Protease HtrA1 Modulates Oxidant- and Cisplatin-induced Cell Death in Ovarian Cancer[1]

Jeremy Chien, Keith C. Bible, Julie Staub, Yean Kit Lee, Shou-Ih Hu, David I. Smith, Robert M. Crowl, Scott H. Kaufmann, Viji Shridhar[2]

Mayo Clinic Cancer Center (J.C., K.C.B., J.S., Y.K.L., D.I.S., S.H.K., V.S.) and Departments of Experimental Pathology (J.C., D.I.S., V.S.) and Oncology (K.C.B., S.H.K.), Mayo Clinic, Rochester, MN 55905; and Arthritis Biology Unit, Novartis Pharmaceuticals, Summit, NJ 07901

Category: Tumor biology

Running title: HtRA1 downregulation in ovarian cancer

Please address correspondence to:
Viji Shridhar, Ph.D.
Division of Experimental Pathology
Mayo Foundation
200 First Street SW
Rochester, MN 55905
Phone (507) 266-2775
FAX (507) 266-5193
Email: shridv@exrch.mayo.edu

Footnotes

[1]Supported in part by DOD grant DAMD17-99-1-9504 (to V.S., D.I.S., and S.H.K) and a John W Anderson Foundation grant (to V.S.) and the Mayo Foundation.

[2]To whom correspondence should be addressed at Division of Experimental Pathology, Hilton 811, Mayo Clinic, 200 First St., S.W., Rochester, MN 55905.

[3]Abbreviations used are: CDDP, cisplatin; LOH, loss of heterozygosity; OSE, ovarian surface eptihelium; PBS, calcium- and magnesium-free Dulbecco's phosphate buffered saline; UCN-01, 7-hydroxystaurosporine; XIAP, X-linked inhibitor of apoptosis protein; zVAD(OMe)-fmk; N-(N$^{\alpha}$-benzyloxycarbonylvalinylalanyl) aspartic acid (O-methyl ester) fluoromethylketone.

Abstract

We report here that HtrA1, identified as one of several under-expressed genes in ovarian cancer, modulates hydrogen peroxide- and cisplatin-induced cell death. Expression of HtrA1 was completely absent in three of seven ovarian cancer cell lines, and can be induced by 5-aza-2'-deoxycytidine. Fifty-nine percent (11/17) of primary ovarian tumors had either a complete absence or markedly reduced levels of HtrA1 expression compared to the brushings of ovarian surface epithelium. Approximately fifty percent of primary ovarian tumors show loss of an allele at microsatellite markers in the vicinity of HtrA1 on 10q26.13. Forced expression of HtrA1 induces cell death in OV202 cells and enhances cell death induced by cisplatin or oxidative stress in HtrA1-null OV167 cells. HtrA1-induced cell death is not inhibited by the broad caspase inhibitor N-(N$^{\alpha}$-benzyloxycarbonylvalinylalanyl) aspartic acid (O-methyl ester) fluoromethylketone [zVAD(OMe)fmk], but instead reflects serine protease activity and results in the release of a catalytically active 37 kDa protease. These observations raise the possibility that HtrA1 is a death-promoting serine protease and that downregulation of HtrA1 in ovarian cancer may contribute to the malignant phenotype by conferring resistance to apoptosis-inducing conditions, including chemotherapeutic agents and oxidative stress.

Introduction

Ovarian cancer is one of the leading causes of gynecological related deaths among women in the United States (1). Of the 26,000 women diagnosed each year with this disorder, over half will die of their disease. These statistics highlight the need for improved understanding of the pathogenesis of this neoplasm.

Like cancers of other tissues, ovarian cancer is considered to result from an accumulation of a series of genetic alterations. Alterations in tumor suppressor genes such as p53 (2, 3), pRB (4), and NOEY2 (5) and oncogenes such as K-ras (6), c-myc (7) and HER-2/neu (8) have been shown to play an important role in ovarian carcinogenesis (9). To search for additional alterations that might play a role in the biology of ovarian cancer, we recently generated suppression subtraction cDNA libraries between normal ovarian epithelium and primary tumors. One of the differentially expressed genes identified from this screen (10) was HtrA1, a human homologue of bacterial *htrA* gene product.

HtrA1 was originally isolated from human fibroblasts as a transformation-sensitive protein due to its down-regulation by SV40 (11). It was also identified as an overexpressed gene in osteoarthritic cartilage compared to non-arthritic controls (12). HtrA1 contains an N-terminal domain Kazal-type trypsin inhibitor motif and a C-terminal trypsin-like protease domain (12). By analogy to the bacterial HtrA protein, which has been extensively characterized with respect to both structure (13) and function (14), the human homolog would be expected to act as a chaperone at low temperature and as a proteolytic enzyme that removes denatured or damaged substrates at elevated temperature (15). Consistent with this hypothesis, HtrA1 has been shown to exhibit protease activity that is completely abolished by mutation of serine 328 (12).

The functions of mammalian HtrA1 are incompletely understood. A mammalian homologue, HtrA2/Omi, is localized to mitochondria but released together with cytochrome c during apoptosis (16-20). Upon release to cytosol, HtrA2 interacts with and antagonizes the function of XIAP[3], thereby promoting apoptosis. Moreover, separate from its action on XIAP, HtrA2 can mediate atypical cell death through its serine protease activity in HEK293 cells (16).

In this report, we describe the loss of HtrA1 expression in ovarian cancer and demonstrate the effects of HtrA1 re-expression in ovarian cancer cell lines. In particular, we present evidence that the *HtrA1* locus is subject to loss of one allele and methylation-induced silencing of the other. Reexpression of HtrA1 induces cell death in OV202 ovarian cancer cells and modulates CDDP-[3] or H_2O_2-induced cell death in OV167 cells. Interestingly, cell death associated with forced expression of HtrA1 is not attenuated by the broad spectrum caspase inhibitor zVAD(OMe)fmk (21), but instead reflects serine protease activity. Taken together, these data suggest that HtrA1 modulate apoptotic signaling and that loss of HtrA1 in ovarian cancer may confer a survival advantage against CDDP- and H_2O_2-induced apoptosis.

Experimental Procedures

Cell culture. OV167, OV177, OV202, OV207, and OV266 were low passage ovarian cancer cell lines established at the Mayo Clinic (22), while OVCAR-3, OVCAR-5, and SKOV-3 were purchased from American Type Culture Collection (Manassas, VA). All cells were grown according to the provider's recommendations.

Tissue processing and Tumors. All the tumors were snap frozen tissues. Tumor contents of the tissues were assessed by H&E stained sections and verified by a pathologist (Dr. Gary Keeney) at the Mayo Clinic. Only tumors with 75-90% tumor content were used for RT-PCR analysis. For control, 20-30 normal ovarian epithelial cell brushings were pooled from patients without cancer and the epithelial nature of these brushings were verified by H&E staining.

Materials. Topotecan and UCN-01were kindly provided by Pharmaceutical Resources Branch of the National Cancer Institute. Paclitaxel, CDDP, and H_2O_2 were purchased from Sigma (St. Louis, MO). All other reagents were obtained as previously described (23-25). Stock (1000-fold concentrated) solutions of paclitaxel, topotecan and UCN-01 were prepared in DMSO and stored at -20°C prior to use. CDDP and H_2O_2 were prepared immediately before use as a 1000-fold concentrated solutions in DMSO and PBS respectively.

Plasmids and antibodies. The plasmids encoding wild-type or S328A HtrA1were generated by PCR cloning into pcDNA3.1 vector as described previously (12). To a generate carboxyl terminus GFP fusion construct of HtrA1, PCR products flanking the entire ORF or C-terminal domain corresponding to codons 153-480 of HtRA1 were cloned into pcDNA3.1/CT-GFP TOPO

vector. Proper construction of all the plasmids was confirmed by DNA sequencing. Antiserum specific for HtrA1 was raised as described previously (12).

Northern Blot Analysis. 15 μg of total RNA was resolved on 1.2% formaldehyde agarose gels and blotted in 1X SPC buffer onto Hybond N membranes (Amersham, Piscataway, NJ). The probes were labeled using the random primer labeling system (Invitrogen, Carlsbad, CA) and purified using spin columns (TE100) from Clontech (Palo Alto, CA). Filters were hybridized at 68°C with radioactive probes in a microhybridization incubator (Robbins Scientific, Sunnyvale, CA) for 1-3 hours in Express Hybridization solution (Clontech) and washed according to the manufacturer's guidelines.

Immunoblotting. Cell lysates were resolved by SDS-PAGE under reducing conditions, followed by transfer onto 0.2-μm PVDF membrane. After the transfer, immunoblotting was carried out as described previously (12).

Semi-quantitative RT-PCR. 50-100 ng of reverse transcribed cDNA was used in a multiplex reaction with the following primers: HtrA1 forward (5'-TAT CGC GGA CGT GGT GGA GAA GAT CG -3') and HtRA1 reverse ('-GTC CAG CTC ATG CCT CTG CCT -3') to yield a 595 bp product and GAPDH forward (5'-ACC ACA GTC CAT GCC ATC AC-3') and GAPDH reverse (5'- TCC ACC ACC CTG TTG CTT GTA-3') to yield a 450 bp product. The PCR reactions contained 50 mM KCl, 10 mM Tris-HCl (pH 8.3), 1.5 mM $MgCl_2$, 400 μM of each HtrA1 primer and 50 μM of each GAPDH primer, and 0.5 units of Taq polymerase (Promega) in a 12.5 μl reaction volume. The conditions for amplification were: 94°C for 3 min, then 30 cycles of 94°C for 30 sec, 58°C for 30 sec, and 72°C for 30 sec in a Perkin Elmer-Cetus 9600 Gene-Amp PCR system. The products of the reaction were resolved on a 1.6% agarose gel. One amplicon

was cut from the gel, purified with QIAquick Gel Extraction Kit (Qiagen, Valencia, CA), and sequenced to verify the specificity of PCR reactions.

Light-Cycler PCR Analysis. Using HtrA1F1 (5'-TCC GCA ACT CAG ACA TGG AC-3') and HtrA1R1 (5'-GGC CTC CCG AGT TTC CAT AG-3') plus RPS9F (5'-TCG CAA AAC TTA TGT GAC CC-3') and RPS9R (5'-TCC AGC ACC CCC AAT C-3') primers, duplex PCR amplification was carried out with Light-Cycler (Roche, Indianapolis, IN) in the presence of SYBR-Green dye according to the following condition: 1 min at 95°C for initial denaturation, followed by 40 cycles at 95°C (10 s), 58°C (15 s), and 72°C (20 s), followed by the measurement of fluorescence at the end of each cycle. After the 40^{th} cycle, melting curve analyses were performed with Light-Cycler software by denaturing the sample at 95°C, rapidly cooling down to 65°C for 15 s, and measuring the fluorescence as the sample temperature was gradually raised to 95°C in the steps of 0.1°C/sec. Each run included a negative control and a known RPS9 control.

LOH analysis of primary ovarian tumors. The markers used in this study are listed in Figure 2A, along with their chromosomal locations. The PCR reaction mix contained: 50 ng of genomic DNA, 50 mM KCl, 10 mM Tris-HCl (pH 8.3), 1.5 mM $MgCl_2$, 200 μM of each primer, 0.05 μl of [α-^{32}P] CTP (10 μCi/μl) and 0.5 units of Taq polymerase (Qiagen, Valencia, CA) in a 10 μl reaction volume. The conditions for amplification were: 94°C for two minutes, then 30 cycles of 94°C for 30 seconds, 52-57°C for 30 seconds, and 72°C for 30 seconds in a Perkin Elmer-Cetus 9600 Gene-Amp PCR system in a 96 well plate. The PCR products were denatured and run on 6% polyacrylamide sequencing gels containing 8 M urea. The gels were dried, autoradiographed for 16-24 h and scored for LOH. Multiple exposures were used before scoring

for LOH. Allelic imbalance indicative of LOH as scored when there was more than 50% loss of intensity of one allele in the tumor sample with respect to the matched allele from normal tissue.

Establishment of HtrA1 stable transfectants. Exponentially growing OV167 cells in 100 mm dishes were washed with serum free medium, and incubated with a mixture of 5 μg of plasmid, 30 μl of LipofectAmine, and 20 μl of Plus reagent (Invitrogen, Carlsbad, CA). After 3 h incubation, complete medium with serum was added. Beginning 24 hours after the start of transfection, G418 was added to select the transfectants. For controls, cells were similarly transfected with empty pcDNA3.1+ vector and selected.

Electroporation. Two days prior to transfection, cells were incubated in antibiotic-free culture medium. On the day of transfection, two million cells in 0.4 ml Cytomix (26) were mixed with 20 μg DNA, and electroporated in 0.4 cm cuvettes using BTX T820 square wave electroporator (BTX, San Diego, CA). Typical settings for electroporation were 2 pulses of 5 ms duration at 330 V for OV202, resulting in 86% transfection efficiency. Immediately after electroporation, cells were allowed to recover for 10 minutes at room temperature before plating in antibiotic-free culture medium.

Assessment of Cell Death. Twenty-four hours after the electroporation, free floating cells in the medium were collected, stained with trypan blue, and counted with hemacytometer. Approximately 20% of cells died from electroporation. The amount of cell death in mock electroporation served as a baseline for determining % cell death in S328A- or HtrA1-transfected groups.

Colony forming assays. To determine population doubling times, 1 x 10^5 cells were seeded in triplicate 100 mm tissue culture plates, incubated for intervals between 24 and 240 h, trypsinized,

and counted on a hemacytometer. Colony forming assays were performed as previously described (23-25). In brief, subconfluent cells were released with trypsin, plated at a density of 4000 cells/plate in multiple 35 mm dishes containing 2 ml culture medium, and incubated for 14-16 h at 37°C to allow cells to attach. Graded concentrations of each drug or equivalent volumes of DMSO (0.1%) were then added to triplicate plates. After a 24 h treatment, plates were washed twice with serum-free MEM and incubated in drug free culture medium for an additional 14 d. The resulting colonies were stained with Coomassie blue and counted manually. Diluent-treated control plates typically contained 75-200 colonies and served as a basis for estimates of colony forming efficiency for the three lines.

Flow Cytometry. Cell cycle analysis was performed as previously reported (23). Briefly, cells were grown to 30-40% confluence in 100 mm tissue culture dishes, released by trypsinization, and sedimented at 200 x g for 5 min. All further steps were performed at 4°C unless otherwise indicated. Samples were fixed in 50% ethanol, treated with RNAse A, stained with propidium iodide and analyzed by flow cytometry on a Becton-Dickinson FACScan (San Jose, CA) using an excitation wavelength of 488 nm and an emission wavelength of 585. Histograms were analyzed using ModFit software (Verity Software House, Topsham, ME).

CDDP Accumulation. Cellular accumulation of CDDP was assessed as previously described (25). In brief, cells grown to 50% confluence on quadruplicate 100 mm tissue culture dishes were treated with CDDP for 2 h, washed *in situ* four times with ice cold PBS and solubilized by direct addition of 3 ml of 70% nitric acid to the first of each set of four plates followed by serial transfer of this solution to each additional plate in each set to solubilize the remaining cells. After a 24 h incubation at 20-22°C, aliquots were removed for estimation of protein (27) and elemental Pt (25).

Cell viability. In order to directly assess cell viability, cells were grown to 30% confluence in 100 mm dishes, treated with 16 μM CDDP for 24 h, harvested at the indicated time points and assessed for either a) their ability to exclude trypan blue or b) apoptotic morphology by staining with Hoechst 33258 as previously described (24, 25). Floating and adherent cells from each dish were combined prior to evaluation with trypan blue or Hoechst staining.

MTT Assay. Five thousand cells plated in 96-well plates, allowed to adhere for 1 d, treated with varying concentration of H_2O_2 for 4 h, washed with PBS, and placed in fresh growth medium. Two days later, cells were incubated with 100 μg/ml MTT for 2 h, washed twice with PBS, and solublized in DMSO. Absorbance at 570 nm was compared to that of untreated cells. Each treatment group contained at least four replicates.

Results

Expression Analysis

Suppression subtraction hybridization identified HtrA1 (previously referred to as PRSS11) as a down-regulated gene in ovarian cancer (10). To follow up on this observation, we examined the mechanism of downregulation and the biological consequences of reexpression of this gene product.

Hybridization with full length coding sequence of HtrA1 to a multiple tissue northern blot revealed that HtrA1 is widely expressed. Particularly noteworthy in the present context is the expression in ovary (Figure 1A), which is lower than that of placenta but equivalent to that of heart and brain. Further analysis revealed that HtrA1 is expressed in OSE cells (Figure 1B), the normal counterpart of ovarian cancer. Notably, compared to short-term culture OSE, the expression of HtrA1 is lost or markedly diminished in several ovarian cancer cell lines by Northern and Western blot analyses (Figure 1B and C respectively).

Examination of primary ovarian tumors also demonstrated down-regulation of HtrA1 expression. Northern blotting (Figure 1D) indicated that HtrA1 is lost or reduced in both early- and late-stage tumors when compared to normal ovarian epithelial cell brushings. Semi-quantitative RT-PCR (Figure 1E) and Light-Cycler analysis (Figure 1F) also indicated reduced levels of HtrA1 expression in several ovarian tumors of different histologies.

Mechanisms of HtrA1 Downregulation

LOH analysis was performed to determine whether the HtrA1 downregulation observed in ovarian cancer reflected allelic loss. Utilizing four genetic markers in the vicinity of the *htrA1* locus (Figure 2A), we analyzed 30 ovarian carcinomas and matched normal DNA for LOH. As indicated in Figure 2B, the marker D10S587, which maps approximately 0.9 Mb telomeric to

htrA1 locus, demonstrated 50% LOH, suggesting that loss of an allele by LOH could account for lowers levels of expression seen at least in some of the primary tumors. Figures 2A and 2B list three additional markers in the same vicinity, their frequency of LOH, cytogenetic band location, and base position determined from UCSC Genome Project Working Draft, relative to the *htrA1* locus.

Loss of a single *htrA1* allele by LOH would only result in reduced expression and would not be sufficient to account for the complete loss of expression of HtrA1 observed in some of the primary tumors. Loss of expression of a gene could be due to deletion of both alleles (homozygous deletion), inactivating mutations within the promoter or in the gene, or epigenetic alterations such as methylation. Therefore, we examined the possibility that hypermethylation might contribute to HtrA1 downregulation. Since the promoter region and exon1 of *htrA1* are highly GC rich, we hypothesized that hypermethylation of promoter or exon 1 might result in inactivation of the gene expression. Treatment of OV207 cells with 0-10 μM of 5 aza 2'-deoxycytidine, a well known methyltransferase inhibitor (28, 29), induced a dose-dependent increase in HtrA1 message by RT-PCR analysis (Figure 2C), suggesting that methylation could represent an additional mechanism that contributes to HtrA1 downergulation. However, our attempts to identify tumor-specific methylation sites in cell lines with complete loss of HtrA1 expression by methylation specific PCR of the putative CpG islands in the promoter and within exon 1 of HtrA1 have been unsuccessful. It is also possible that hypermethylation of specific factor(s) regulating the expression of HtrA1 could result in loss of HtrA1 expression.

Homology between HtrA1 and HtrA2

To gain further insight into potential biological effects of HtRA1 downregulation, a database search for homologous polypeptides was performed. This analysis demonstrated that the most closely related polypeptide is the recently cloned proapoptotic mitochondrial protein, Omi/HtrA2, which shares 53% amino acid identity (75%) homology over their C-terminal regions beginning with amino acid 146 of HtRA1 (Figure 3). This region contains highly homologous (65% identical) trypsin-like domains as well as related PDZ protein-protein interaction domains (Figure 3). These homologies raised the possibility that HtrA1 might be involved in the regulation of apoptosis. However, unlike HtrA2, HtrA1 does not contain an N-terminal mitochondrial targeting sequence (highlighted by a gray box in HtrA2 sequence), but instead contains a Kazal-type trypsin inhibitor (box with dotted line).

Exogenous Expression of HtrA1 Induces Cell Death in OV202

To determine the functional significance of HtrA1 downregulation in ovarian cancer, we utilized two ovarian cancer cell lines, OV202 and OV167. Both of these cell lines lack endogenous HtRA1 protein (Figure 1C). Exogenous expression of HtrA1 in OV202 induced cell death (Figure 4A) in a manner similar to that described in HEK293 cells following the transfection of HtrA2 (16). Moreover, the cell rounding observed with HtrA1 expression in OV202 was not prevented by 100 μM zVAD(OMe)-fmk (Figure 4B), suggesting that this phenomenon may be caspase-independent. In contrast, OV202 cells transfected with the serine protease mutant S328A displayed a normal phenotype (Figure 4B, inset). Approximately $3.89 \pm 0.26 \times 10^5$ (out of 2×10^6) cells died within 24 h after electroporation with the vector (mock) transfection. By contrast, a significantly higher number ($7.48 \pm 0.13 \times 10^5$ of 2×10^6) of cells died after transfection with the wild-type HtrA1 (Figure 4C). This increase in cell death was not

observed with the serine protease mutant S328A (16.98 ± 14.74% increase with S328A vs 92.45 ± 3.27% increase with HtrA1) (Figure 4D), eliminating the possibility that higher level of cell death is the result of transfection artifact. Proteolytic cleavage of HtrA1, resulting in 37-40 kDa products, was also observed in OV202 cells transfected with HtrA1 (Figure 4E). This proteolytic cleavage could not be prevented by co-tranfection with a dominant-negative caspase-9 (dnCasp-9) construct that inhibits caspase-9 activation or pre-incubation with zVAD(OMe)-fmk during transfection. However, proteolytic cleavage was not observed in cells transfected with serine protease mutant S328A. Since the antibody was raised to the peptides corresponding to the C-terminal region of HtrA1 (12), the fragments detected represent products of the HtrA1 C-terminal domain. The smallest fragment detected is approximately 37 kDa, most likely corresponding to the C-terminal HtrA1 containing PDZ and trypsin domains. To determine whether the 37 kDa fragment retains the ability to induce cell death, cDNA encoding the C-terminal domain (codons 153-480) was transfected into OV202. As indicated in Figure 4F, the 37 kDa fragment (HtrA-CT) was more effective in inducing cell rounding than full-length HtrA (HtrA-FL).

Exogenous Expression of HtrA1 Enhances Sensitivity to Oxidative Stress in OV167

In contrast to OV202, exogenous expression of HtrA1 in OV167 did not induce cell death. Accordingly, a stable clone of OV167 expressing HtrA1 provided a convenient system to examine the role of HtrA1 in response to stress. Since mammalian HtrA2, a homologue of HtrA1, was previoiusly shown to be involved in oxidative stress response during ischemia-reperfusion injury (30), we investigated whether HtrA1 could also modulate oxidative stress responses in ovarian cancer cells. After parental, vector-, and HtrA1-transfected OV167 cells were treated with varying concentration of H_2O_2 for 4 h, cell viability was determined 2 days

later by MTT assay. As shown in Figure 5A, HtrA1-transfected OV167 cells displayed a marked sensitivity to H_2O_2 ($p<0.05$). Phase-contrast microscopic examination of cells treated with 600 μM H_2O_2 for 4 h indicated extensive apoptosis in HtrA1-transfected OV167 compared to parental or vector-transfected OV167 (Figure 5B). Western blot analysis showed the absence of HtrA1 expression in parental and vector clone, and the presence of HtrA1 expression in HtrA1 transfected clone. Additionally, the treatment of HtrA1 expressing OV167 with 600 μM H_2O_2 resulted in appearance of the 37 kDa catalytically active C-terminal domain.

CDDP treatment induces HtrA1 expression in normal ovarian epithelial cells

Exogenous Expression of HtrA1 Enhances CDDP Sensivity of OV167

Examination of the three OV167 cell lines (parental, stable transfectants of vector and HtrA1 in OV167) demonstrated no consistent differences between the HtrA1 expressing and the HtrA1 null lines with respect to doubling times (data not shown). Likewise, the transfected lines were fairly similar with respect to their sensitivities to paclitaxel and topotecan as assessed by colony forming assays (Figure 6A and B). In contrast, the HtrA1- and vector-transfected lines differed significantly with respect to their sensitivities to CDDP (Figure 6C). In particular, the vector-transfected line almost 3-fold more resistant to CDDP (IC_{90}= 7.7 – 2.5 M, n = 4) compared to the HtrA1 transfectant (IC_{90}= 2.8 – 1.0 M, $p<0.005$). To confirm that the observed differences in colony formation reflected differences in cell killing, sensitivities of the lines to CDDP were also assayed by directly assessing apoptotic morphological changes (using Hoechst 33258 staining) and subsequent cell death (using trypan blue staining). Trypan blue staining confirmed that the HtrA1 transfected line was more sensitive to CDDP-induced cytotoxicity (Figure 6D), while Hoechst staining demonstrated that it was similarly more sensitive to CDDP-induced apoptosis (Figure 6D inset). In an effort to determine whether

enhanced drug accumulation might be responsible for the enhanced sensitivity observed in the HtrA1-transfected line, CDDP accumulation was assessed using a mass spectroscopic assay for intracellular platinum (25). These studies showed no significant differences in platinum accumulation following a 24-hour treatment of the three cell lines with CDDP.

Discussion

In an attempt to identify differentially expressed genes in ovarian cancer, we generated four suppression-subtraction cDNA libraries from two early and two late-stage tumors subtracted against normal ovarian epithelium. One of the differentially expressed genes identified from this screen was HtrA1 (human homologue of bacterial *htrA* gene product). The product of this gene, which was identified as down-regulated in all four libraries (10), belongs to the HtrA family of serine protease that is well conserved from bacteria to humans. The bacterial HtrA gene product is one of the most well-characterized proteins of the HtrA family of serine proteases (31). HtrA is localized within the periplasmic space of bacteria (32); and its presence is necessary for bacterial thermotolerance. Moreover, it has recently been shown that bacterial HtrA has dual role, acting as a chaperone at normal temperature and as an active protease at high temperature (13, 15).

Human HtrA1 also shares extensive homology with the proapoptotic mammalian protease HtrA2/Omi, particularly in the C-terminal trypsin-like and PDF domains. However, HtrA1 does not contain the mitochondrial targeting sequence and XIAP-interacting peptide sequence that are present in HtrA2. Nonetheless, forced overexpression of HtrA1 and HtrA2 elicits a similar cellular response: atypical cell death characterized by rounding and detachment of cells. This is perhaps not unexpected given the fact that other proteases also kill cells (20, 33).

In OV202 cells, this death was not inhibited by the broad spectrum caspase inhibitor zVAD(OMe)-fmk. This atypical cell death was not observed after expression of a mutant lacking serine protease activity, suggesting that death induced by HtrA1 required serine protease activity. Additional experiments demonstrated that serine protease activity is required for proteolytic processing of HtrA1. There is increasing evidence that caspase-independent cell

death mechanisms may play a role in both cancer and neurodegenerative diseases (34, 35). In prostate cancer LNCaP cells (36) and leukemia cells (37), inhibitor studies have suggested a possible role for serine proteases in radiation-induced cell death. The identity of the putative proteases, however, has remained unclear.

This atypical cell death was not, however, observed in all cell lines. Although exogenous expression of HtrA1 induces atypical cell death in OV202 cells, it does not produce a similar effect in OV167 cells. This observation is somewhat similar to the differential response to exogenously expressed HtrA2, which elicits atypical cell death in HEK293 cells but not in U2OS cells (18). It is possible that differences in the genetic background, particularly the endogenous levels of protease inhibitors, contribute to the differential response to exogenously expressed HtrA1 (38). It is also possible that the presence or deficiency of regulatory mechanisms controlling the activation of HtrA1 could account for a differential response to exogenously expressed HtrA1. Our findings suggest that catalytically processed 37 kD protein was more effective in inducing cell death than full length protein, raising the possibility that processing of full length protein may be a requirement for the induction of cell death. It has been reported that bacterial HtrA does not undergo auto-proteolytic cleavage *in vitro*, but instead appears to require additional activating factors *in vivo* (39).

The lack of cell death upon forced overexpression in OV167 cells permitted an analysis of the effects of HtrA1 as a modulator of other apoptotic stimuli. Results of this analysis indicated that introduction of HtrA1 into OV167 cells was associated with enhanced sensitivity to the chemotherapeutic agent CDDP as well as the oxidizing agent H_2O_2. Interestingly, CDDP treatment also resulted in HtrA1 induction in normal ovarian surface epithelial cells. These observations suggest that HtrA1 might contribute to CDDP sensitivity and HtrA1 loss might

participate in CDDP resistance. Further experiments examining the relationship between HtrA1 expression and CDDP response appear to be warranted.

In summary, our studies suggest that loss of HtrA1 in ovarian carcinoma is common and may be of potential functional significance. In particular, HtrA1 loss appears to contribute to resistance to high levels of oxidative stress. In addition, HtrA1 loss is associated with *de novo* resistance to the antineoplastic agent CDDP in the OV167 cell line. These observations suggest that the dual chaperone/protease function of HtrA1 might play a role in the repair of normal OSE cells after minor insults and the demise of these same cells after severe damage. This duality of function is highly reminiscent of tumor suppressors that participate in both cellular repair and demise, such as p53 (40).

Acknowledgements

We thank James Tarara from Optical Morphology Core for his technical assistance with laser scanning confocal microscopy, Kim R. Kalli for providing us with short-term culture of ovarian surface epithelial cells, and Edward A. Sausville for UCN-01.

References

1. Society, A. C. Cancer facts and figures, 2002.
2. Kupryjanczyk, J., Thor, A. D., Beauchamp, R., Merritt, V., Edgerton, S. M., Bell, D. A., and Yandell, D. W. p53 gene mutations and protein accumulation in human ovarian cancer, Proc Natl Acad Sci U S A. *90:* 4961-5., 1993.
3. Kohler, M. F., Marks, J. R., Wiseman, R. W., Jacobs, I. J., Davidoff, A. M., Clarke-Pearson, D. L., Soper, J. T., Bast, R. C., Jr., and Berchuck, A. Spectrum of mutation and frequency of allelic deletion of the p53 gene in ovarian cancer, J Natl Cancer Inst. *85:* 1513-9., 1993.
4. Li, S. B., Schwartz, P. E., Lee, W. H., and Yang-Feng, T. L. Allele loss at the retinoblastoma locus in human ovarian cancer, J Natl Cancer Inst. *83:* 637-40., 1991.
5. Yu, Y., Xu, F., Peng, H., Fang, X., Zhao, S., Li, Y., Cuevas, B., Kuo, W. L., Gray, J. W., Siciliano, M., Mills, G. B., and Bast, R. C., Jr. NOEY2 (ARHI), an imprinted putative tumor suppressor gene in ovarian and breast carcinomas, Proc Natl Acad Sci U S A. *96:* 214-9., 1999.
6. Enomoto, T., Weghorst, C. M., Inoue, M., Tanizawa, O., and Rice, J. M. K-ras activation occurs frequently in mucinous adenocarcinomas and rarely in other common epithelial tumors of the human ovary, Am J Pathol. *139:* 777-85., 1991.
7. Katsaros, D., Theillet, C., Zola, P., Louason, G., Sanfilippo, B., Isaia, E., Arisio, R., Giardina, G., and Sismondi, P. Concurrent abnormal expression of erbB-2, myc and ras genes is associated with poor outcome of ovarian cancer patients, Anticancer Res. *15:* 1501-10., 1995.
8. Ross, J. S., Yang, F., Kallakury, B. V., Sheehan, C. E., Ambros, R. A., and Muraca, P. J. HER-2/neu oncogene amplification by fluorescence in situ hybridization in epithelial tumors of the ovary, Am J Clin Pathol. *111:* 311-6., 1999.
9. Orsulic, S., Li, Y., Soslow, R. A., Vitale-Cross, L. A., Gutkind, J. S., and Varmus, H. E. Induction of ovarian cancer by defined multiple genetic changes in a mouse model system, Cancer Cell. *1:* 53-62., 2002.
10. Shridhar, V., Sen, A., Chien, J., Staub, J., Avula, R., Kovats, S., Lee, J., Lillie, J., and Smith, D. I. Identification of underexpressed genes in early- and late-stage primary ovarian tumors by suppression subtraction hybridization, Cancer Res. *62:* 262-70., 2002.
11. Zumbrunn, J. and Trueb, B. Primary structure of a putative serine protease specific for IGF- binding proteins, FEBS Lett. *398:* 187-92., 1996.
12. Hu, S. I., Carozza, M., Klein, M., Nantermet, P., Luk, D., and Crowl, R. M. Human HtrA, an evolutionarily conserved serine protease identified as a differentially expressed gene product in osteoarthritic cartilage, J Biol Chem. *273:* 34406-12., 1998.
13. Krojer, T., Garrido-Franco, M., Huber, R., Ehrmann, M., and Clausen, T. Crystal structure of DegP (HtrA) reveals a new protease-chaperone machine, Nature. *416:* 455-9., 2002.
14. Clausen, T., Southan, C., and Ehrmann, M. The HtrA Family of Proteases: Implications for Protein Composition and Cell Fate, Mol Cell. *10:* 443-455, 2002.

15. Spiess, C., Beil, A., and Ehrmann, M. A temperature-dependent switch from chaperone to protease in a widely conserved heat shock protein, Cell. *97:* 339-47., 1999.
16. Suzuki, Y., Imai, Y., Nakayama, H., Takahashi, K., Takio, K., and Takahashi, R. A serine protease, HtrA2, is released from the mitochondria and interacts with XIAP, inducing cell death, Mol Cell. *8:* 613-21., 2001.
17. Hegde, R., Srinivasula, S. M., Zhang, Z., Wassell, R., Mukattash, R., Cilenti, L., DuBois, G., Lazebnik, Y., Zervos, A. S., Fernandes-Alnemri, T., and Alnemri, E. S. Identification of Omi/HtrA2 as a mitochondrial apoptotic serine protease that disrupts inhibitor of apoptosis protein-caspase interaction, J Biol Chem. *277:* 432-8., 2002.
18. Martins, L. M., Iaccarino, I., Tenev, T., Gschmeissner, S., Totty, N. F., Lemoine, N. R., Savopoulos, J., Gray, C. W., Creasy, C. L., Dingwall, C., and Downward, J. The serine protease Omi/HtrA2 regulates apoptosis by binding XIAP through a reaper-like motif, J Biol Chem. *277:* 439-44., 2002.
19. Martins, L. M. The serine protease Omi/HtrA2: a second mammalian protein with a Reaper- like function, Cell Death Differ. *9:* 699-701., 2002.
20. Verhagen, A. M., Silke, J., Ekert, P. G., Pakusch, M., Kaufmann, H., Connolly, L. M., Day, C. L., Tikoo, A., Burke, R., Wrobel, C., Moritz, R. L., Simpson, R. J., and Vaux, D. L. HtrA2 promotes cell death through its serine protease activity and its ability to antagonize inhibitor of apoptosis proteins, J Biol Chem. *277:* 445-54., 2002.
21. Garcia-Calvo, M., Peterson, E. P., Leiting, B., Ruel, R., Nicholson, D. W., and Thornberry, N. A. Inhibition of human caspases by peptide-based and macromolecular inhibitors, J Biol Chem. *273:* 32608-13., 1998.
22. Conover, C. A., Hartmann, L. C., Bradley, S., Stalboerger, P., Klee, G. G., Kalli, K. R., and Jenkins, R. B. Biological characterization of human epithelial ovarian carcinoma cells in primary culture: the insulin-like growth factor system, Exp Cell Res. *238:* 439-49., 1998.
23. Bible, K. C. and Kaufmann, S. H. Cytotoxic synergy between flavopiridol (NSC 649890, L86-8275) and various antineoplastic agents: the importance of sequence of administration, Cancer Res. *57:* 3375-80., 1997.
24. Bible, K. C. and Kaufmann, S. H. Flavopiridol: a cytotoxic flavone that induces cell death in noncycling A549 human lung carcinoma cells, Cancer Res. *56:* 4856-61., 1996.
25. Bible, K. C., Boerner, S. A., Kirkland, K., Anderl, K. L., Bartelt, D., Jr., Svingen, P. A., Kottke, T. J., Lee, Y. K., Eckdahl, S., Stalboerger, P. G., Jenkins, R. B., and Kaufmann, S. H. Characterization of an ovarian carcinoma cell line resistant to cisplatin and flavopiridol, Clin Cancer Res. *6:* 661-70., 2000.
26. van den Hoff, M. J., Moorman, A. F., and Lamers, W. H. Electroporation in 'intracellular' buffer increases cell survival, Nucleic Acids Res. *20:* 2902., 1992.
27. Bible, K. C., Boerner, S. A., and Kaufmann, S. H. A one-step method for protein estimation in biological samples: nitration of tyrosine in nitric acid, Anal Biochem. *267:* 217-21., 1999.

28. Saitoh, F., Hiraishi, K., Adachi, M., and Hozumi, M. Induction by 5-aza-2'-deoxycytidine, an inhibitor of DNA methylation, of Le(y) antigen, apoptosis and differentiation in human lung cancer cells, Anticancer Res. *15:* 2137-43., 1995.
29. Persengiev, S. P. and Kilpatrick, D. L. The DNA methyltransferase inhibitor 5-azacytidine specifically alters the expression of helix-loop-helix proteins Id1, Id2 and Id3 during neuronal differentiation, Neuroreport. *8:* 2091-5., 1997.
30. Faccio, L., Fusco, C., Chen, A., Martinotti, S., Bonventre, J. V., and Zervos, A. S. Characterization of a novel human serine protease that has extensive homology to bacterial heat shock endoprotease HtrA and is regulated by kidney ischemia, J Biol Chem. *275:* 2581-8., 2000.
31. Pallen, M. J. and Wren, B. W. The HtrA family of serine proteases, Mol Microbiol. *26:* 209-21., 1997.
32. Skorko-Glonek, J., Lipinska, B., Krzewski, K., Zolese, G., Bertoli, E., and Tanfani, F. HtrA heat shock protease interacts with phospholipid membranes and undergoes conformational changes, J Biol Chem. *272:* 8974-82., 1997.
33. Williams, M. S. and Henkart, P. A. Apoptotic cell death induced by intracellular proteolysis, J Immunol. *153:* 4247-55., 1994.
34. Wolf, B. B. and Green, D. R. Apoptosis: letting slip the dogs of war, Curr Biol. *12:* R177-9., 2002.
35. Patel, T., Gores, G. J., and Kaufmann, S. H. The role of proteases during apoptosis, Faseb J. *10:* 587-97., 1996.
36. Kimura, K. and Gelmann, E. P. Propapoptotic effects of NF-kappaB in LNCaP prostate cancer cells lead to serine protease activation, Cell Death Differ. *9:* 972-80., 2002.
37. Gong, B., Chen, Q., Endlich, B., Mazumder, S., and Almasan, A. Ionizing radiation-induced, Bax-mediated cell death is dependent on activation of cysteine and serine proteases, Cell Growth Differ. *10:* 491-502., 1999.
38. Askew, Y. S., Pak, S. C., Luke, C. J., Askew, D. J., Cataltepe, S., Mills, D. R., Kato, H., Lehoczky, J., Dewar, K., Birren, B., and Silverman, G. A. SERPINB12 is a novel member of the human ov-serpin family that is widely expressed and inhibits trypsin-like serine proteinases, J Biol Chem. *276:* 49320-30., 2001.
39. Skorko-Glonek, J., Krzewski, K., Lipinska, B., Bertoli, E., and Tanfani, F. Comparison of the structure of wild-type HtrA heat shock protease and mutant HtrA proteins. A Fourier transform infrared spectroscopic study, J Biol Chem. *270:* 11140-6., 1995.
40. Vousden, K. H. and Lu, X. Live or let die: the cell's response to p53, Nat Rev Cancer. *2:* 594-604., 2002.

Figure Legends

Figure 1. Expression Analysis. (A) Northern blot analysis of HtrA1 expression in normal tissues. The highest level of HtrA1 transcripts was detected in placenta followed by brain, heart, and ovary. (B) Northern analysis of expression of HtrA1 in ovarian cancer cell lines compared with short-term culture OSE. HtrA1 expression is not detected in OV167, OV177, OV207, and OV266 by Northern blot analysis. (C) Similar pattern of HtrA1 expression in ovarian cell lines, with the exception in OV202, was detected by Western blot analysis. (D) Diminished HtrA1 expression is observed in 7 out of 8 primary tumors by Northern blot. (E, F) Semi-quantitative and quantitative RT-PCR of primary tumors. Absence or diminished expression of the HtrA1 transcript, compared to normal ovarian epithelial cells (NOE), is detected in primary tumors by semi-quantitive RT-PCR (E) and by quantitative Light-Cycler (F). GAPDH is used as loading or internal controls.

Figure 2. Mechanisms of Inactivation. (A) Markers used for LOH, corresponding cytogenetic band location, and base position relative to *htrA1* locus. (B) The *htrA1* locus is associated with a region of deletion in ovarian cancer. Using four makers located in the vicinity of the *htrA1* locus, 30 sets of normal and tumor samples were analyzed for LOH. Percentage of LOH is calculated for each marker and shown in Panel A with corresponding representative autoradigraphs for each marker. (C) 5 aza-2'-deoxycytidine induces a dose-dependent increase of HtrA1 transcript in OV207. Duplex RT-PCR amplification products of HtrA1 and GAPDH were subjected to agarose gel electrophoresis and shown in Panel B.

Figure 3. Homology and Sequence Alignments of HtrA1 and HtrA2. Both polypeptides containg trypsin-like protease domains and PDZ protein-protein interaction domains in their C-termini. In the N-terminal region, HtrA1 contains an insulin-like growth factor binding protein (IGFBP) domain and a Kazal-type trypsin inhibitor domain (gray box), whereas HtrA2 contains a mitochondrial targeting sequence (highlighted in gray). A signal peptide cleavage site in HtrA1 is indicated by the arrowhead. The sequence of HtrA2 removed after mitochondrial targeting is underlined.

Figure 4. Exogenous expression of HtrA1 induces cell death. (A) OV202 were electroporated with 20 μg of plasmid encoding serine protease mutant HtrA1 (S328A) or wild-type HtrA1 (HtrA1-WT). After 24 h, GFP-positive cells were visualized by fluorescence microscopy. Cells transfected with HtrA1 were rounded up, whereas cells transfected with mutant remained flattened. (B) GFP-positive OV202 cells with round morphology were counted, and expressed as the percentage of total GFP-positive cells. (C) Comparison between the total number of cell deaths induced by S328A and wild-type HtrA1. Twenty four hours after the electroporation, floating cells were collected by centrifugation for 10 min at 500 x g. The cell pallet was resuspended in 100 μl trypan blue, and dead cells were counted by hemacytometer in three independent counts. (D) Comparison of % cell death induced by S328A and wild-type HtrA1 normalized with cell death from mock transfection. (E) Immunoblot of whole cell lysates indicating the catalytic products of HtrA1 in OV202 transfected with wild-type HtrA1 (HtrA1-WT). (F, G) Comparison of % cell rounding in OV202 transfected with either vector, serine protease mutant full length HtrA1 (S328A-FL), wild-type full length HtrA1 (HtrA1-FL), or C-terminal HtrA1 (HtrA1-CT). Schematic representation of full length and C-

terminal HtrA1 is also shown. The error bars represent the standard error of means (SEM) calculated from triplicate samples. Asterisks indicate a statistically signficant difference from the control as determined by one-way ANOVA ($p<0.05$).

Figure 5. HtrA1 expression increases the sensitivity of OV167 cells to oxidative stress. (A) Exogenous expression of HtrA1 decreases the viability of OV167 under oxidative stress. Parental, vector-, and HtrA1-transfected OV167 cells were treated with various concentration of H_2O_2 for 4 h. Cell viability was assessed by MTT assay 2 d later. Absorbance was converted into % cell viability by normalizing the aborbance measured from untreated groups as 100%. Error bars represent SEM calculated from quadruplicates. (B) Phase-contrast microscopy of cells treated with H_2O_2. Cells were treated with 600 μM H_2O_2 for 6 h, and phase-contrast micrographs were taken by Nikon Spot II digital camera. HtrA1-expressing OV167 cells display marked cell death. (C) Stress-induced proteolytic cleavage of HtrA1. Total lysates taken from parental, vector-, and HtrA1-tansfected OV167 treated with 600 μM H_2O_2 for 4 h, were subjected to SDS-PAGE followed by immunoblot with anti-HtrA1 polyclonal antibody, as described elsewhere (Hu et al, 1998). The total lystates taken from cells treated with UCN-01 or H_2O_2 produce a 37 kD HtRA1 fragment indicated by the arrowhead.

Figure 6. Effects of paclitaxel, topotecan and CDDP in HtrA-null and HtrA-expressing ovarian cell lines. A-C. Effects of paclitaxel (**A**), topotecan (**B**) or CDDP (**C**) on colony formation in OV167 cell lines. Cells were exposed to the indicated drug for 24 h, washed, and incubated in drug-free medium for 12-14 days to allow colonies to form. Each data point represents the mean colony count from triplicate plates. Error bars, ±1SD. Results are each

representative of four independent experiments with each agent. **D.** Effects of CDDP on viability of OV167 cell lines. Cells were exposed to 16 μM CDDP for 24 h and incubated in drug-free medium for the indicated length of time. After combining floating and adherent cells from each plate, cell viability was assessed by trypan blue exclusion, while apoptosis was assessed by examination of nuclear morphology after Hoescht 33258 staining (inset). Data shown are representative of four independent experiments. In the inset, p values represent results of two-sided Student's t tests using pooled estimates of sample variances.

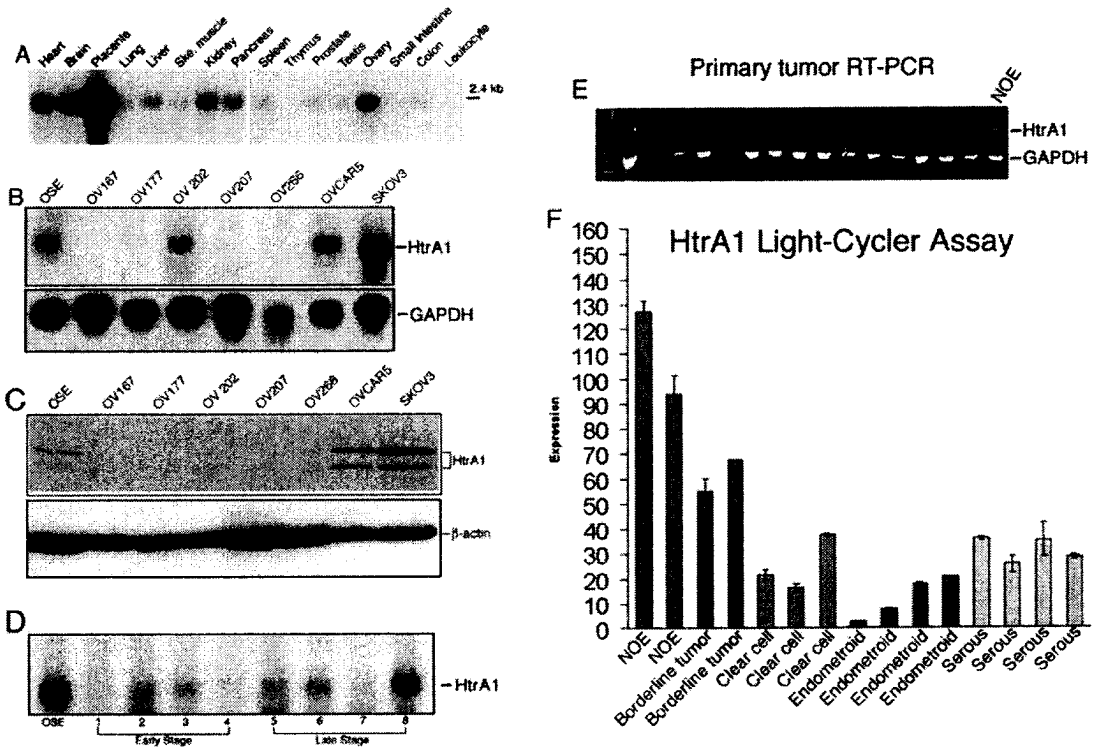
A
Heart
Brain
Placenta
Lung
Liver
Skel. muscle
Kidney
Pancreas
Spleen
Thymus
Prostate
Testis
Ovary
Small intestine
Colon
Leukocyte
2.4 kb
B
OSE
OV167
OV177
OV 202
OV207
OV266
OVCAR5
SKOV3
HtrA1
GAPDH
C
OSE
OV167
OV177
OV 202
OV207
OV266
OVCAR5
SKOV3
HtrA1
β-actin
D
HtrA1
OSE
1
2
3
4
5
6
7
8
Early Stage
Late Stage
E
Primary tumor RT-PCR
NOE
HtrA1
GAPDH
F
HtrA1 Light-Cycler Assay
Expression
160
150
140
130
120
110
100
90
80
70
60
50
40
30
20
10
0
NOE
NOE
Borderline tumor
Borderline tumor
Clear cell
Clear cell
Clear cell
Endometroid
Endometroid
Endometroid
Endometroid
Serous
Serous
Serous
Serous

Figure 1.

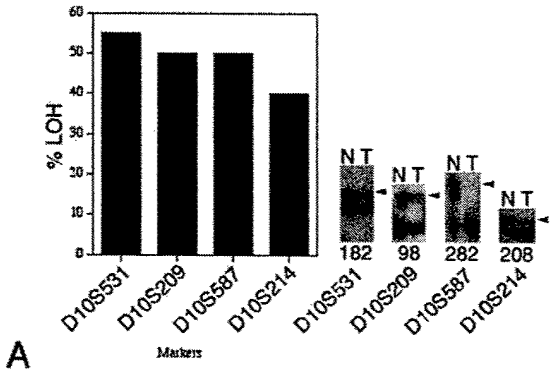

A

Table1 : Markers used for LOH analysis and % LOH in primary tumors

Markers	% LOH	Cytogenetic Band Location	Base Position	Mbs away from HtrA1
D10S531	55 (6/11)	10q25.3	125000000	-7.4*
D10S209	50 (4/8)	10q26.12	130100000	-2.3*
D10S587	50 (7/14)	10q26.13	133300000	0.9
D10S214	40 (4/10)	10q26.2	134900000	2.5

* Upstream of HtrA1

The numbers in parenthesis are the number of tumors with LOH/total number of informative tumors.

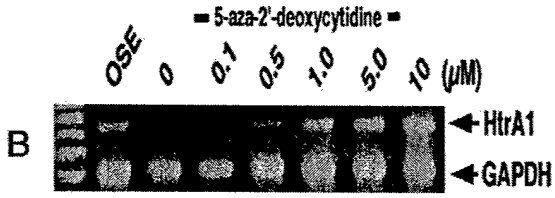

B

Figure 2.

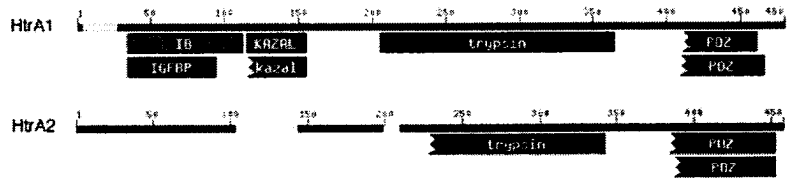


```
HtrA2   MAAPRAGRG--AGWSLRAWRALGGIRWGRRPRLTPDLRALLTSGTSDPRARVTYG--TPS
HtrA1   MQIPRAALLPLLLLLLAAPASAQLSRAGRSAPLAAGCPDRCEPARCPPQPEHCEGGRARD
        *  ***.         * *  : :  * ** . *:..       .. . *:..   *  : .

HtrA2   LWARLSV-GVTEPRAC-LTSGTPGPRAQLTA--VTPDTRTREASENSGTRSRAWLAVALG
HtrA1   ACGCCEVCGAPEGAACGLQEGPCGEGLQCVVPFGVPASATVRRRAQAGLCVCASSEPVCG
          .  .* *..*  ** * .*. *   * ..   .* : * .   ::*    *    . *

HtrA2   AGG---AVLLLLWGGGRG------PPAVLAAVPS-----PPPASPRSQYNFIADVVEKTA
HtrA1   SDANTYANLCQLRAASRRSERLHRPPVIVLQRGACGQGQEDPNSLRHKYNFIADVVEKIA
        :..   * *  * ...*       **.::    :        * * * :********** *

HtrA2   PAVVYIEILDRHPFLGREVPISNGSGFVVAADGLIVTNAHVVADRRRVRVRLLSGDTYEA
HtrA1   PAVVHIELFRKLPFSKREVPVASGSGFIVSEDGLIVTNAHVVTNKHRVKVELKNGATYEA
        ****:**:: : **  ****:: .****:*: **********:::**:*.* .* ****

HtrA2   VVTAVDPVAIATLRIQTKEPLPTLPLGRSADVRQGEFVVAMGSPFALQNTITSGIVSSA
HtrA1   KIKDVDEKAIALIKIDHQGKLPVLLLGRSSELRPGEFVVAIGSPFSLQNTVTTGIVSTT
         :. **  **** ::*: :  **.* ****:::* ******:****:****:*:****::

HtrA2   QRPARDLGLPQTNVEYIQTDAAIDFGNSGGPLVNLDGEVIGVNTMKVTAGISFAIPSDRL
HtrA1   QRGGKELGLRNSDMDYIQTDAIINYGNSGGPLVNLDGEVIGINTLKVTAGISFAIPSDKI
        ** .::*** :::::****** *:*****************:**:**************::

HtrA2   REFLHRGEKKNSSSGISGSQRRYIGVMMLTLSPSILAELQLREPSFPDVQHGVLIHKVIL
HtrA1   KKFLTESHDR-QAKGKAITKKKYIGIRMMSLTSSKAKELKDRHRDFPDVISGAYIIEVIP
        ::** ....: .:.* : ::::***: *::*:.*   **: *. .**** *. * :**

HtrA2   GSPAHRAGLRPGDVILAIGEQMVQNAEDVYEAVRTQSQLAVQIRRGRETLTLYVTPEVTE
HtrA1   DTPAEAGGLKENDVIISINGQSVVSANDVSDVIKRESTLNMVVRRGNEDIMITVIPEEID
        .:**. .**: .***::*. * * .*:** :.:: :* * : :***.* : : * **  :

HtrA2   -
HtrA1   P
```

Figure 3.

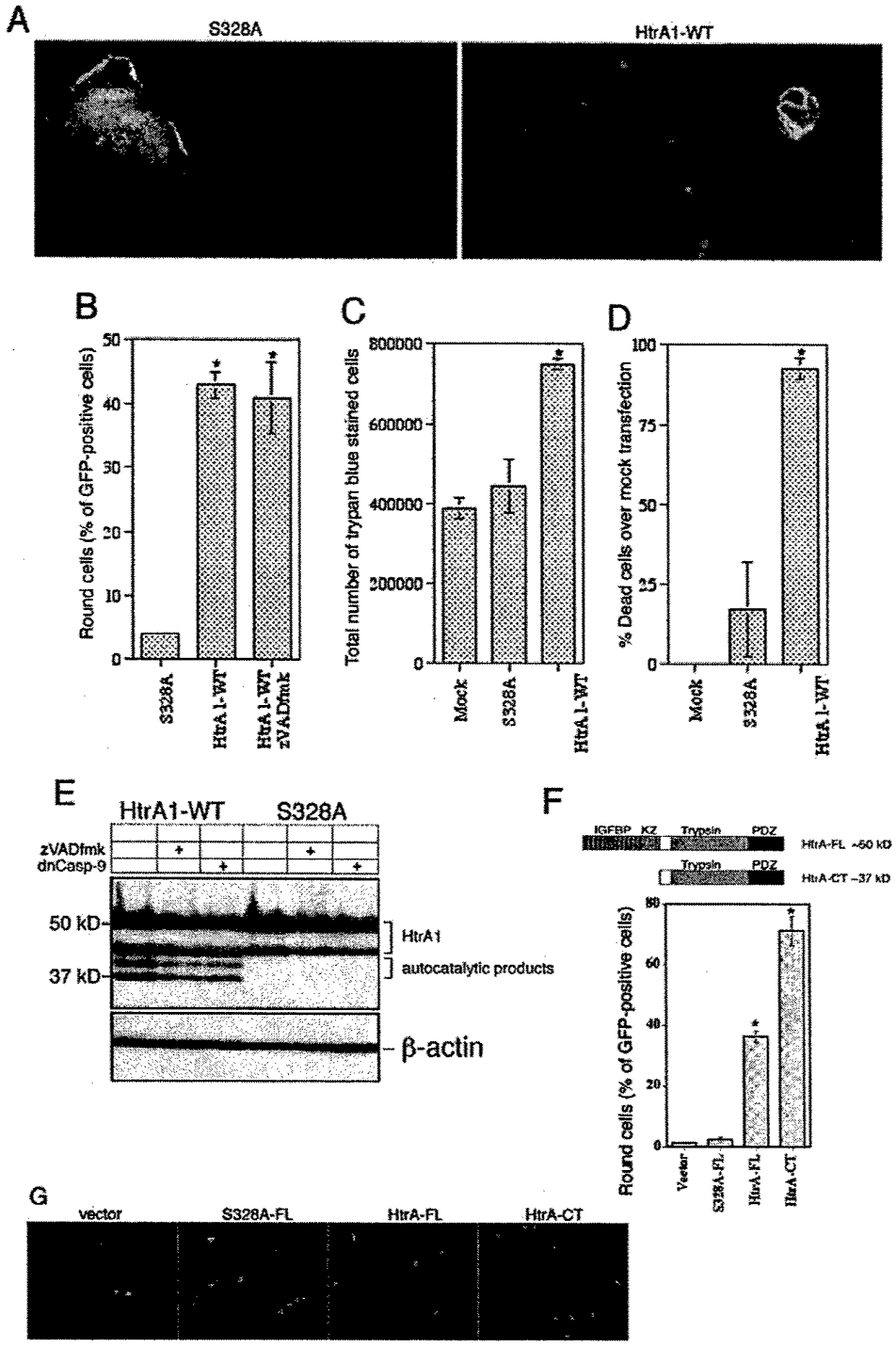
A
S328A
HtrA1-WT
B
Round cells (% of GFP-positive cells)
S328A
HtrA1-WT
HtrA1-WT zVADfmk
C
Total number of trypan blue stained cells
Mock
S328A
HtrA1-WT
D
% Dead cells over mock transfection
Mock
S328A
HtrA1-WT
E
HtrA1-WT
S328A
zVADfmk
dnCasp-9
50 kD
37 kD
HtrA1
autocatalytic products
β-actin
F
IGFBP
KZ
Trypsin
PDZ
HtrA-FL ~50 kD
Trypsin
PDZ
HtrA-CT ~37 kD
Round cells (% of GFP-positive cells)
Vector
S328A-FL
HtrA-FL
HtrA-CT
G
vector
S328A-FL
HtrA-FL
HtrA-CT

Figure 4.

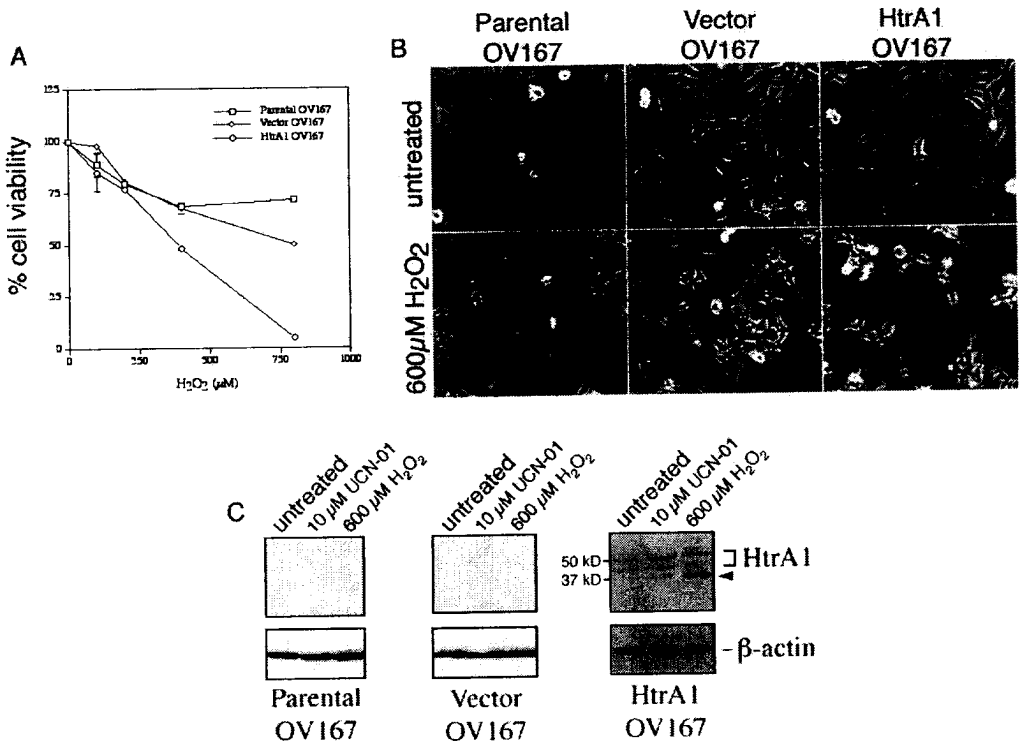
A
% cell viability
Parental OV167
Vector OV167
HtrA1 OV167
H_2O_2 (μM)
B
Parental OV167
Vector OV167
HtrA1 OV167
untreated
600μM H_2O_2
C
untreated
10 μM UCN-01
600 μM H_2O_2
50 kD
37 kD
HtrA1
β-actin
Parental OV167
Vector OV167
HtrA1 OV167

Figure 5.

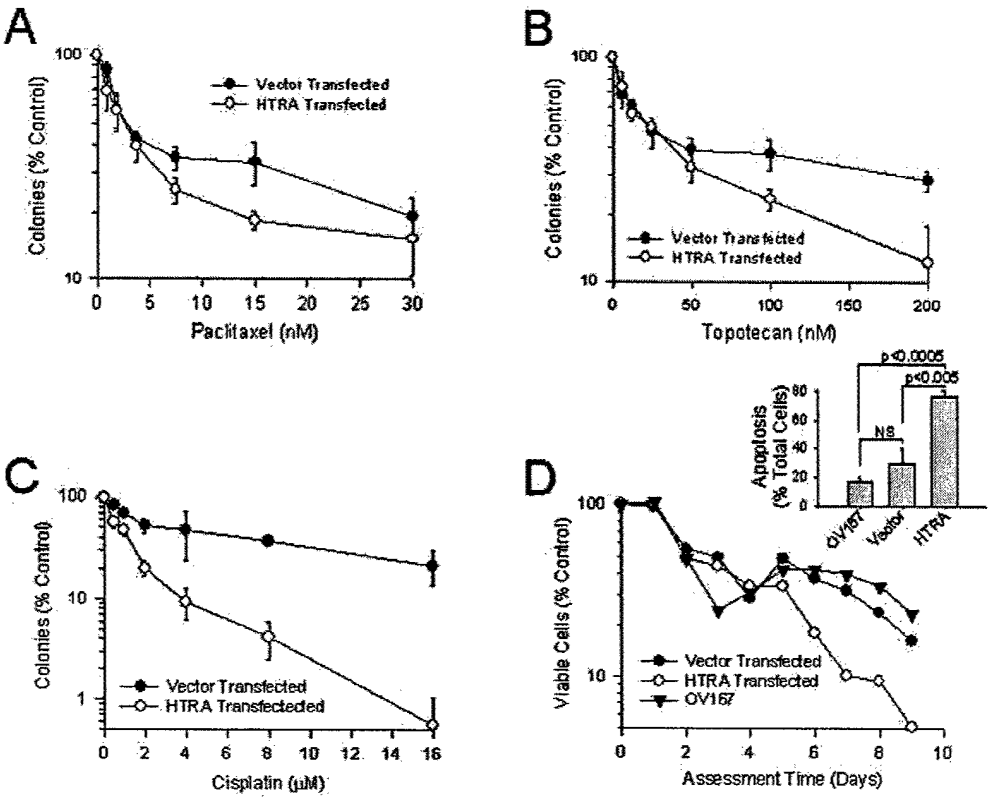
A
Colonies (% Control)
Vector Transfected
HTRA Transfected
Paclitaxel (nM)
B
Colonies (% Control)
Vector Transfected
HTRA Transfected
Topotecan (nM)
C
Colonies (% Control)
Vector Transfected
HTRA Transfectedected
Cisplatin (μM)
D
Apoptosis (% Total Cells)
p<0.0005
p<0.005
NS
OV167
Vector
HTRA
Viable Cells (% Control)
Vector Transfected
HTRA Transfected
OV167
Assessment Time (Days)

Figure 6.